Observations **and Modeling** of Wave Current Interactions

Leonel Romero

Earth Research Institute - UCSB

Collaborators:
Carter Ohlmann (UCSB), Enric Pallàs-Sanz (CICESE),
James C. Mcwilliams (UCLA), Cigdem Akan (UNF), Yusuke Uchiyama (Kobe University) , Nick Statom (SIO)

Air-Sea Interaction

•70% of the earths surface is covered by water

•Oceans play an important role regulating the weather and climate

•Coupling between the ocean and the atmosphere is modulated by surface waves.

•Surface waves modulate the exchange of momentum, heat and gases across the air-sea interface.

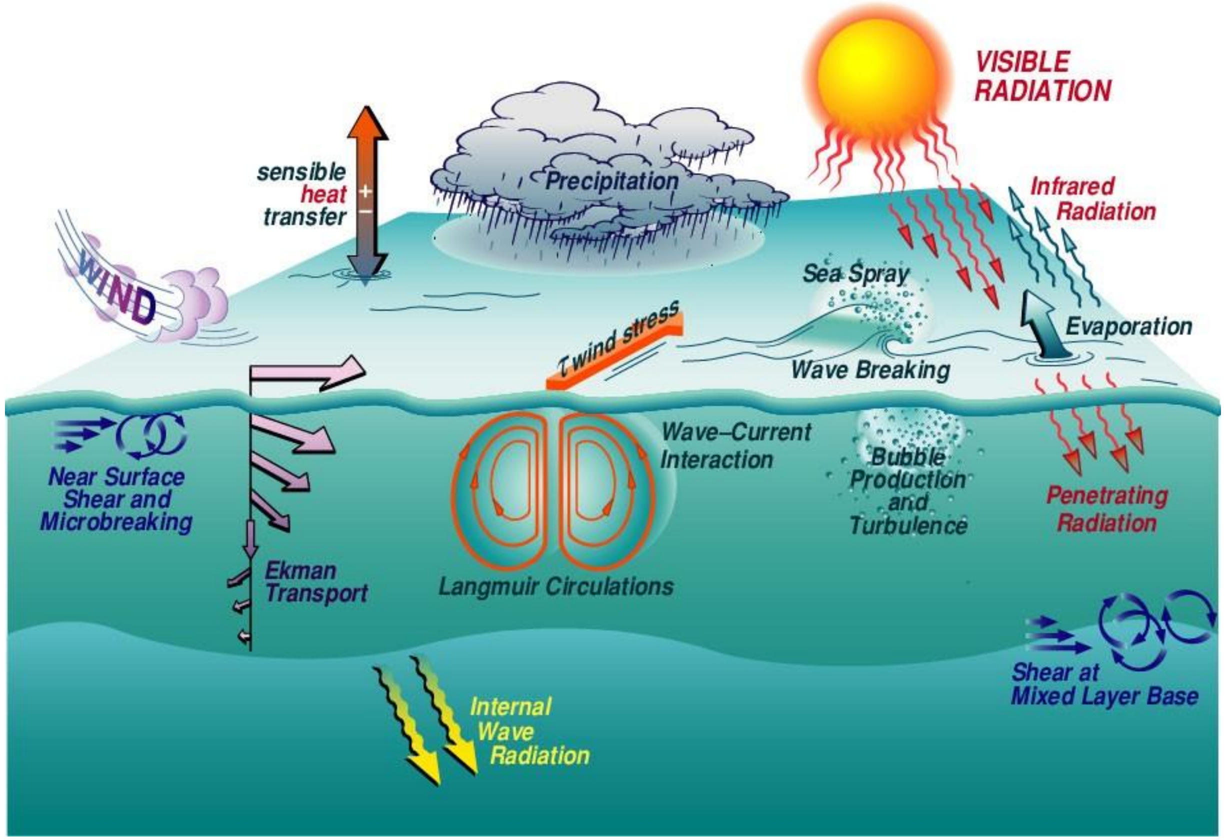

Source CBLAST website:
http://www.whoi.edu/science/AOPE/dept/cbl.jpg

Oceanic Boundary Layer:

- 1) Wave breaking
  - Energy dissipation
  - Drives upper ocean currents
  - Turbulence/Mixing
  - Gas exchange
  - Aerosol production

- 2) Langmuir Circulation
  - Turbulence
  - Mixing

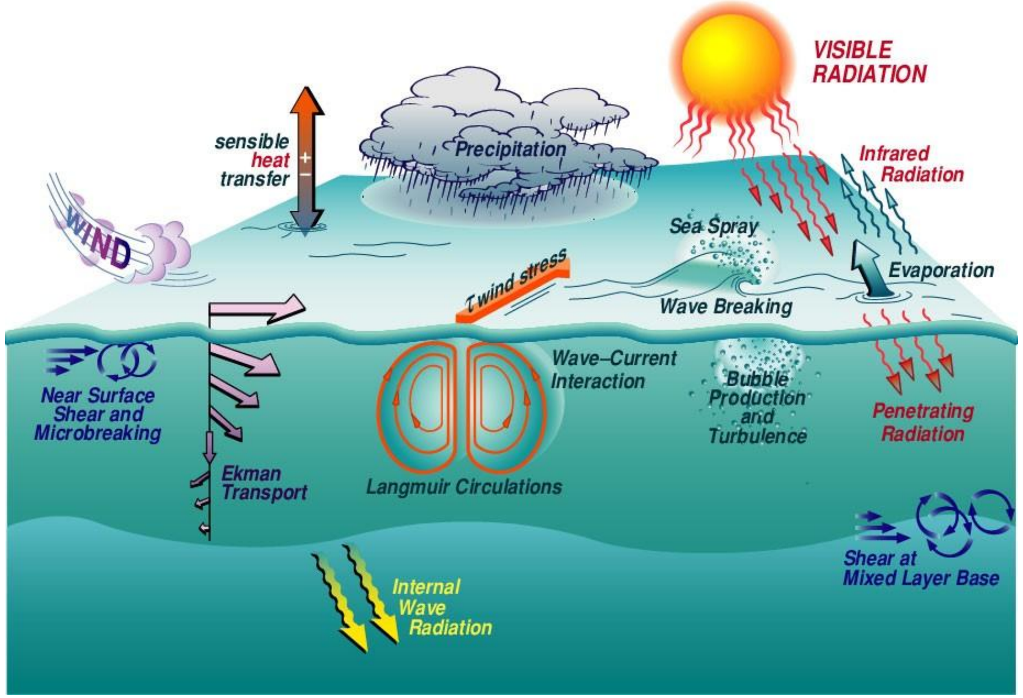

Field experiments

- Location: South Padre Island, TX
- Environmental Conditions
    - Mainly upwelling and downwelling winds
- Number of experiments
    - 2 experiments during spring and fall 2016
- Experiment characteristics
    - 5-7 days of field observations within a 14 day waiting period under different environmental conditions.
    - Each day 4 patches of dye and 4 clusters of drifters were released at 2, 4, 8 and 12 km from the shore (water depth between 10 and 20 m)
    - Measurements were collected for up 5 hours

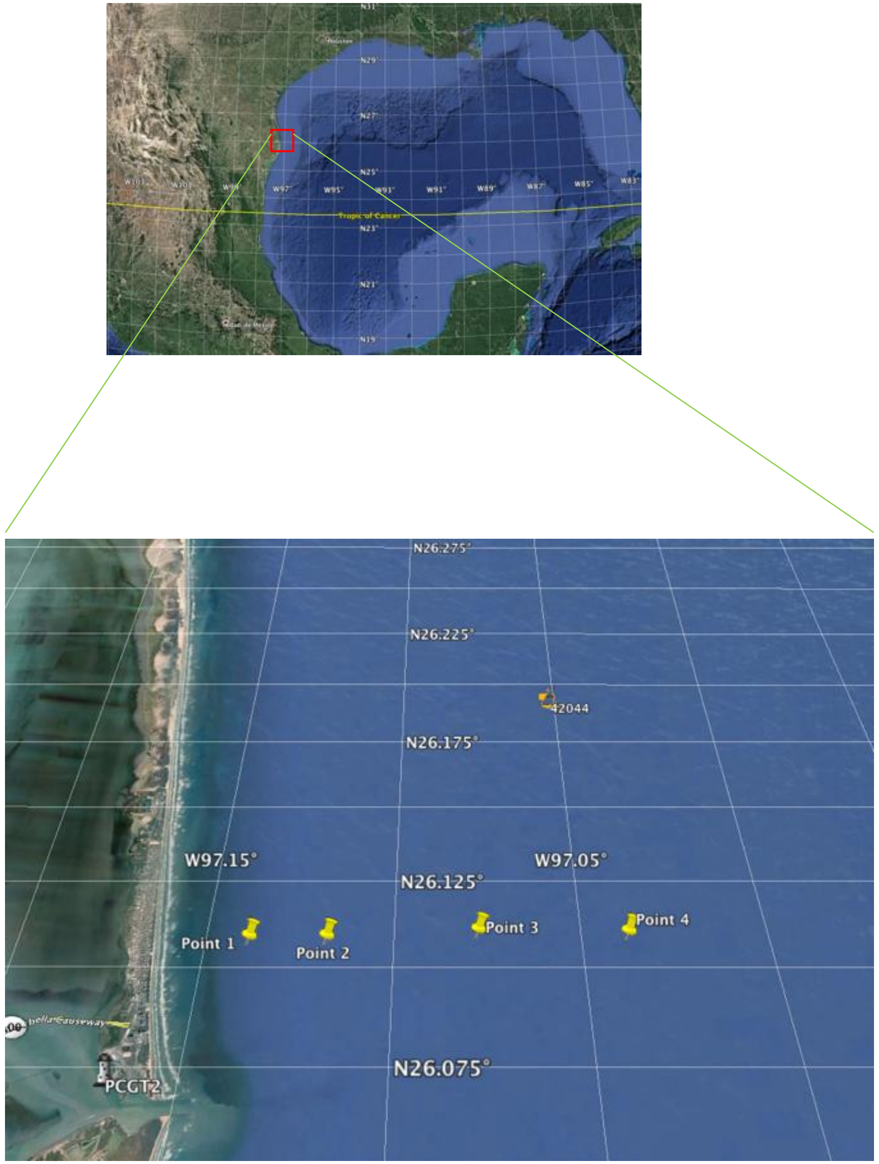

stations

In-situ Measurements

- Platform: small fishing boat (Salt Walker)
- Instrumentation/Supplies:
  - Hand deployed CTD/fluorometer system (Seabird SBE-19+)
  - 16 Microstar drifters drogued at 1 m
  - Tow body with dye fluorometer and GPS for real-time plume tracking (Turner Designs C-fins)
  - 270 gallon tank with a pump and a diffuser
  - 4 gallons of rhodamine dye/ day
  - 2 gallons of alcohol /day

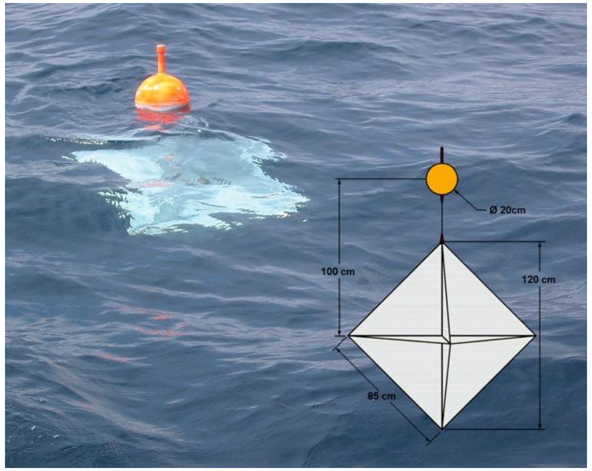

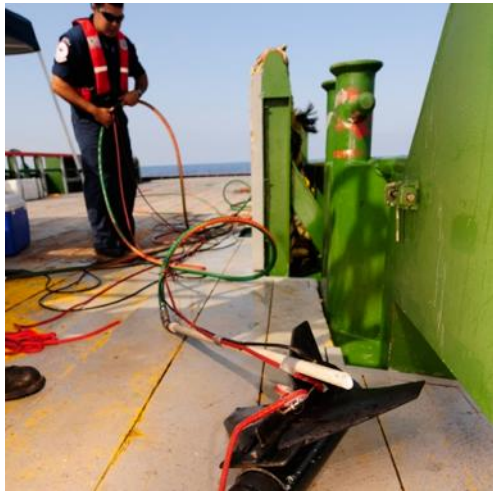

Airborne measurements

Platform:

Aspen Helicopters Partenavia Observer

Instrumentation (SIO) :

The Modular Aerial Sensing System (Melville et al., 2016)

-Hyperspectral sensor – track dye patches

-Infrared camera – detect flow structures

-Scanning lidar – surface waves

-Inertial Motion Unit w/GPS

Flights

-Seven flights 5 hours long each per experiment out of Brownsville Airport, Texas

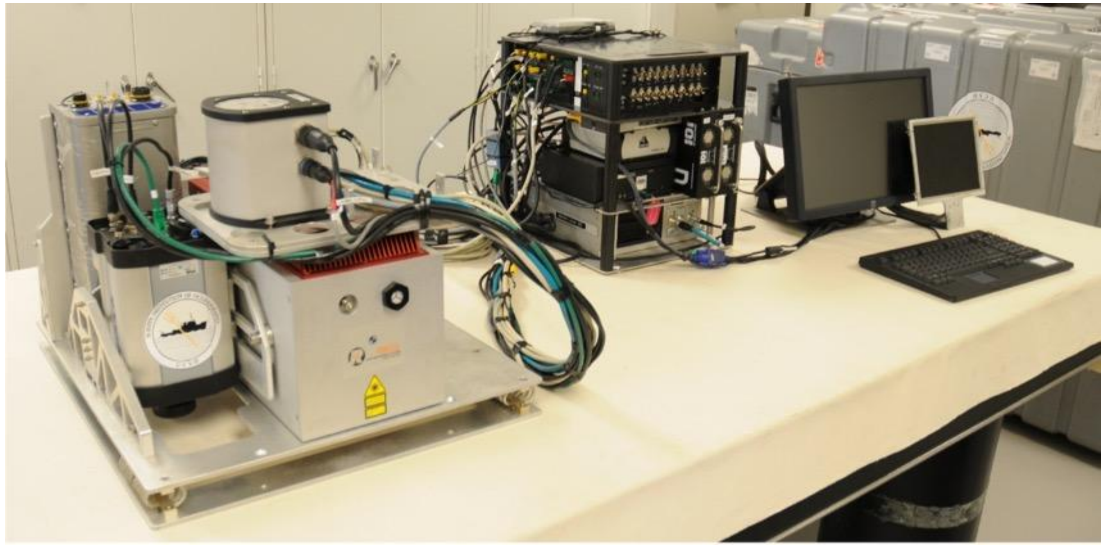

Dye and drifter deployments

- Four drifters in a square configuration 100 m apart allowing measurements of the current gradients and dispersion
- Circular dye patches with a diameter of 100 m

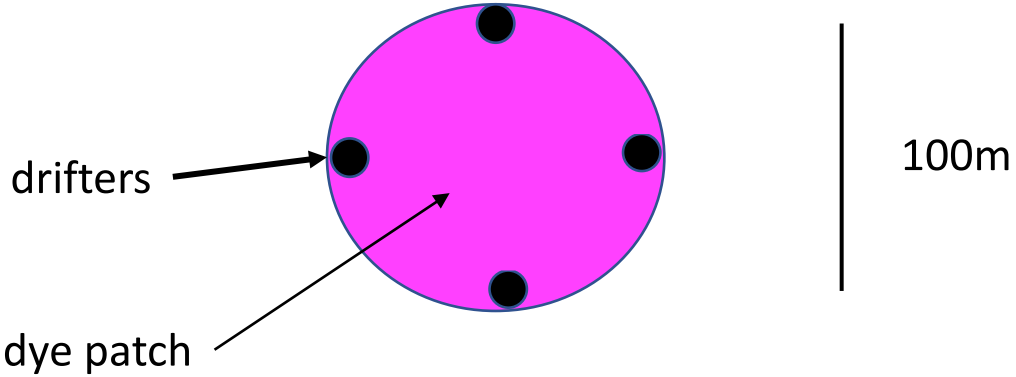

- Drifters are used to guide the boat as it fills in the circle with dye

Boat track during dye deployment

- After deployment the dye typically was vertically mixed reaching ~ 3 m below the surface

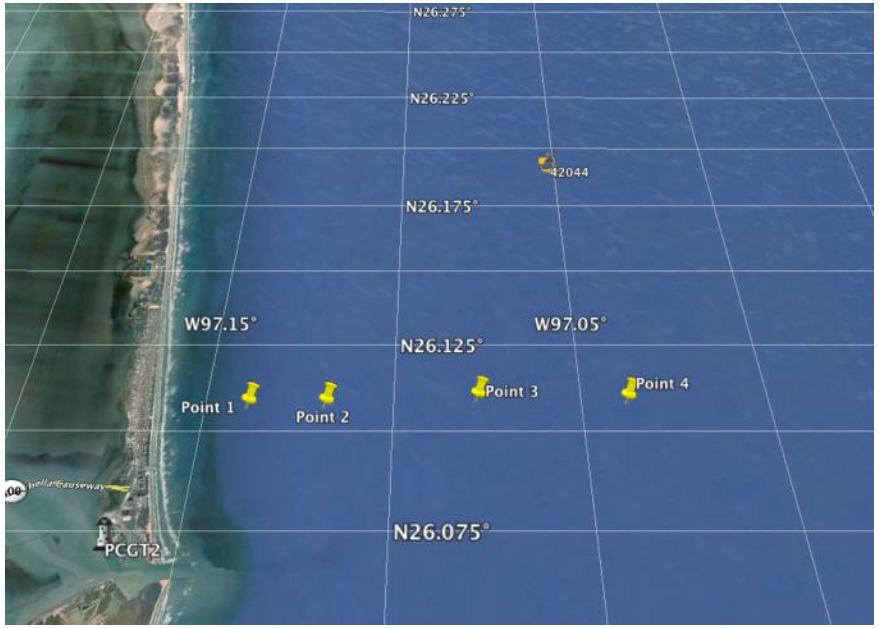

Dye patch

Evolution of a dye patch measured with hyperspectral sensor

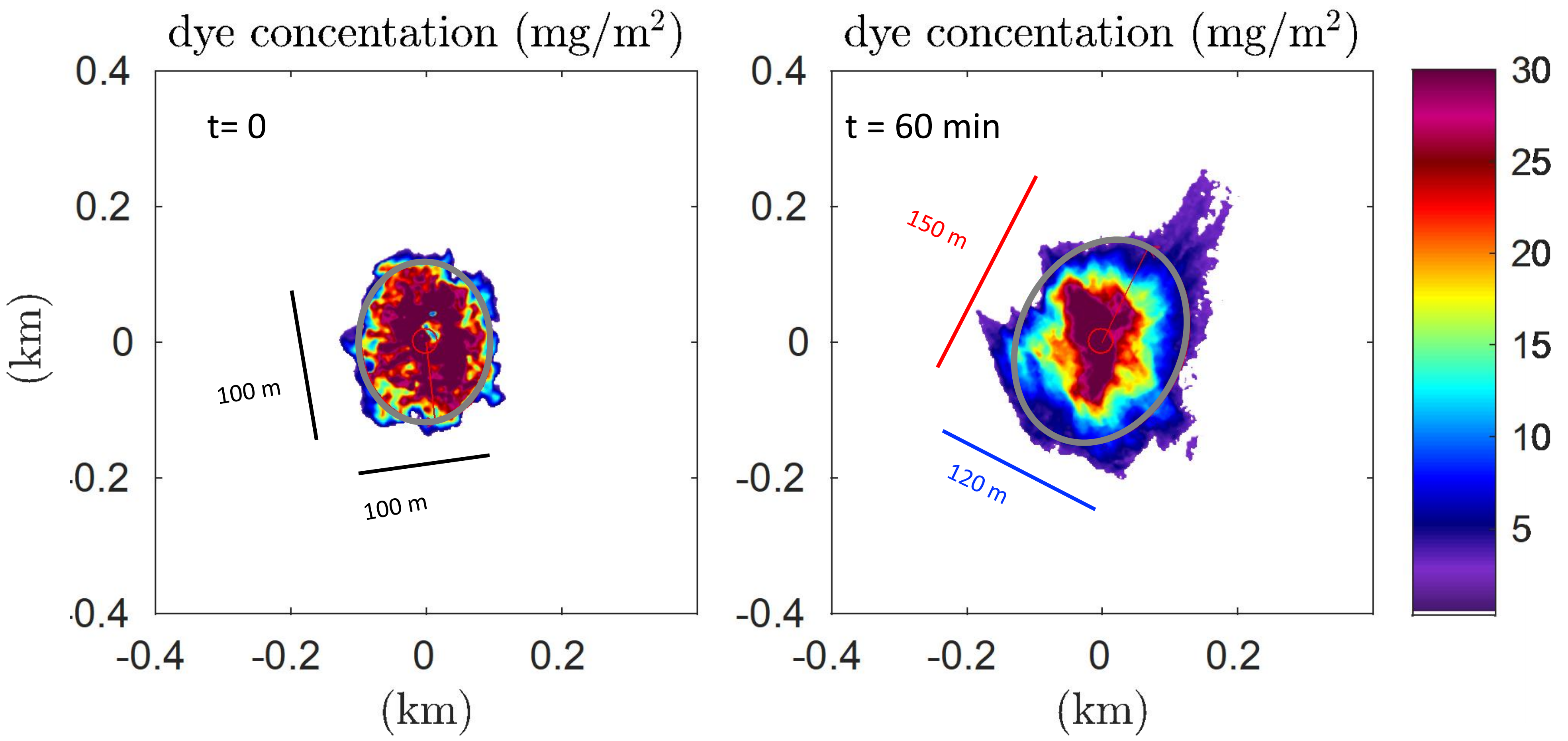

- Dye patch expands significantly over an hour period
- Dye concentration distributions allow us to calculate the horizontal dispersion through the mean-square width and the orientation of the principal component
- Dispersion is represented with principal axis ellipses

Time evolution and dispersion of a dye patch measured remotely

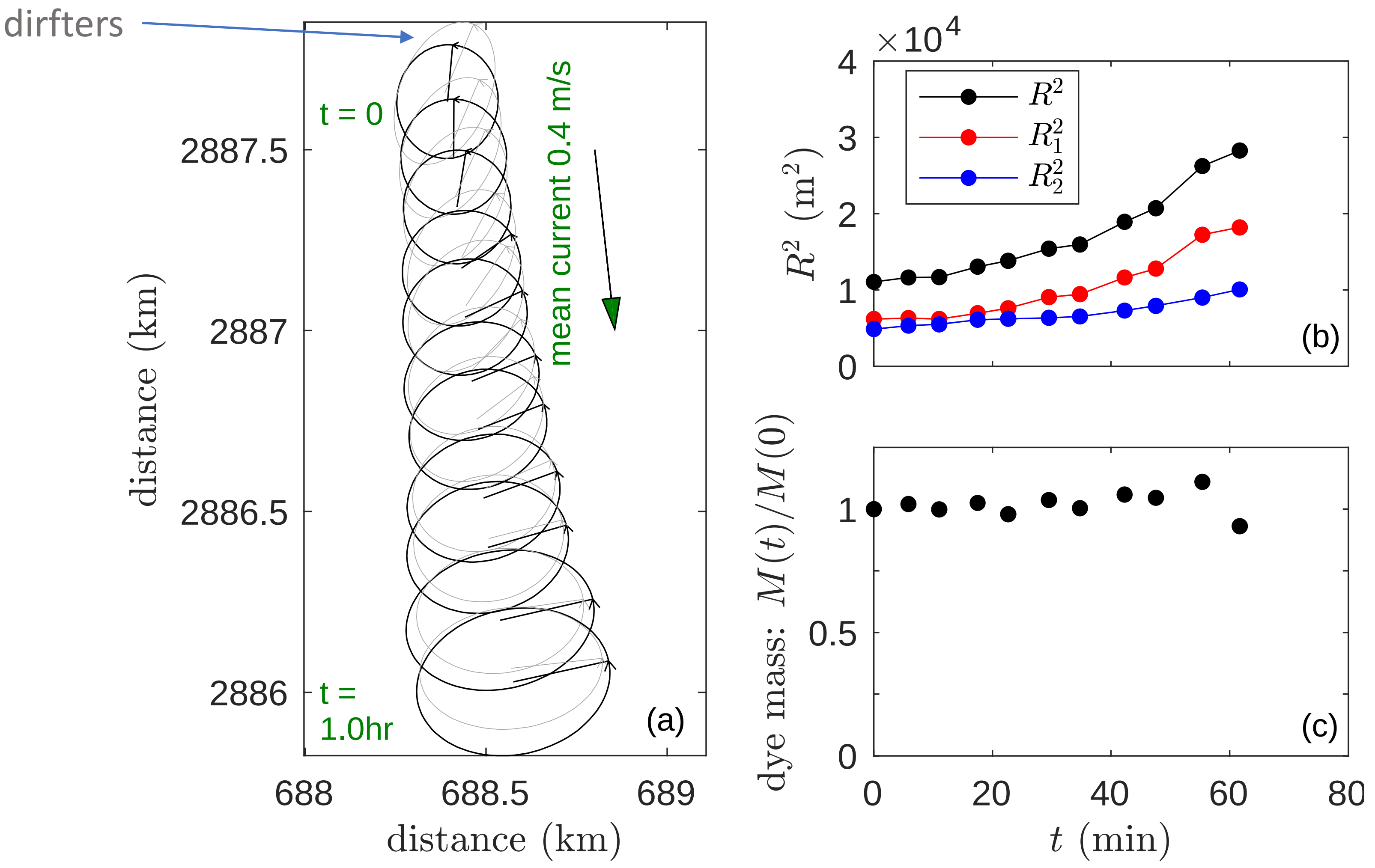

Total dispersion

principal component

Dye is approximately conserved after 50 min

- Dispersion is anisotropic

Evolution of a dye patch deployed near a freshwater front

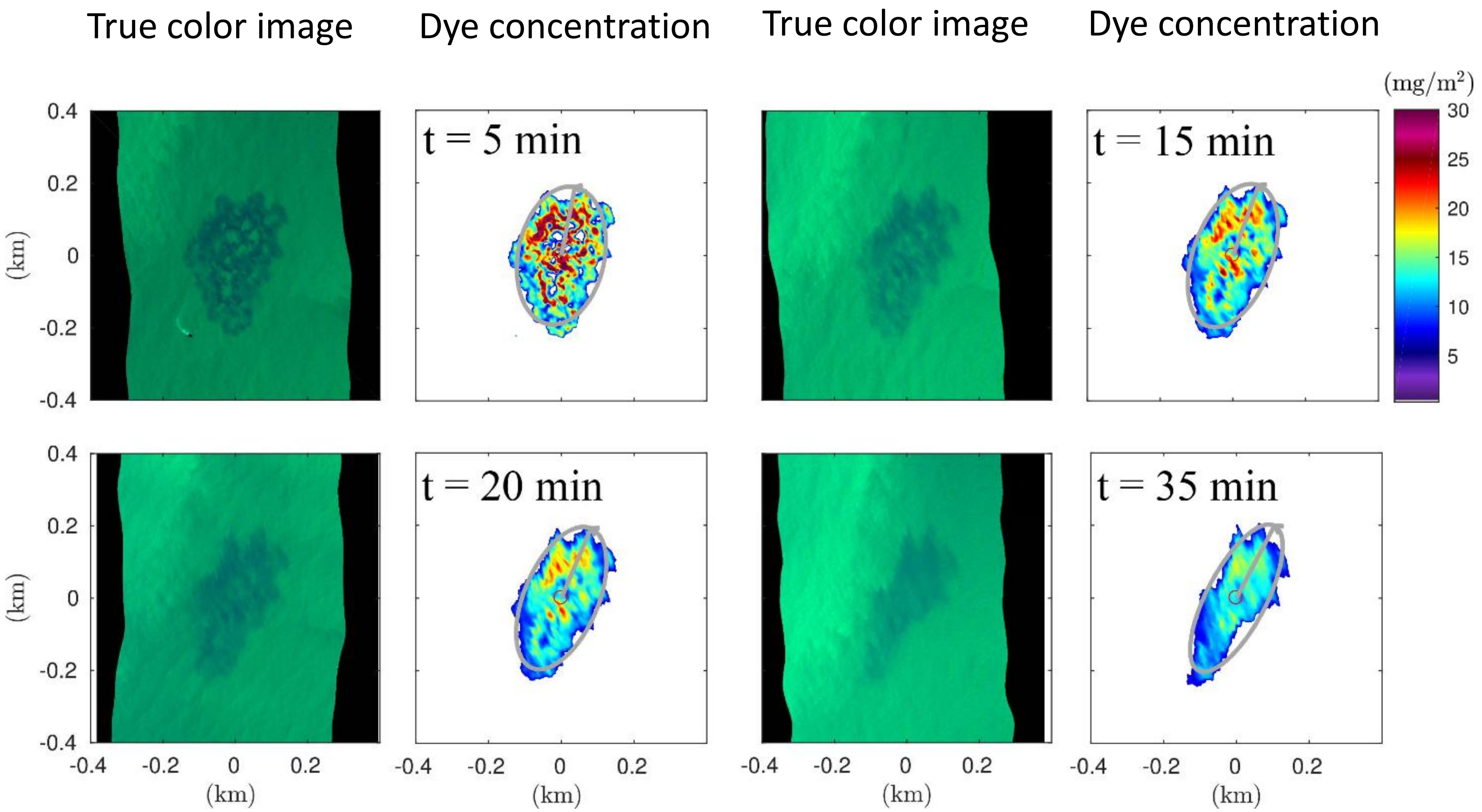

-Dye patch stretches along-front and gets narrower cross-front

-Dye concentration decreases rapidly

-Consistent with submesoscale dynamics with surface convergence and strong downwelling (e.g., Capet et al. 2008

-Remote sensing data allows us to identify different processes that play a dominant role on dispersion

Langmuir like Coherent Streaks

- Dye organizes along streaks mostly aligned the wind (black arrow)
- Downwind “Y-junctions” are typical features of Langmuir cells (Obs. and models)
- Dye spreading is anisotropic approximately along the mean wind direction

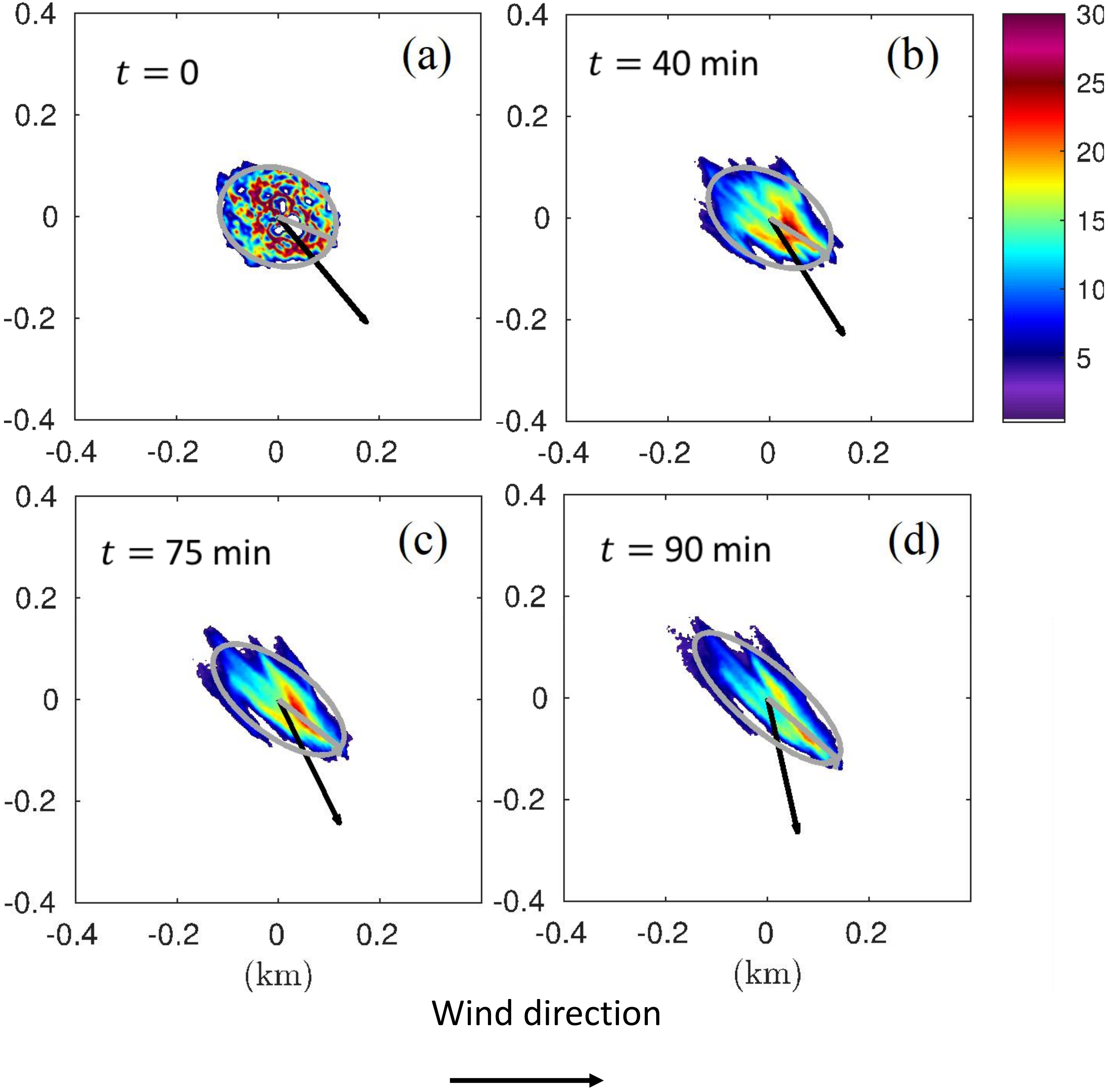

Langmuir like Coherent Streaks

- Dye organizes along streaks mostly aligned the wind (black arrow)
- Dye spreading is anisotropic, being largest approximately cross-wind
- Width of the Streaks reaches ~ 100 m, or 5 times the water depth (c.f., Super Langmuir Cells - Gargett and Wells 2007)

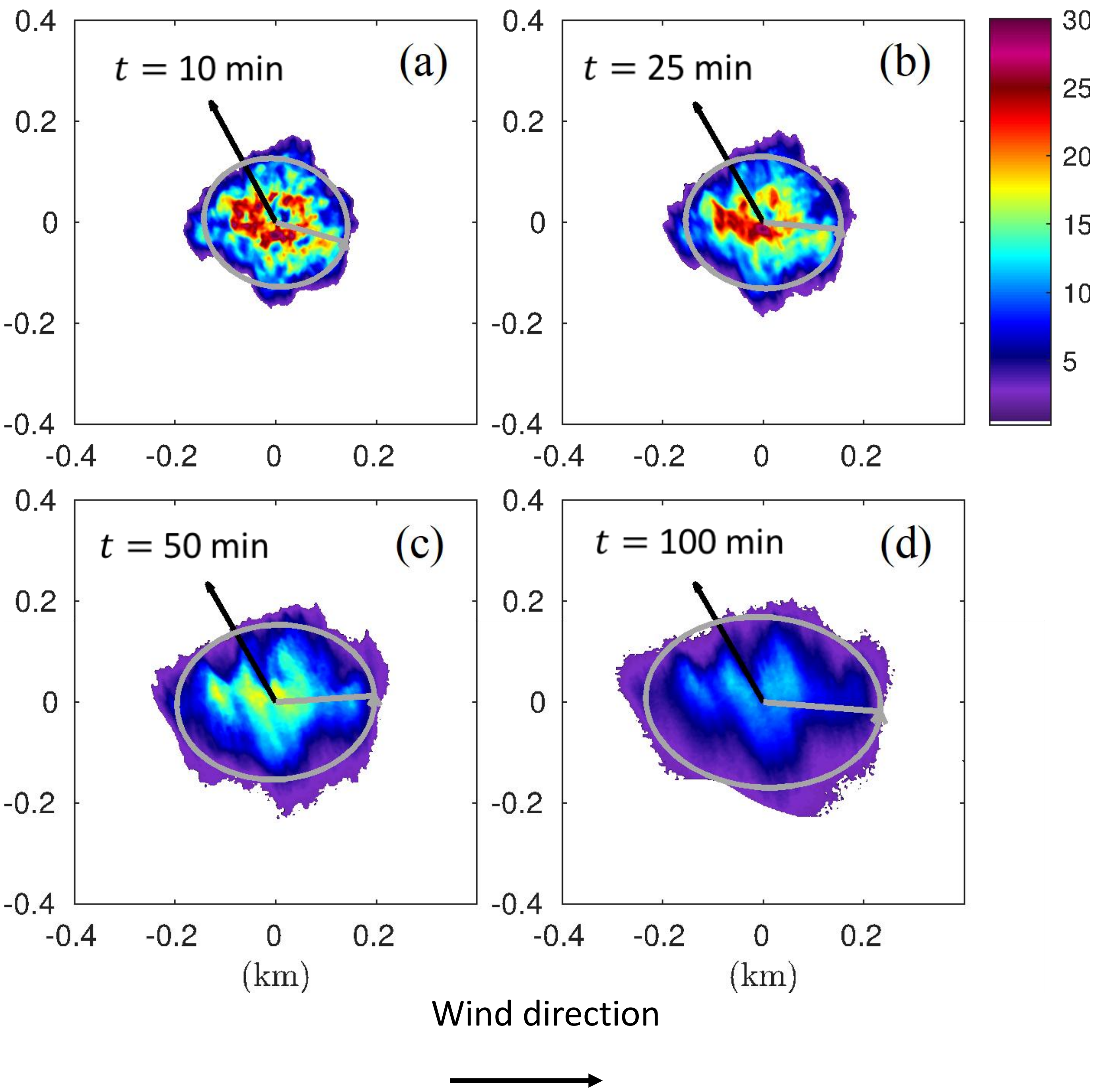

Aligned vs misaligned Winds and Waves

May 31 (p3)

$w_{dye} \sim 0$
$w_{drifter}$= n/a
MLD= 5 m
$U_{10} = 9$ m/s
$H_s = 0.9$ m
$La_t = 0.35$

June 6 (p4)

$w_{dye} \sim 0$
$w_{drifter} = 0$
MLD= 5 m
$U_{10} = 7$ m/s
$H_s = 0.6$ m
$La_t = 0.8$

Dye Patch

Directional wave energy spectra from lidar

Temperature wavenumber spectra

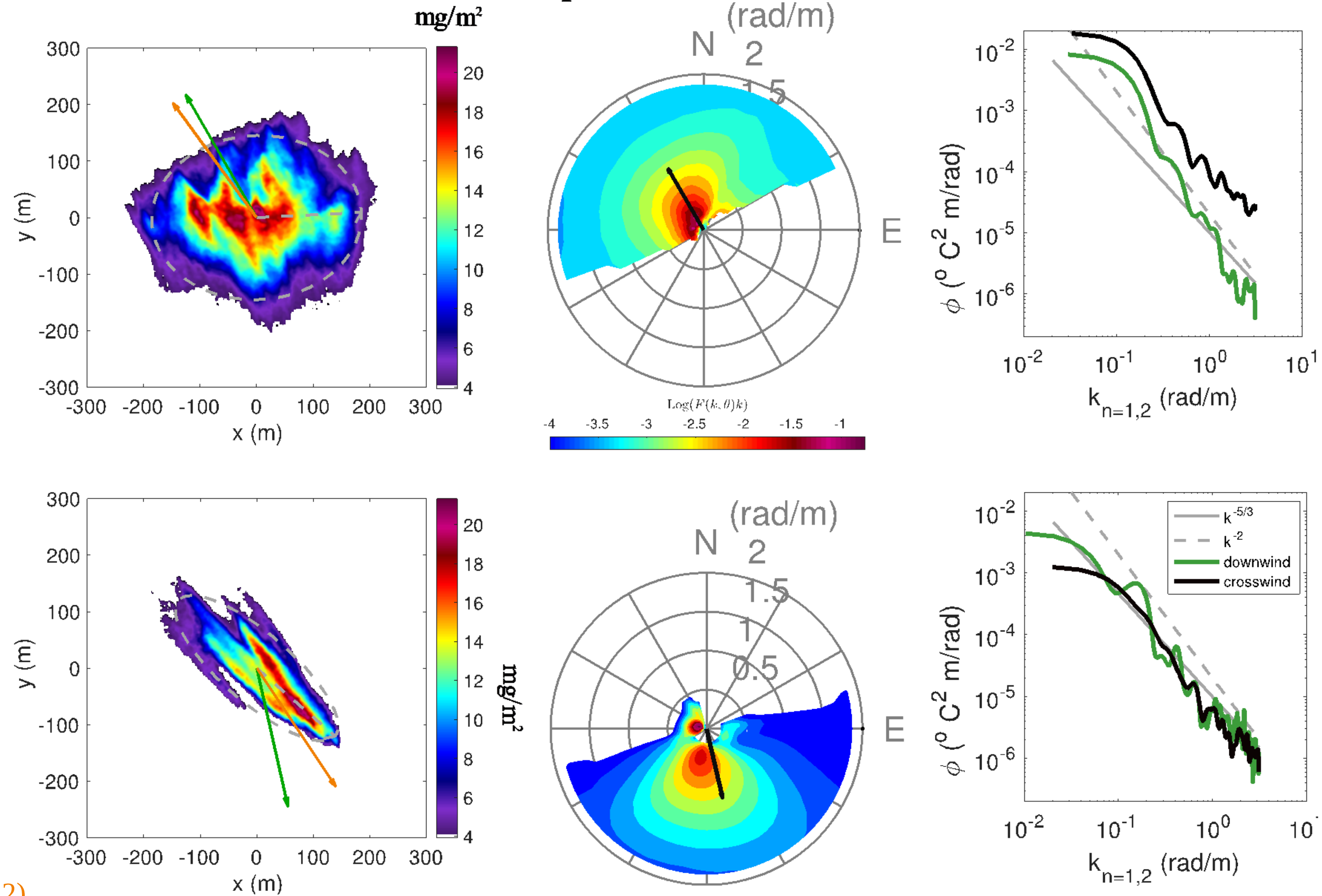

Arrows:
→ Wind direction
→ Law of the wall (Van Roekel et al. 2012)

Characterization of vertical transport

- Vertical velocities from from clusters of drifters (≥ 3)
  - Current gradients: $\boldsymbol{u}_i = \boldsymbol{U} + \boldsymbol{u}_x\, x_{rel_i} + \boldsymbol{u}_y\, y_{rel_i}$
  - Vertical velocity from continuity: $w = \int_0^{z_d} \frac{du}{dx} + \frac{dv}{dy}\, dz$
- Vertical velocities from conservation of dye mass (M)
  - $\frac{dM}{dt} = w\,\bar{C} dA \approx \frac{wM}{z_d} \quad \rightarrow \quad w \approx \frac{dM}{dt}\frac{z_d}{M}$
- Surface convergence at submesoscale fronts give values of up to 10 f and vertical velocities up to 100 m/day (much larger than that for mesoscale fronts)

Downwelling at a Freshwater Front

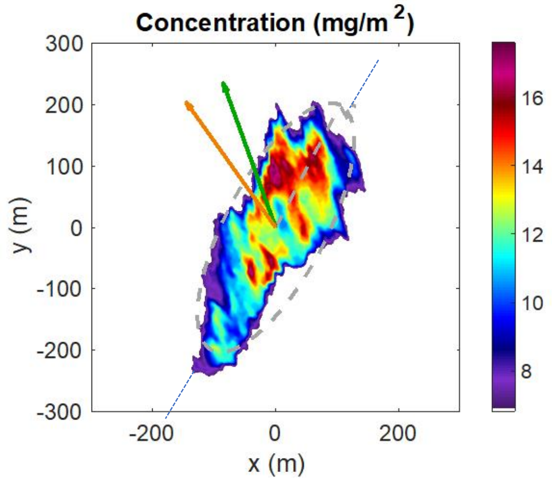

$w_{dye} =$ $-83 \pm 10\ \frac{m}{day}$

$w_{drifter} =$ $-60 \pm 14\ \frac{m}{day}$

$U_{10} = 8$ m/s

$H_s = 1.6$ m

$La_t = 0.35$

Vertical transport by Langmuir Circulation

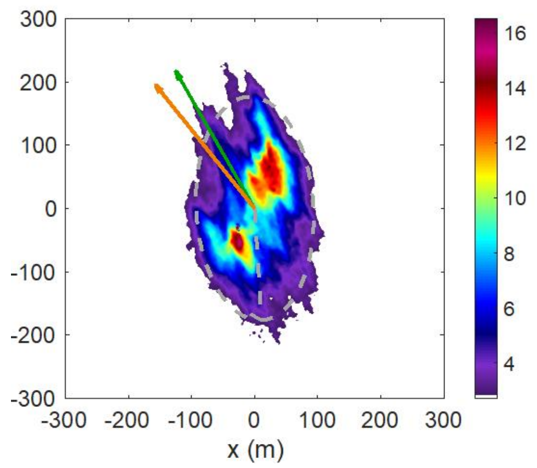

$w_{dye} =$ $-34 \pm 4\ \frac{m}{day}$

$w_{drifter} =$ $-11 \pm 6\ \frac{m}{day}$

MLD= 10 m

$U_{10} = 6$ m/s

$H_s = 0.9$ m

$La_t = 0.35$

Wave Breaking

- wind speed of 15 m/s

actively
breaking fronts

old patches
of foam

+Photo taken from an aircraft in the Gulf of Tehuantepec, Feb. 2004

Generation of Surface Wind Waves

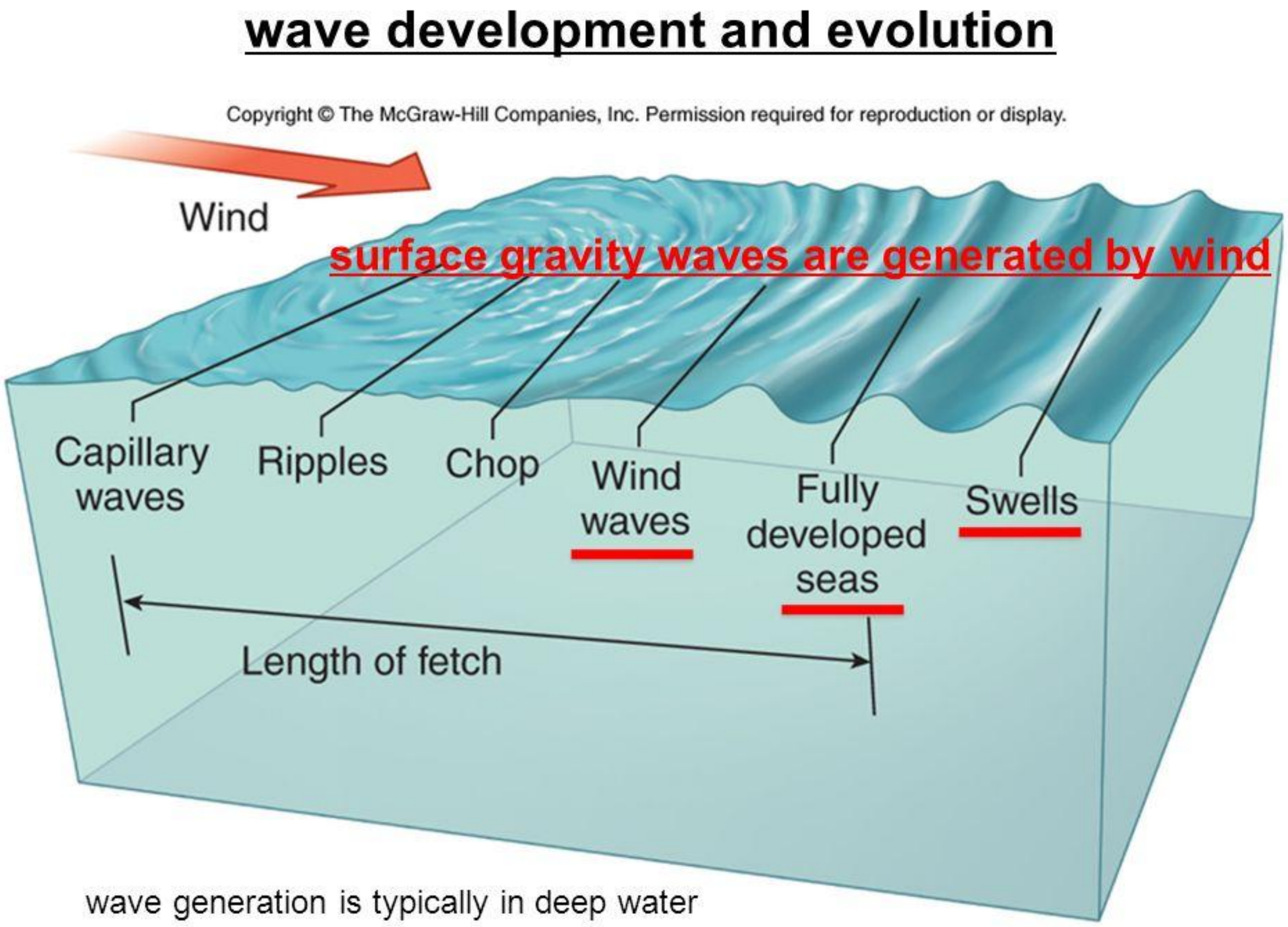

95% of the energy imparted by the wind is lost locally due to wave breaking, inducing mixing and driving currents
5% of the energy becomes swell

Wave Breaking

- wind speed of 15 m/s

old patches of foam

actively breaking fronts

+Photo taken from an aircraft in the Gulf of Tehuantepec, Feb. 2004

Whitecaps in Hurricane Conditions

Hurricane Isabel (2003) –wind speed 60 m/s

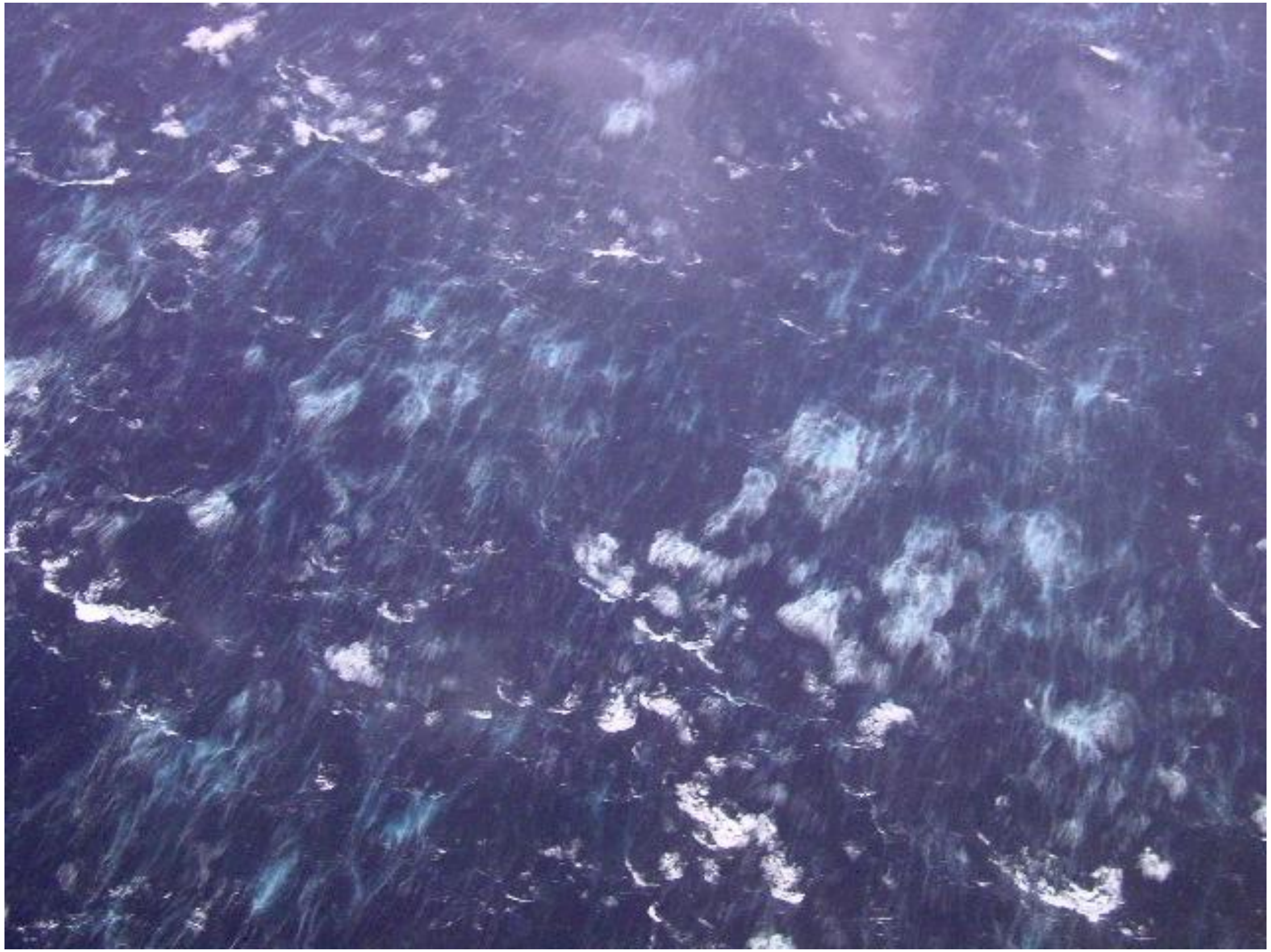

http://www.aoml.noaa.gov/hrd/Storm_pages/isabel2003/photo.html

Whitecap Coverage vs Wind Speed

- 2004 and before

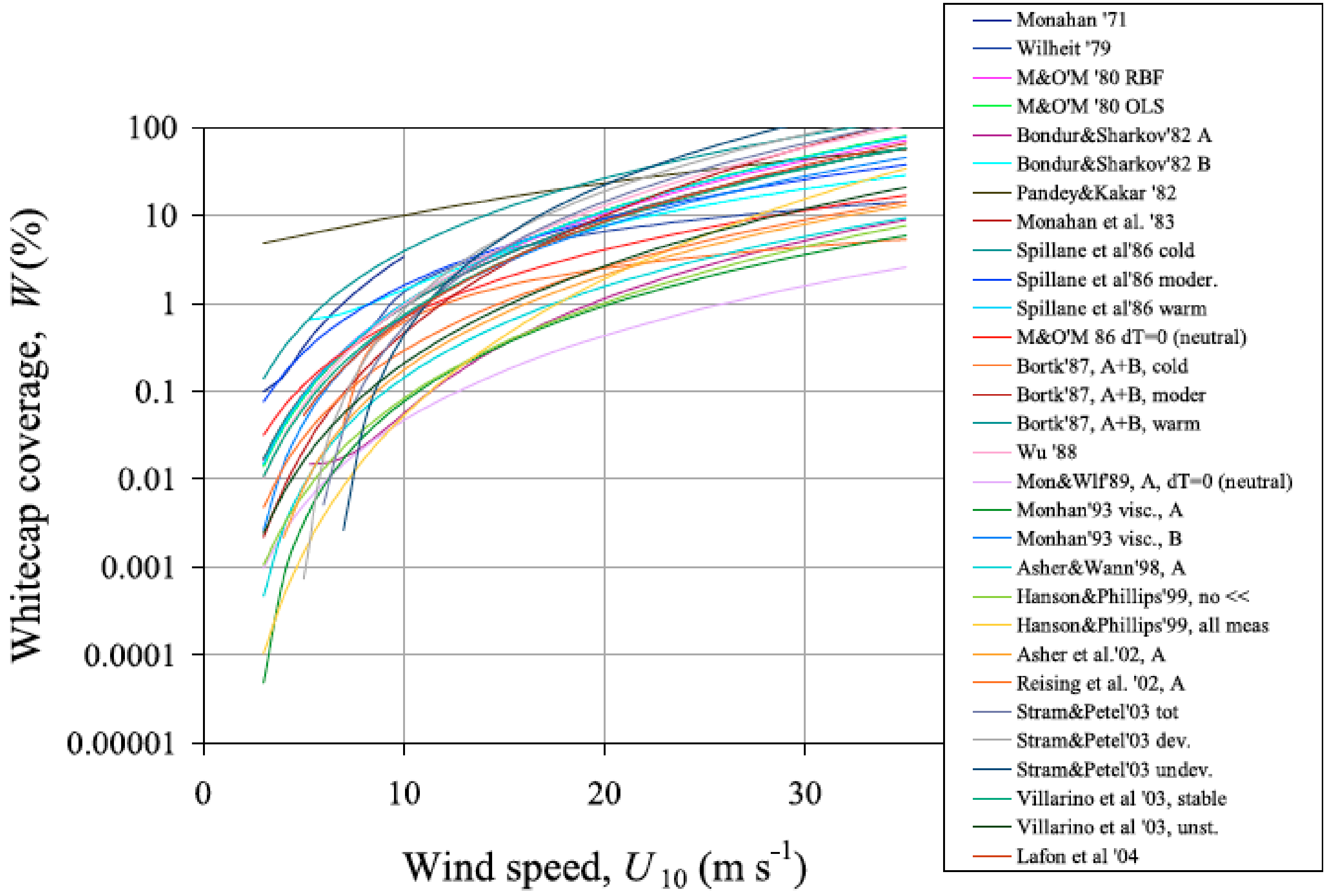

Figure 1. Various parameterizations for $W(U_{10})$ relation.

Modern Measurements: Whitecap Coverage vs Wind Speed

- Overall smaller variability
- Variability is large particularly at low winds
- Saturation or roll off at high winds

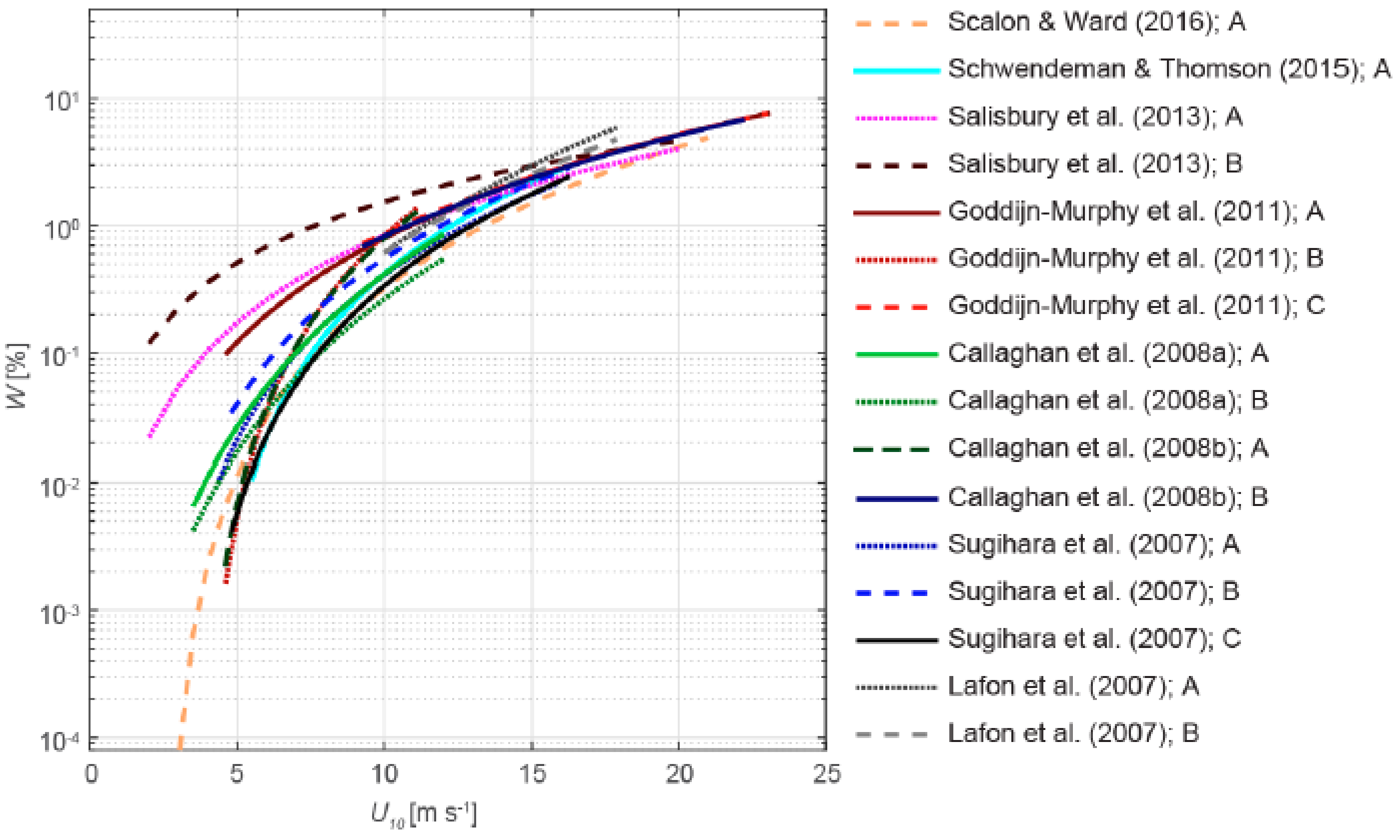

Brummer et al. 2018

Modern Measurements: Whitecap Coverage vs Wind Speed

- Variability is large particularly at low winds

- Saturation or (Roll off) at high winds

W ~ 4 %

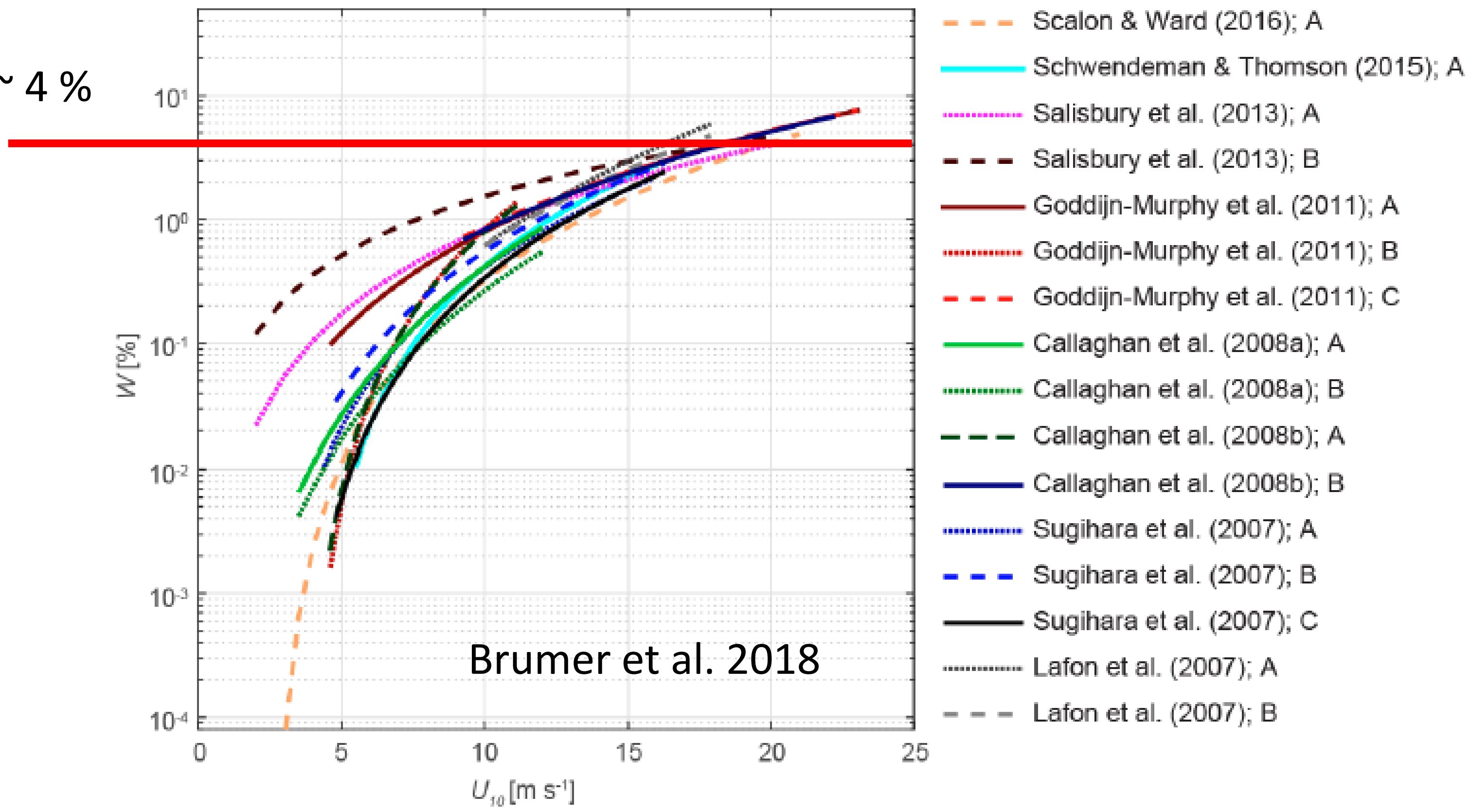

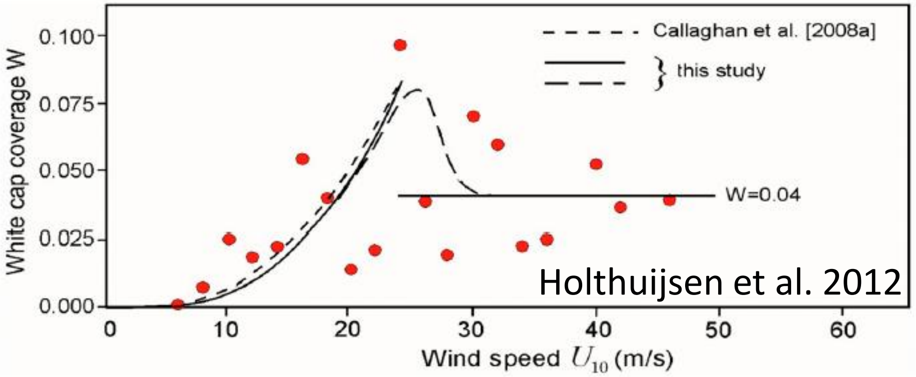

Brummer et al. 2018

Enhanced Breaking due to Wave Current Interactions

Bodega Bay, 2010 (HiRes)

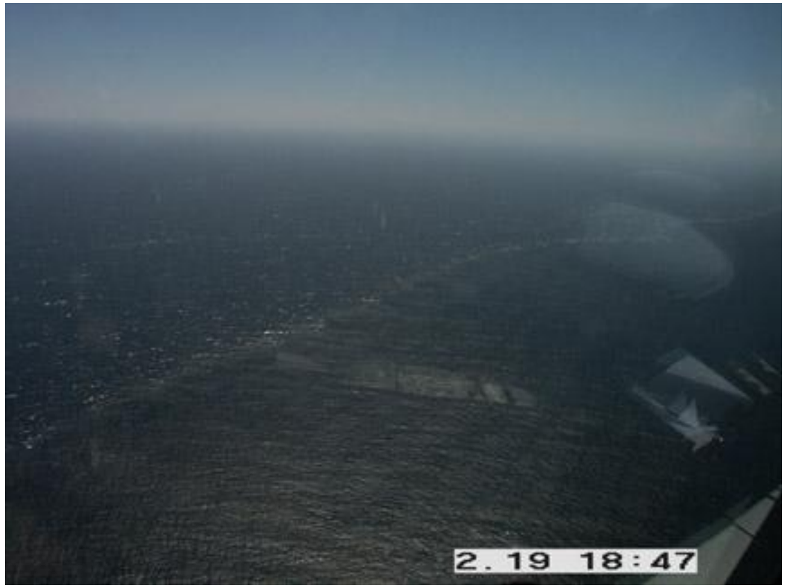

Gulf of Tehuantepec, 2004 (Melville et al. 2005)

HiRes Air-Sea Interaction Experiment
June, 2010

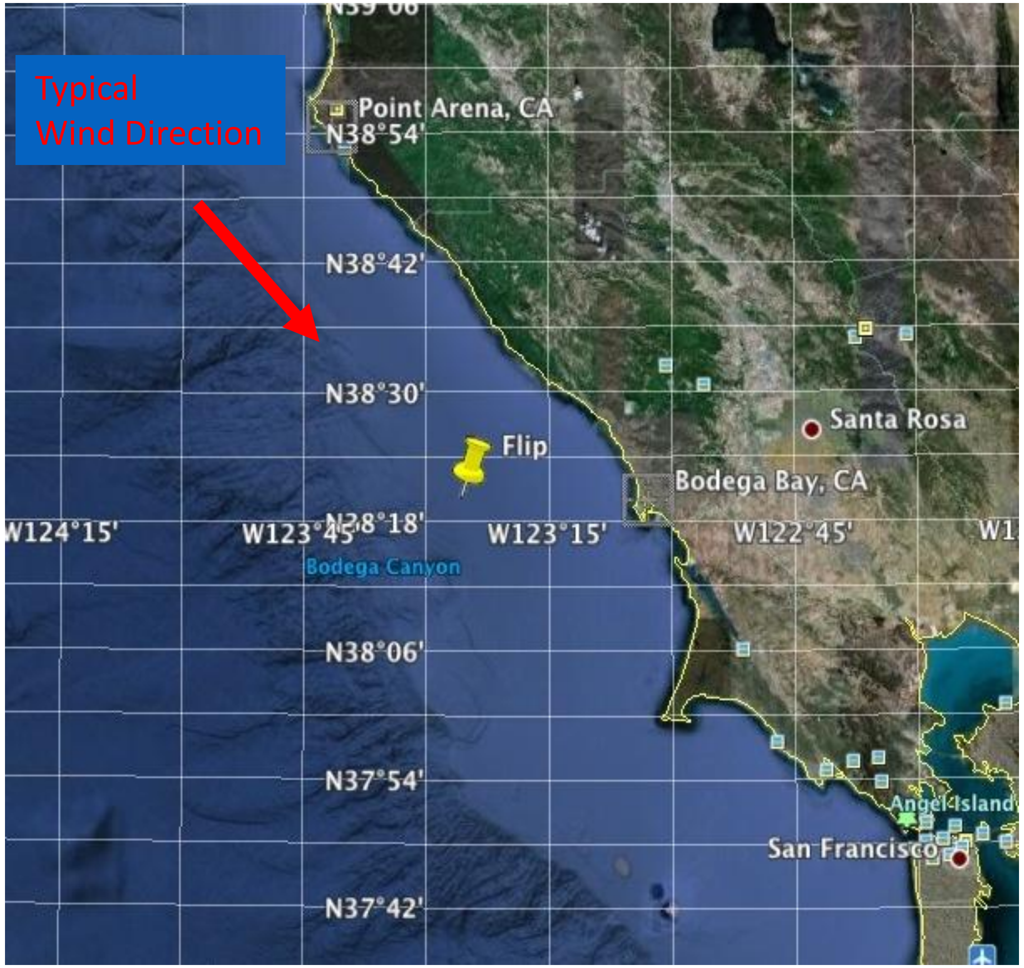

Environmental Conditions

- Wind speed : 10 – 15 m/s
- Waves: up to 4 m wave height
- Surface currents: up to 1 m/s

Platforms

- RV Flip
- **CIRPAS Twin Otter (TO) Aircraft**
- **Partenavia Aircraft**
- RV Sproul

Instrumentation

- Scanning LIDAR (NASA Airborne Topographic Mapper – ATM)
- Fixed LIDAR
- Atmospheric turbulent fluxes (wind, temperature, humidity)
- Nadir looking visible imagery
- Nadir looking Infrared imagery
- SST sensor and aerosols measurement package

CIRPAS Twin Otter

Line of Enhanced Breaking

June 17th , 2010

13 m/s winds
due SE

satellite
SST

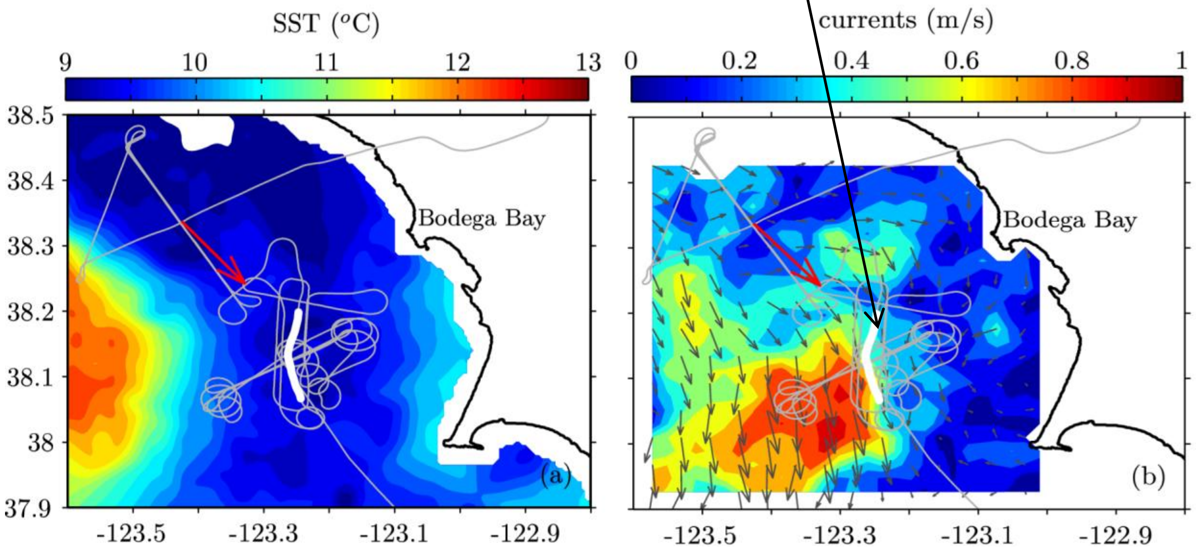

HF radar
currents

Current Induced Refraction

*Vertical Vorticity / C_g = Curvature of a ray (Kenyon, 1971;Dysthe, 2001)

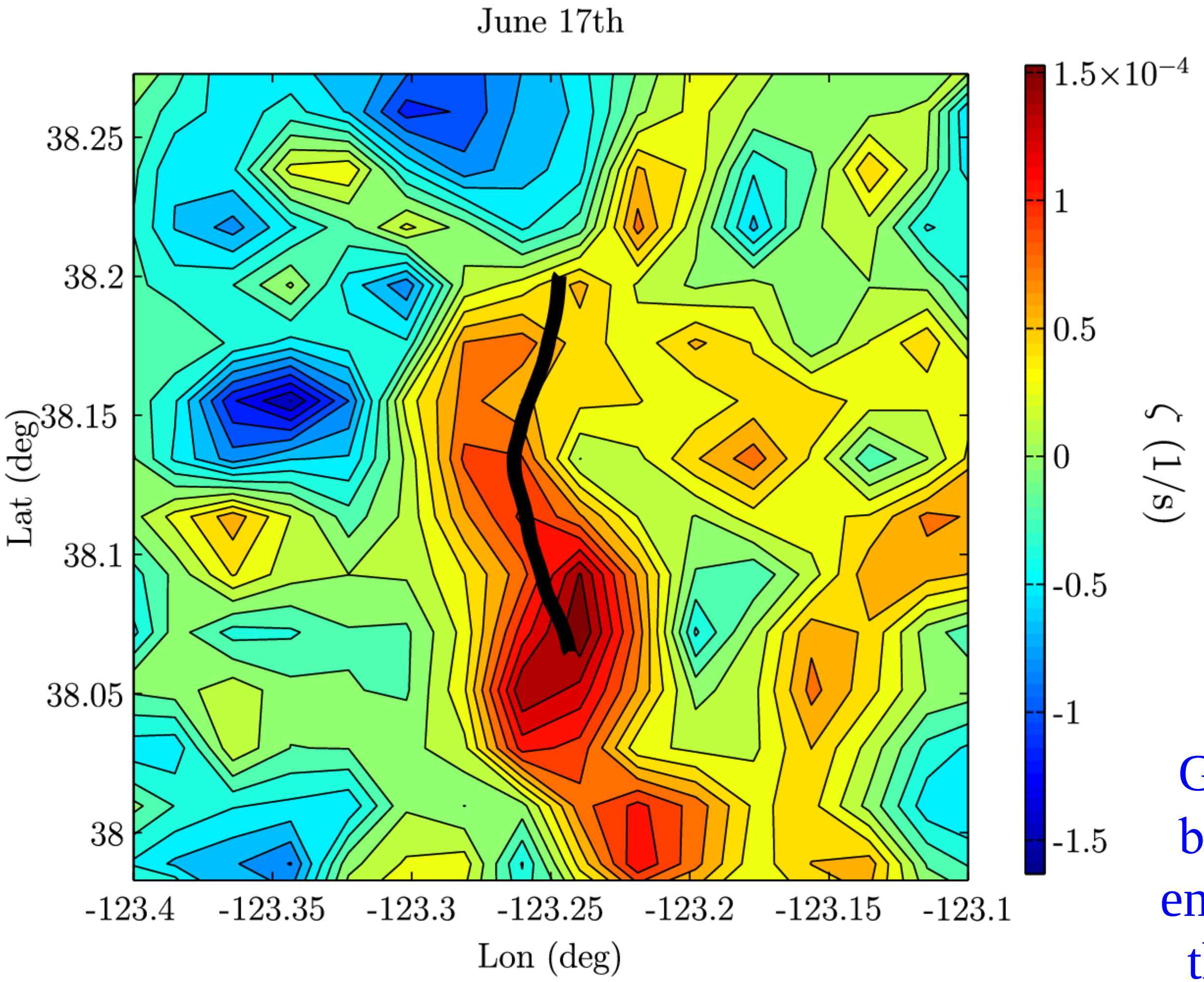

Relative Vorticity

$\zeta = v_x - u_y$

Good correspondence between the "line" of enhanced breaking and the vorticity filament

HI-RES Experiment June 2010

Cross Front Data

Sea Surface Temperature

Vertical Vorticity of the Current

Whitecap Coverage

Wind Speed at 30m above the mean sea level

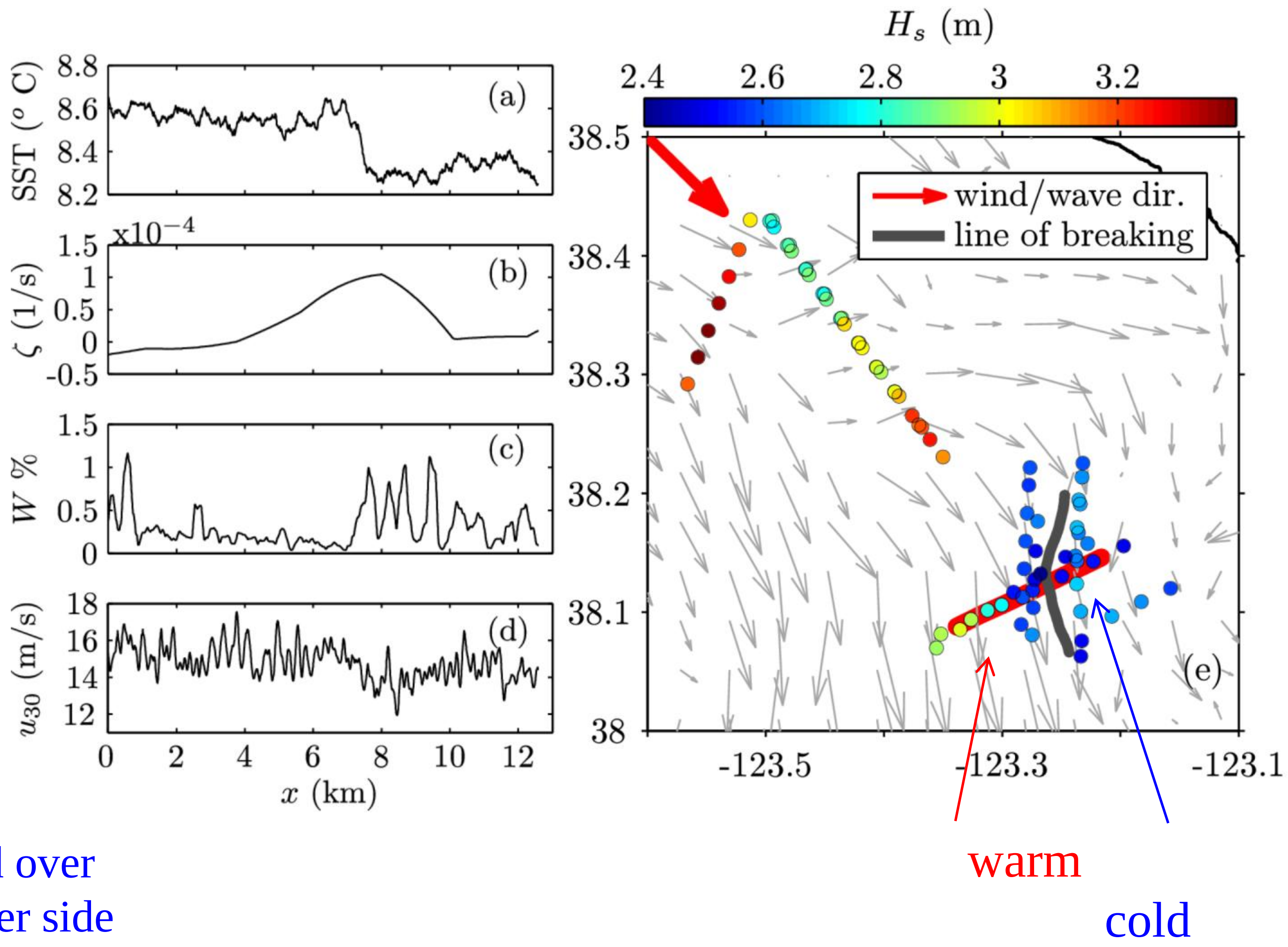

*reduced wind speed over the rougher and colder side (cf. Friehe et al. 1991)

Infrared and Visible Imagery

Sea Surface Temperature

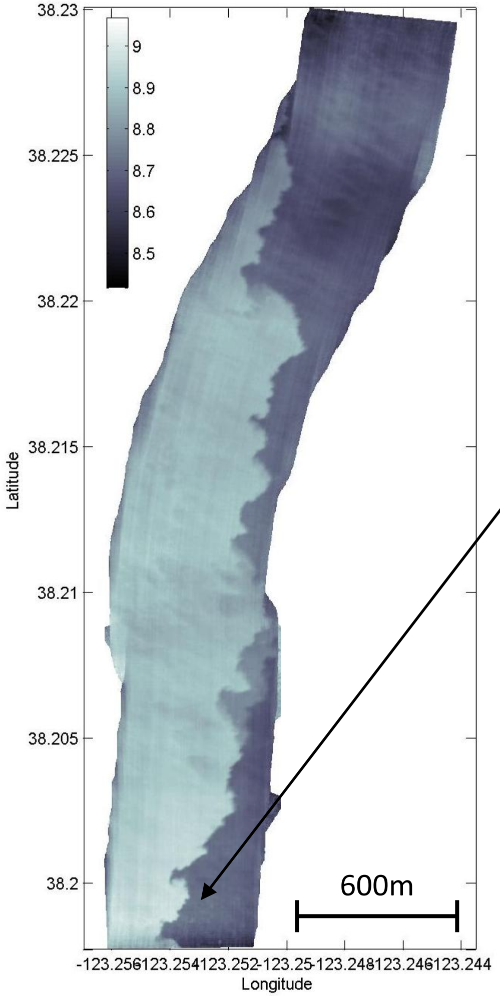

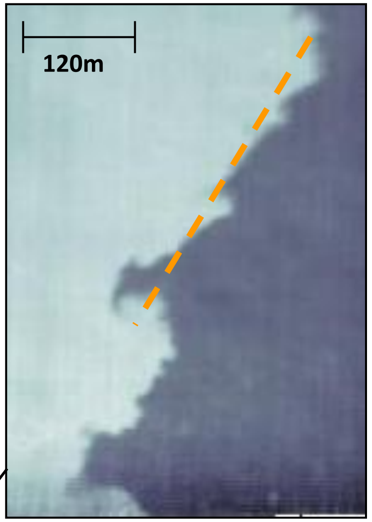

Visible video imagery

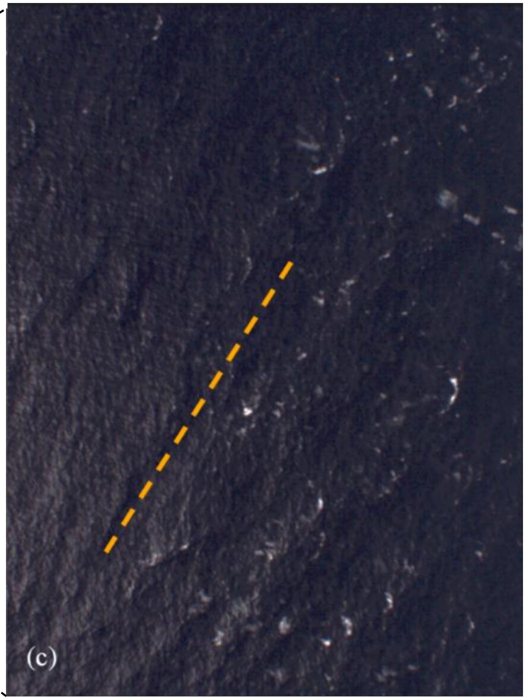

HI-RES Experiment June 2010

2x2m Spatial resolution
From Twin Otter IR Imager

Breaking Statistics across the Front

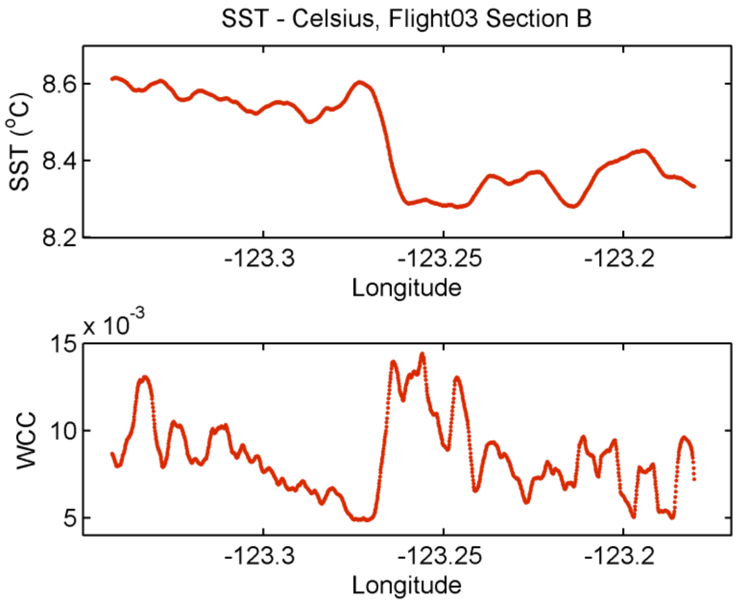

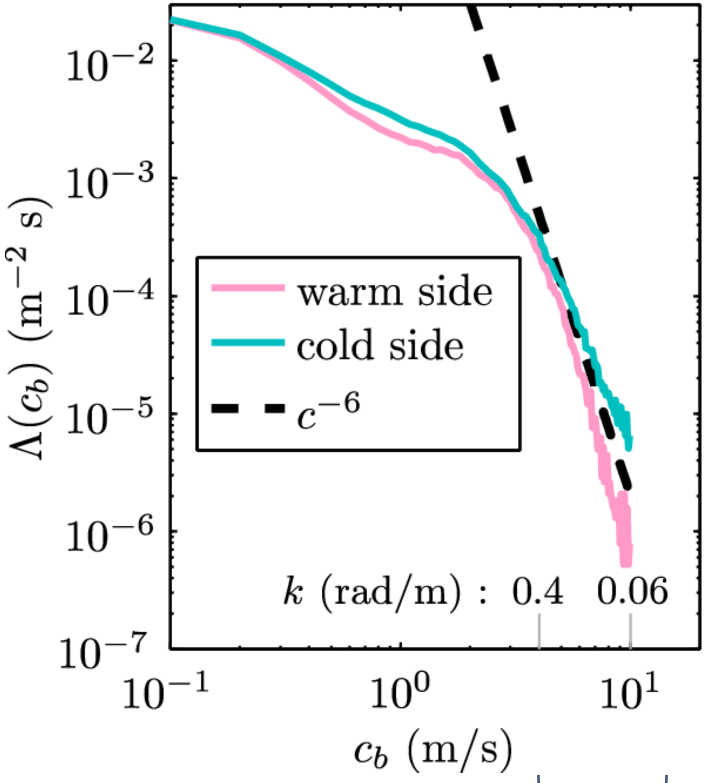

Largest variability of Lambda
c: 10 and 4 m/s

the wavenumber is calculated from the linear dispersion relationship and $c_b = \alpha\ c$, with α=0.8 (Rapp and Melville 1990)

Moments of the Spectrum

- 1d or Omnidirectional spectrum

$$\phi(k) = \int_{-\pi/2}^{\pi/2} F(k,\theta) k d\theta$$

- Saturation spectrum

$$B(k) = \phi(k) k^3$$

- Directional spreading

$$\sigma(k) = \left(\frac{\int_{-\pi/2}^{\pi/2} F(k,\theta)\theta'^2 d\theta'}{\int_{-\pi/2}^{\pi/2} F(k,\theta) d\theta} \right)^{1/2}$$

- Normalized Saturation

$$\tilde{B}(k) = B/\sigma$$

Both measures of the saturation are important parameters for the characterization of wave breaking (Banner et al. 2002)

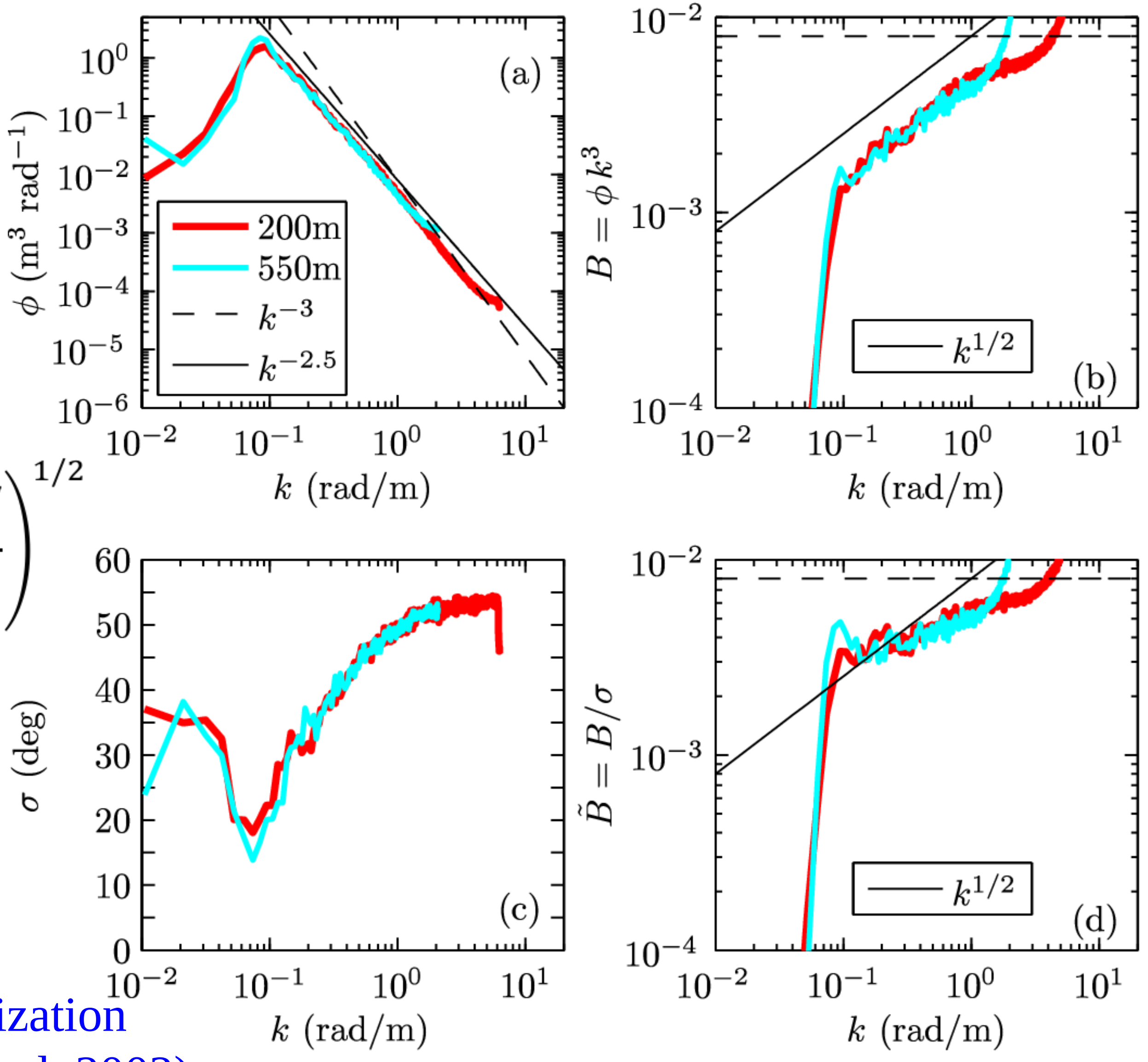

Normalized Saturation vs Whitecap Coverage

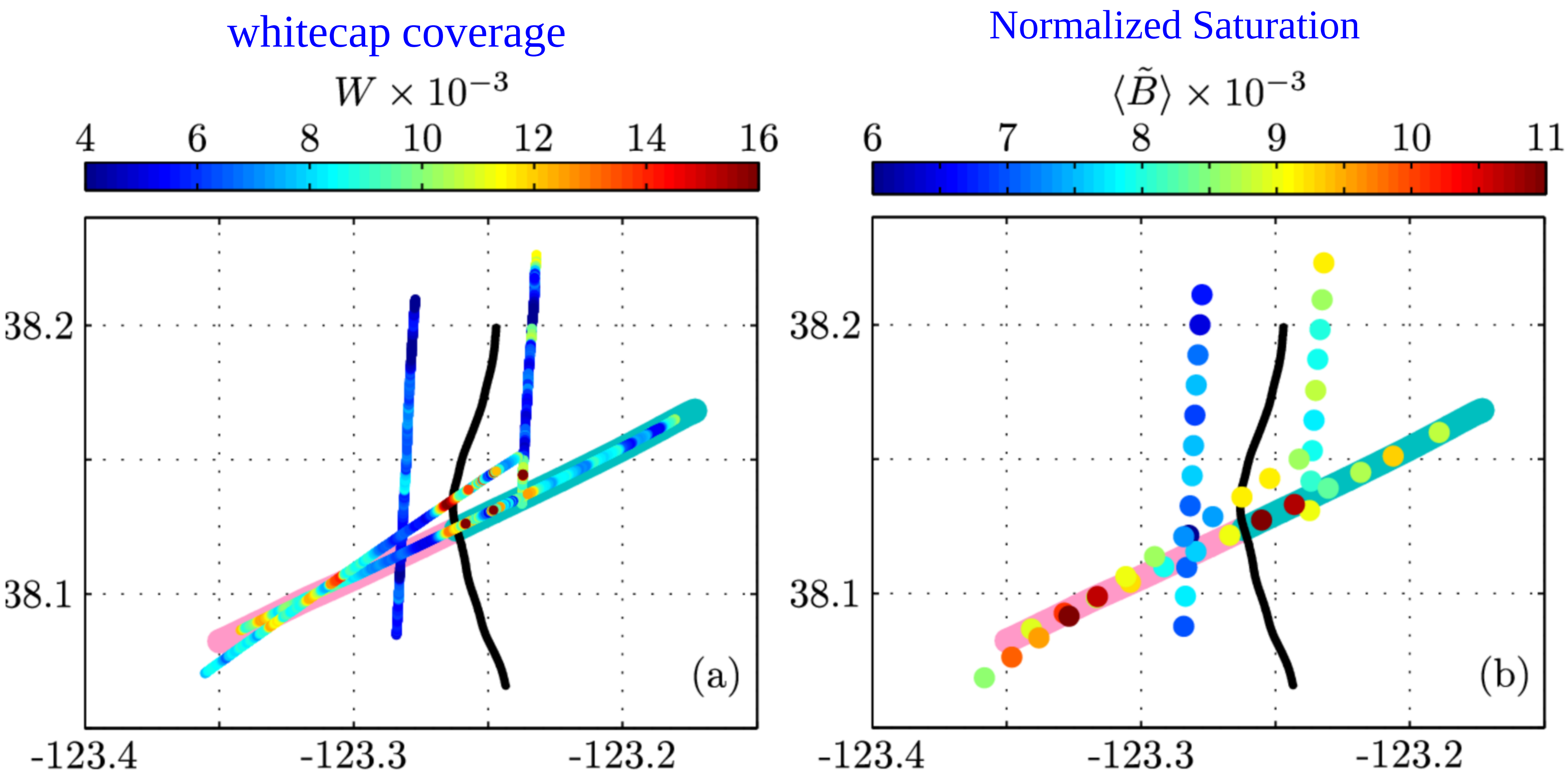

There is good correspondence between both variables (r = 0.76)

Ray Tracing

* Following: Gerber 1993; Dysthe 2001

Vertical Vorticity: $\zeta = v_x - u_y$

+

$-\zeta / c_g$ = Curvature of a ray (Kenyon, 1971;Dysthe, 2001)

Dominant waves : wavelength =110 m   Shorter waves: wavelength = 15m

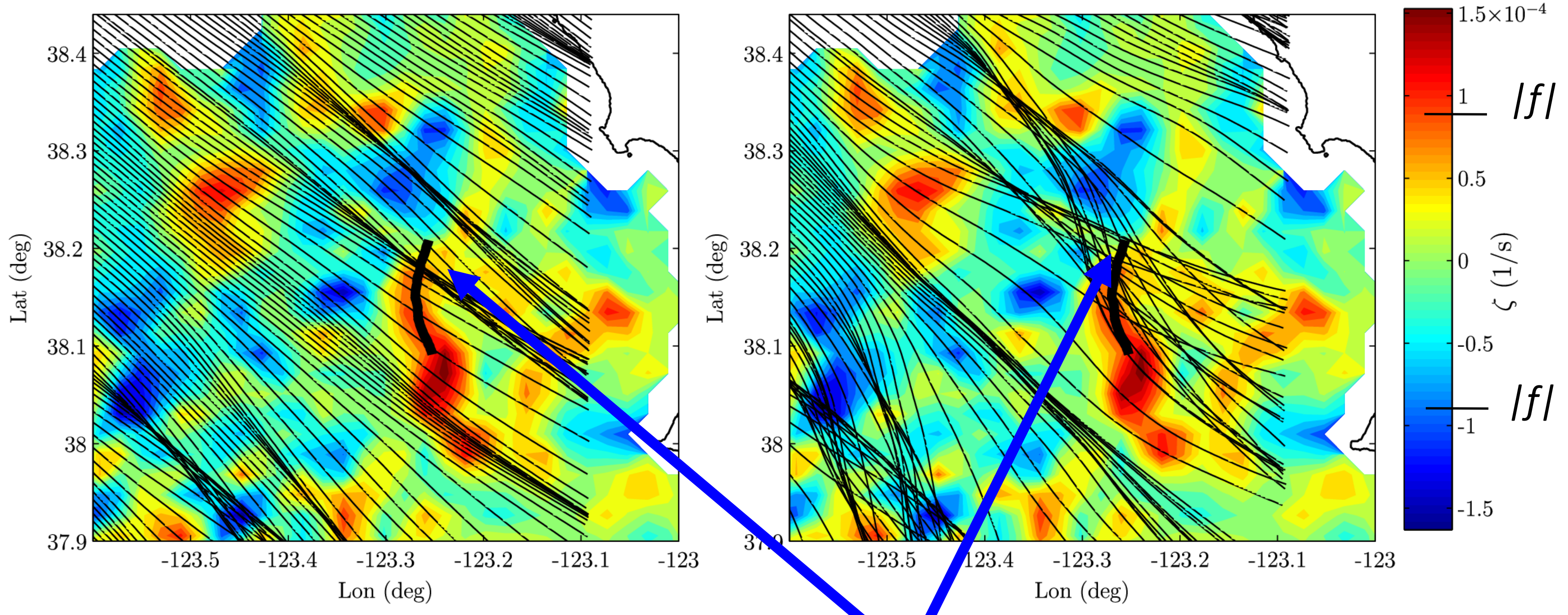

Line of enhanced breaking

Conclusions

- Novel airborne observations over areas with significant wave-current interactions
- Tight coupling between the surface winds, waves and currents at horizontal scales of 1 km.
- Wave height varied by about 25% due to wave-current interactions, whereas whitecap coverage varied substantially by an order of magnitude
- Whitecap coverage correlated with spectral moments, particularly with the normalized saturation

Numerical Modeling of Wave-Current interactions in the Presence of Submesoscale Ocean Features

Goal:

Better understand the interaction between surface waves and submesoscale currents, including feedbacks

Modeling Framework

- Spectral wave model WaveWatchIII (ww3) coupled offline to
  - Regional Ocean Modeling System (ROMS)
  - Weather Research and Forecasting Model (WRF)
- Nested grid from a 300 m grid down to 100 m
- Spectral grid
  - 24 azimuthal points (15^{o} resolution)
  - 18 Frequencies with periods between 5 s and 27 s (most energetic)
- Both ROMS and WRF are forced with realistic forcing (without data assimilation, except at the boundaries of the largest domain)
- WW3 uses buoy observations for boundary conditions.

Wave Model included Current Effects on Waves (CEW)

- Wave Action Conservation Equation: $\frac{\partial N}{\partial t} + (\vec{c}_g + \vec{U}) \cdot \nabla N - \nabla \Omega \cdot \frac{\partial N}{\partial \vec{k}} = S$

  advection refraction

  $N(\vec{k}) = \frac{F(\vec{k})}{\sigma(k)}$: the wave action

  $F(\vec{k})$: directional wavenumber spectrum

  $\sigma(\vec{k}) = \sqrt{g\, k \tanh kh}$: intrinsic frequency,

  $\Omega(\vec{k}) = \sigma(k) + \vec{U} \cdot \vec{k}$: Doppler-shifted frequency,

  $\vec{U}$: ocean surface current (i.e., upper most current vector from ROMS)

  S : source terms (wind forcing, wave-wave interactions, **dissipation**, ...)

- Directional frequency spectrum: $F(\omega, \theta) = \frac{\partial k}{\partial \omega} F(k, \theta) k$
- $\langle \eta^2 \rangle = \int \int F(\omega, \theta) d\theta d\omega = \int \int F(k, \theta) k d\theta dk$

Source Terms

S_{in}: **wind input (Janssen 1989, 1991, Ardhuin et al. 2010)**

S_{nl} : **nonlinear fluxes due to resonant wave-wave interactions (Webb-Resio-Tracy or DIA)**
DIA: direct interaction approximation Hasselmann et al. 1985

S_{ds} : **dissipation, primarily due to wave breaking**
(new parameterization based on Romero and Melville 2011, Romero et al. 2012)

Romero and Melville 2011: Statistics of wave steepness is consistent with weakly non-Gaussian statistics

Romero et al. 2010: Parameterization of strength of wave breaking as a function of the spectral saturation based on field observations and modeling

New model extends the analytical results of Romero and Melville 2011 at the spectral peak over the entire spectrum, assuming self similarity.

Model was tuned and validated against available observations

**Numerical Framework: WAVEWATCH III

Spectral Statistics of Breaking Fronts: $\Lambda(c)$

- Following Phillips 1985
  - L= $\int \Lambda(c)\, dc$:Length of breaking crests per unit surface area
  - Moments of
    - Breaking probability ~ $\int \Lambda(c) c\, dc$
    - Whitecap coverage ~ $\int \Lambda(c) c^2\, dc$
    - Gas transfer velocity ~ $\int \mathrm{b(c)} \Lambda(c) c^3\, dc$
    - Momentum flux ~ $\int \mathrm{b(c)} \Lambda(c) c^4\, dc$
    - Energy dissipation ~ $\int \mathrm{b(c)} \Lambda(c) c^5\, dc$
- $\Lambda(c) \sim c^6$ within the equilibrium range above the spectral peak ($S_{in} \sim S_{nl} \sim S_{ds}$)
- Strength of wave breaking: $\mathrm{b}(\mathrm{c}, B) = A\left((B)^{\frac{1}{2}} - (B_T)^{\frac{1}{2}}\right)^{\frac{5}{2}}$ (Romero et al 2012; Drazen et al. 2008)
- $\Lambda(k) \sim \exp(-\frac{1}{2}\left(\frac{BT}{B(k)}\right)^2)$, $\Lambda(k,\theta)(-\frac{2g^2}{c^6}) = \Lambda(c,\theta)$, *BT* is a constant.

Infrared Measurements of $\Lambda(c)$

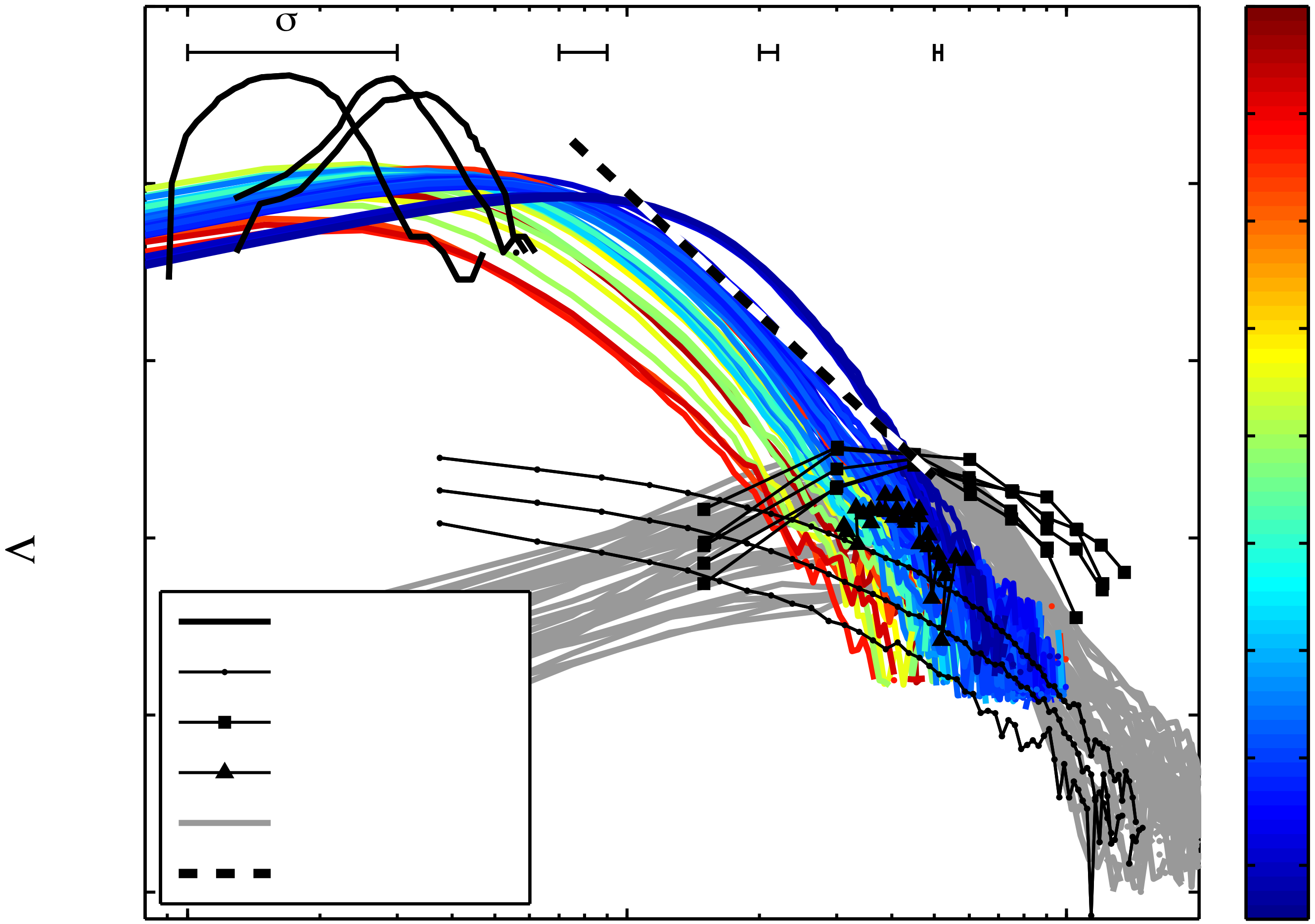

Sutherland and Melville 2013

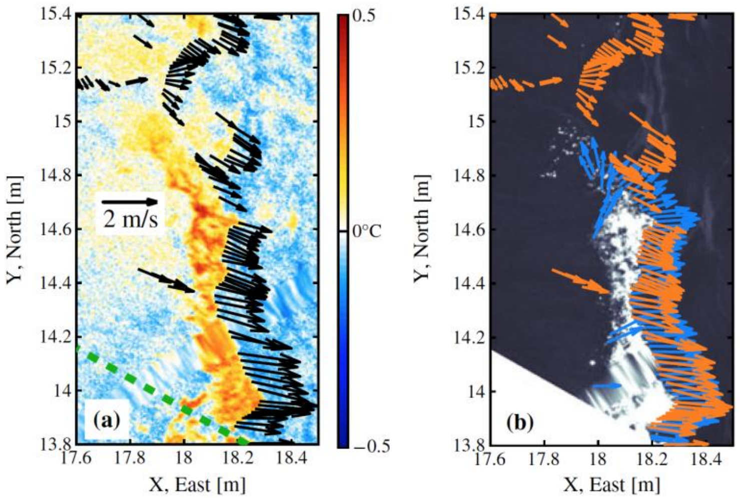

The new model parameterizes $\Lambda(c)$ as a function of the spectral saturation with a few tuning parameters

Distribution of Breaking Fronts: $\Lambda(c)$

Sutherland and Melville 2013

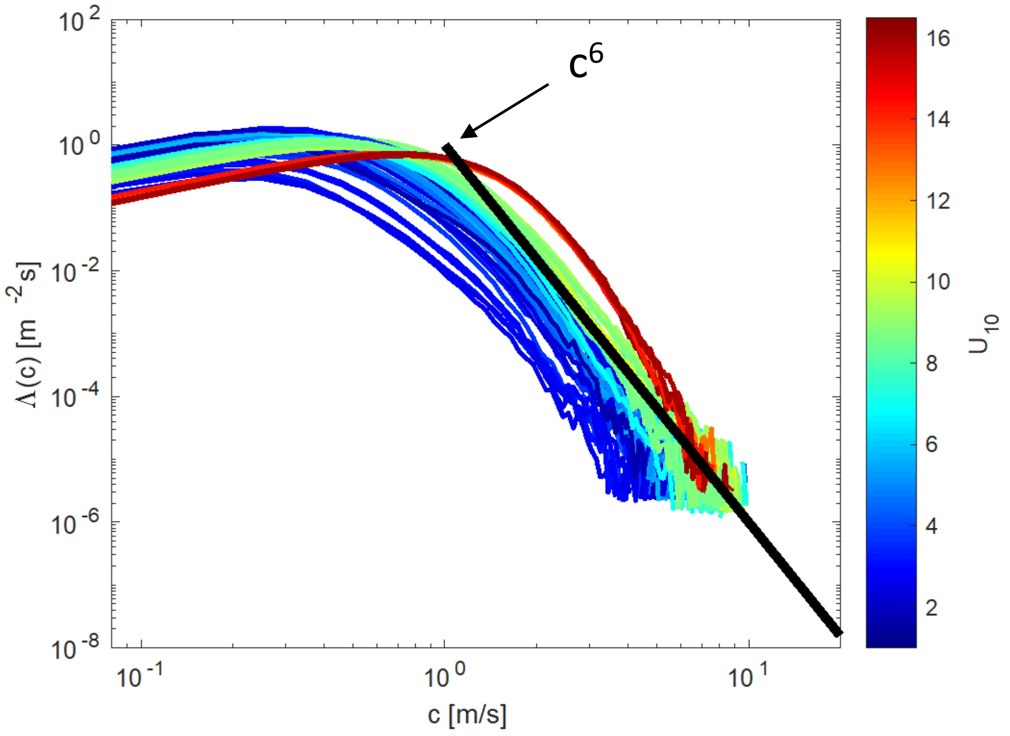

Model Simulations over a similar range of wind speeds (not 1:1)

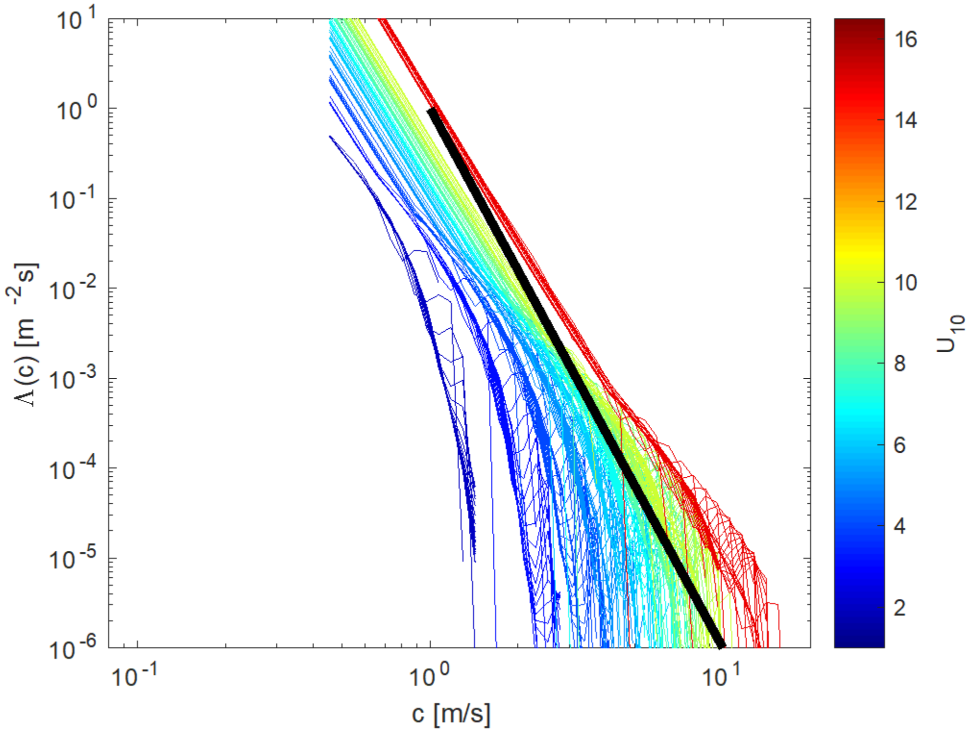

c^6 is consistent with Phillips 1985

Distribution of Breaking Fronts: $\Lambda(c)$

Sutherland and Melville 2013

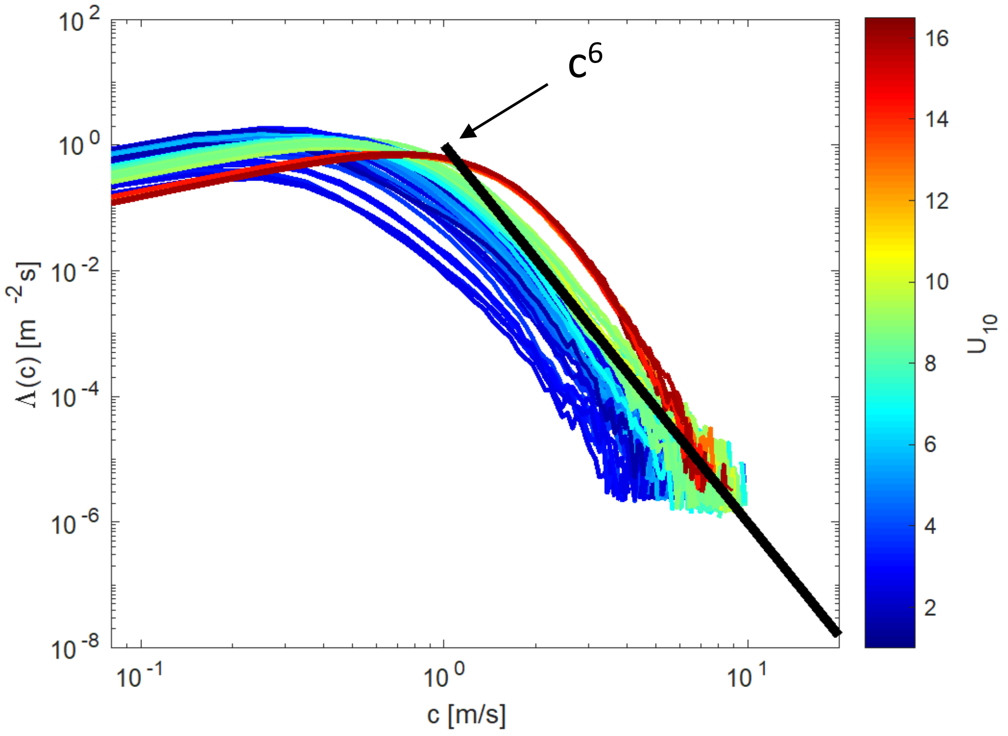

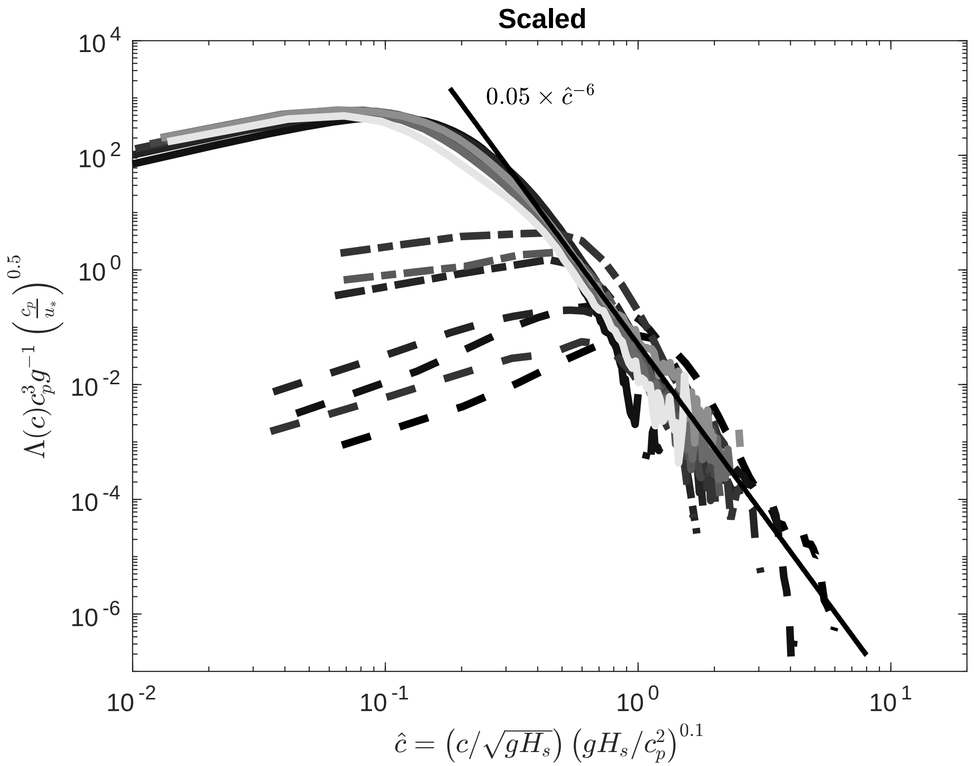

$$\hat{\Lambda}(c) = \Lambda(c) c_p^3 g^{-1} \left(\frac{c_p}{u_*}\right)^{0.5}$$

$$\hat{c} = \left(c/\sqrt{gH_s}\right)\left(gH_s/c_p^2\right)^{0.1}$$

Distribution of Breaking Fronts: $\Lambda(c)$

Sutherland and Melville 2013

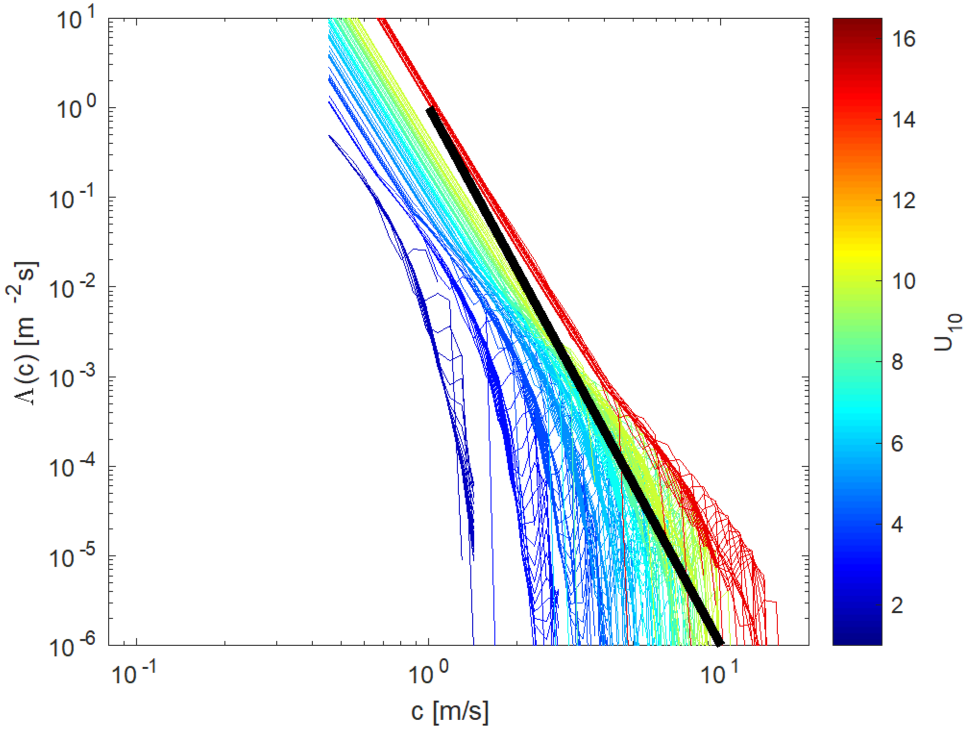

Scaled

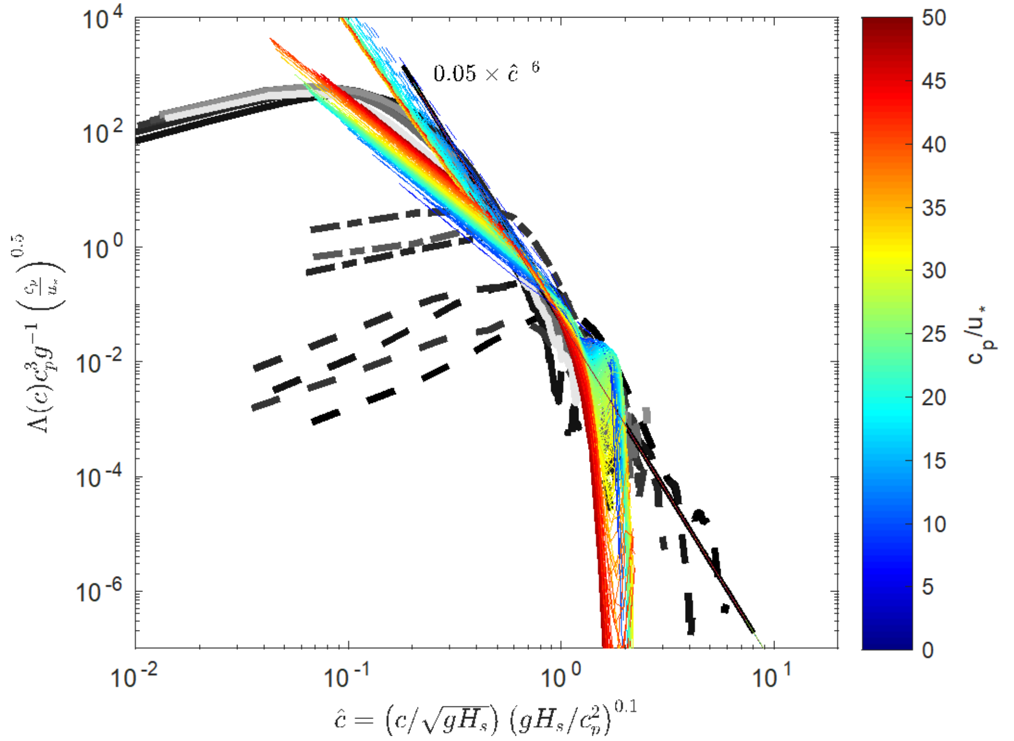

$$\hat{\Lambda}(c) = \Lambda(c)c_p^3 g^{-1}\left(\frac{c_p}{u_*}\right)^{0.5}$$

$$\hat{c} = \left(c/\sqrt{gH_s}\right)\left(gH_s/c_p^2\right)^{0.1}$$

Model performance

Sig. wave height

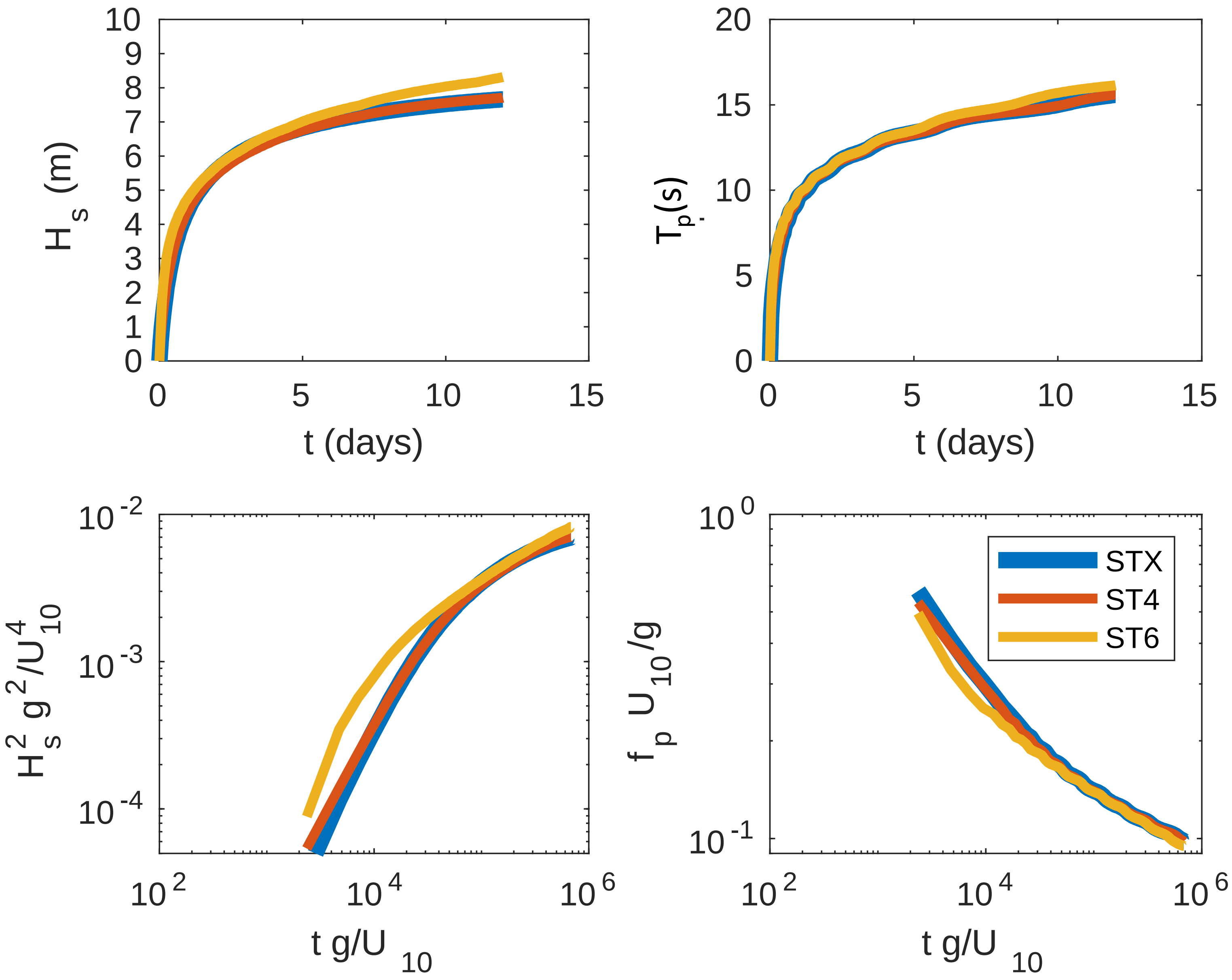

Peak Period

STX: this study

ST4: Ardhuin et al. 2010

ST6: Zieger et al. 2015

Drag coefficient and Whitecap coverage at high winds

Drag coefficient
Vs
Wind speed

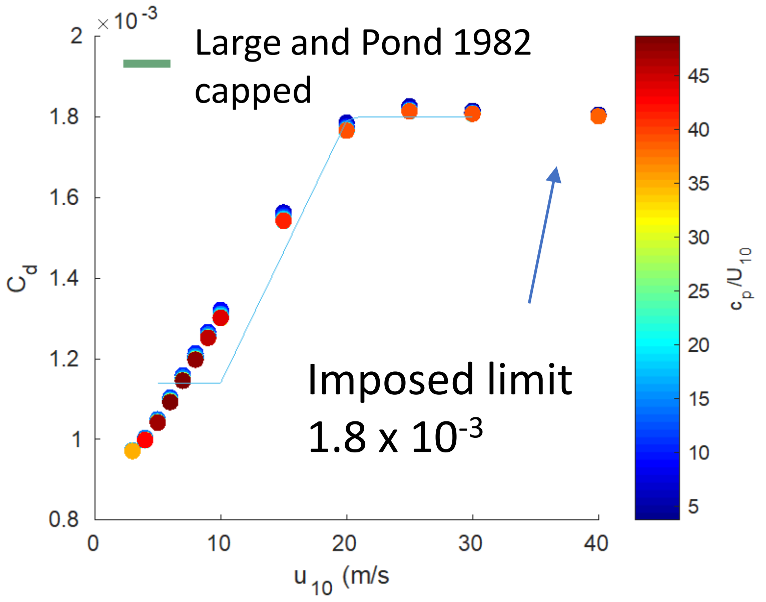

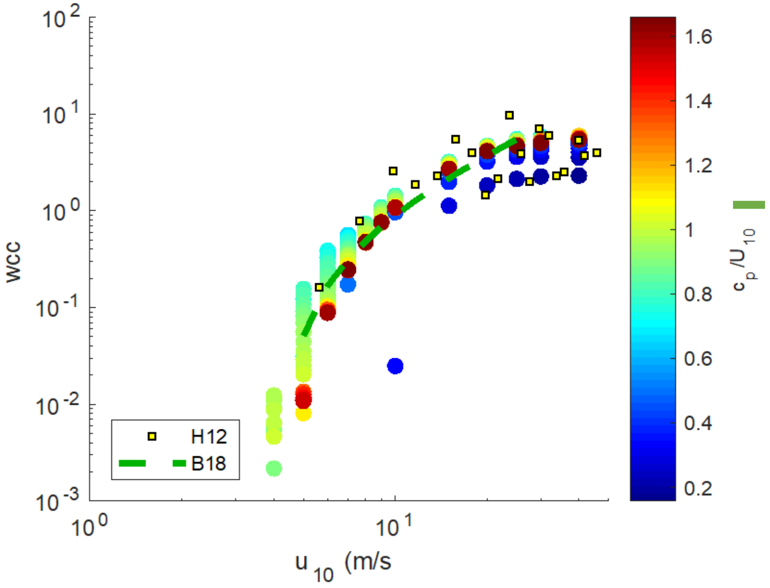

: Holthuijsen et al. 2012

: Brumer et al. 2017

Whitecap Coverage
vs
Wind speed

1.8 x10^{-3}

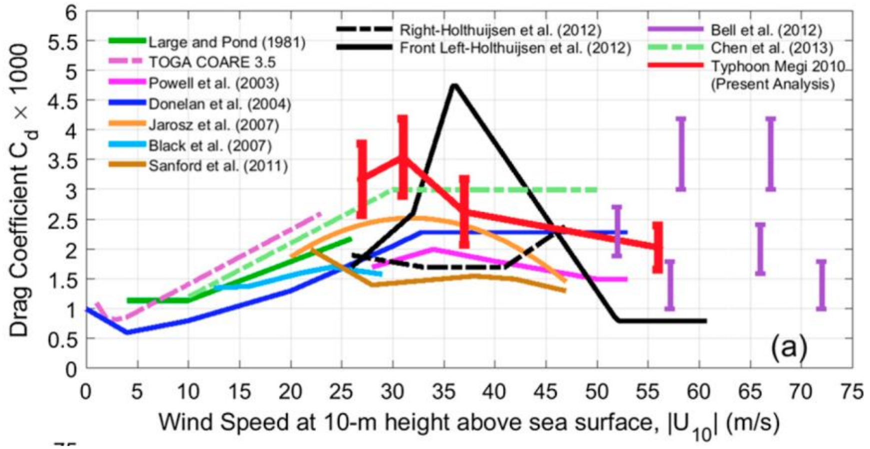

Hsu et al. 2017

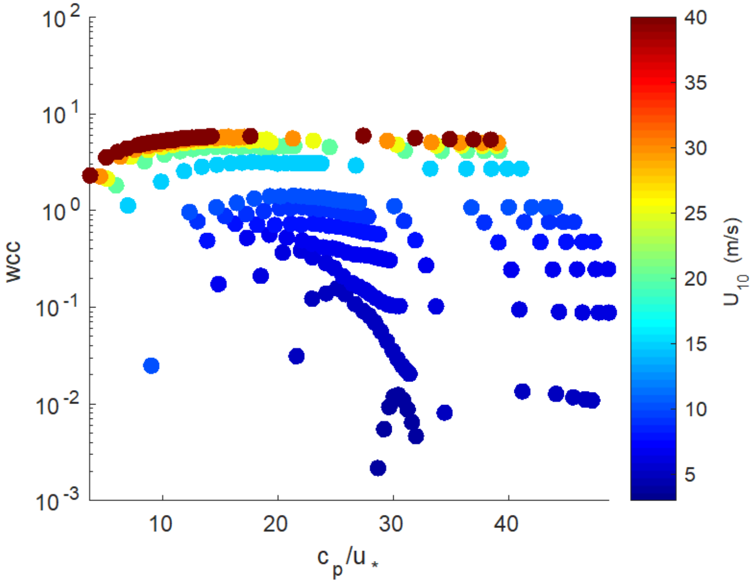

Nested Grids: 270 m and 100 m resolution

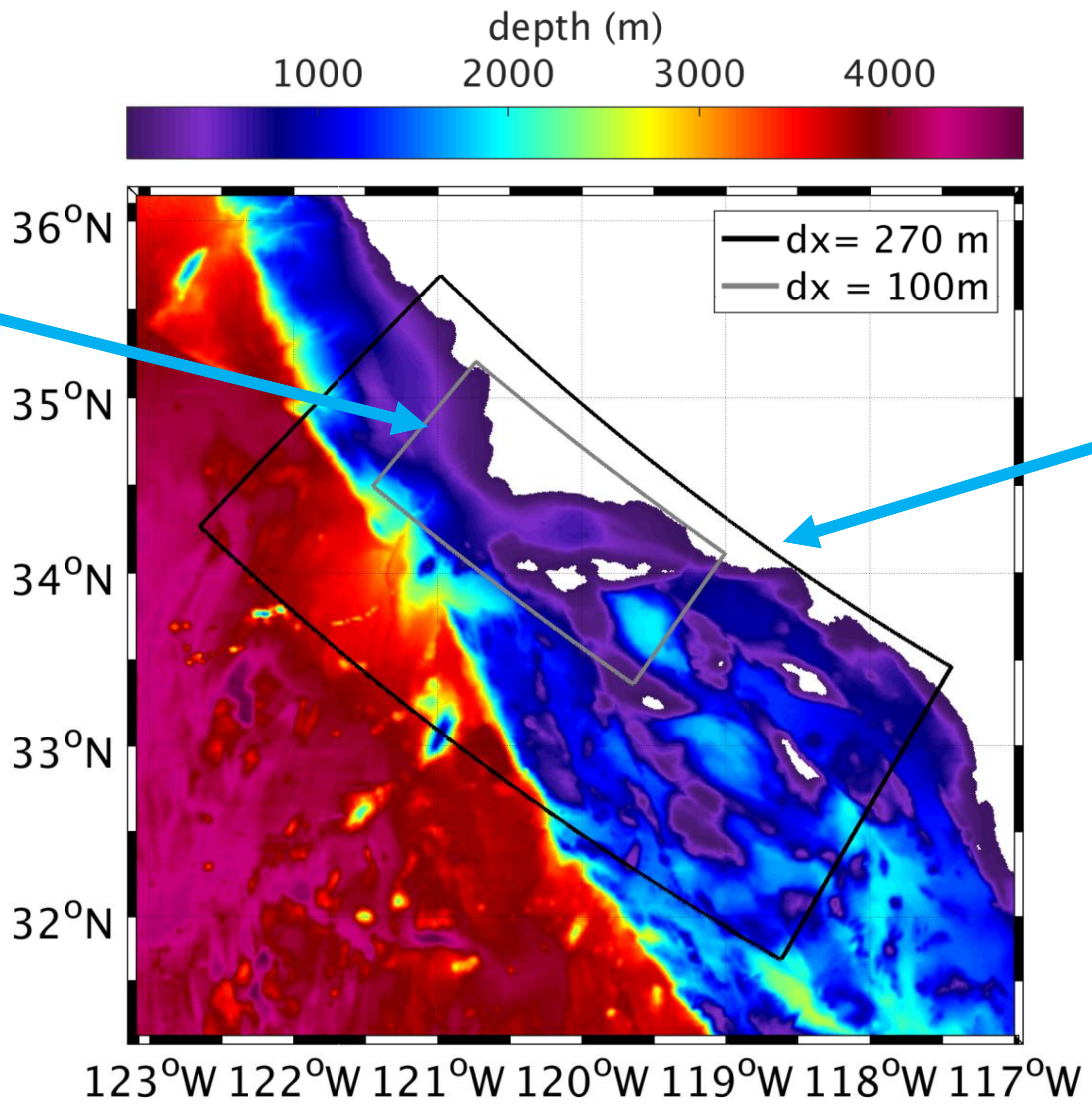

Santa Maria Basin

Southern California Bight

Blended bathymetry:
Global 30 arc second
(SRTM30+, Becker et al. 2009)
NOAA coastal relief model
(1-3 arc seconds)

Wave Data from Coastal Data Information Program (CDIP)

Period: Winter (2006/2007) , and Spring (2007)
Boundary conditions: Harvest Buoy (☆)
All other buoys for model validation

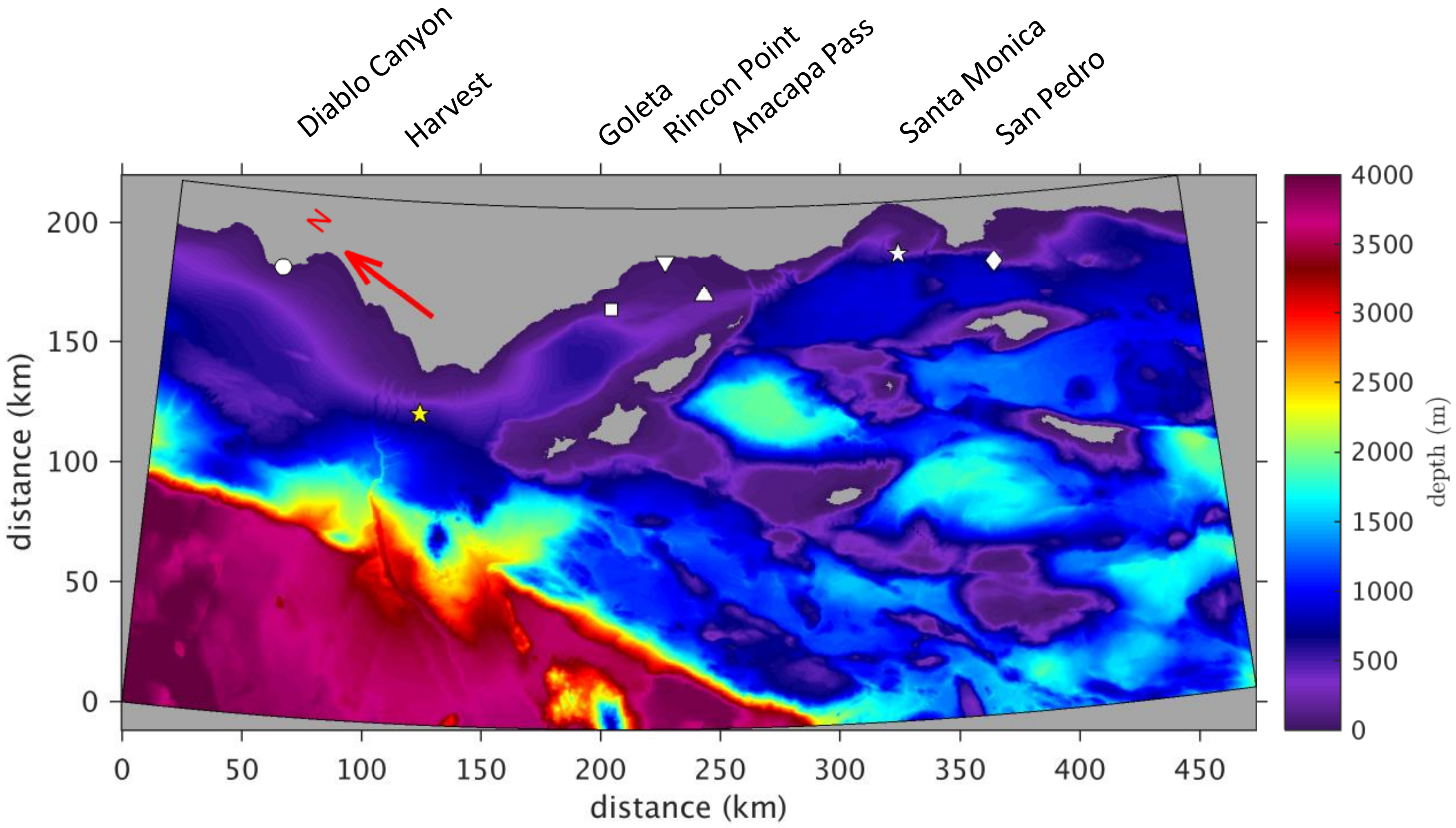

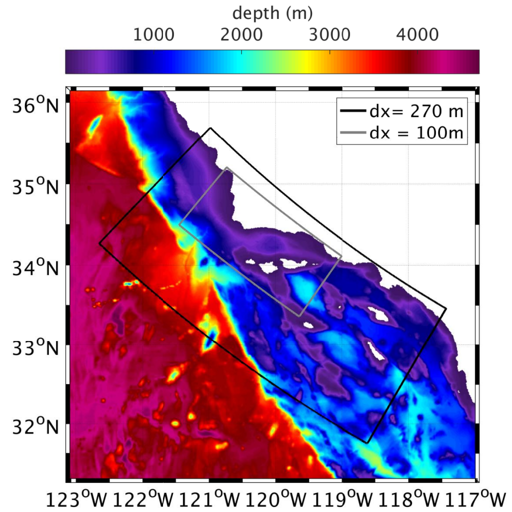

Boundary Conditions

- Harvest buoy data are smoothed with at 2.5 hour filter
- Directional spectra are reconstructed from directional Fourier coefficients using Maximum Entropy Method (Lygre and Krogstad, 1986)
- Temporal lag (T_{lag}) accounting for the wave travel time between the boundary and buoy location using the linear dispersion relationship (cf., O'Reilly et al. 2016)

$$T_{lag} = r / C_g \sim \text{few hours}$$

- T_{lag} is accounted for all spectral components projected along the path between the boundary points and the Harvest buoy

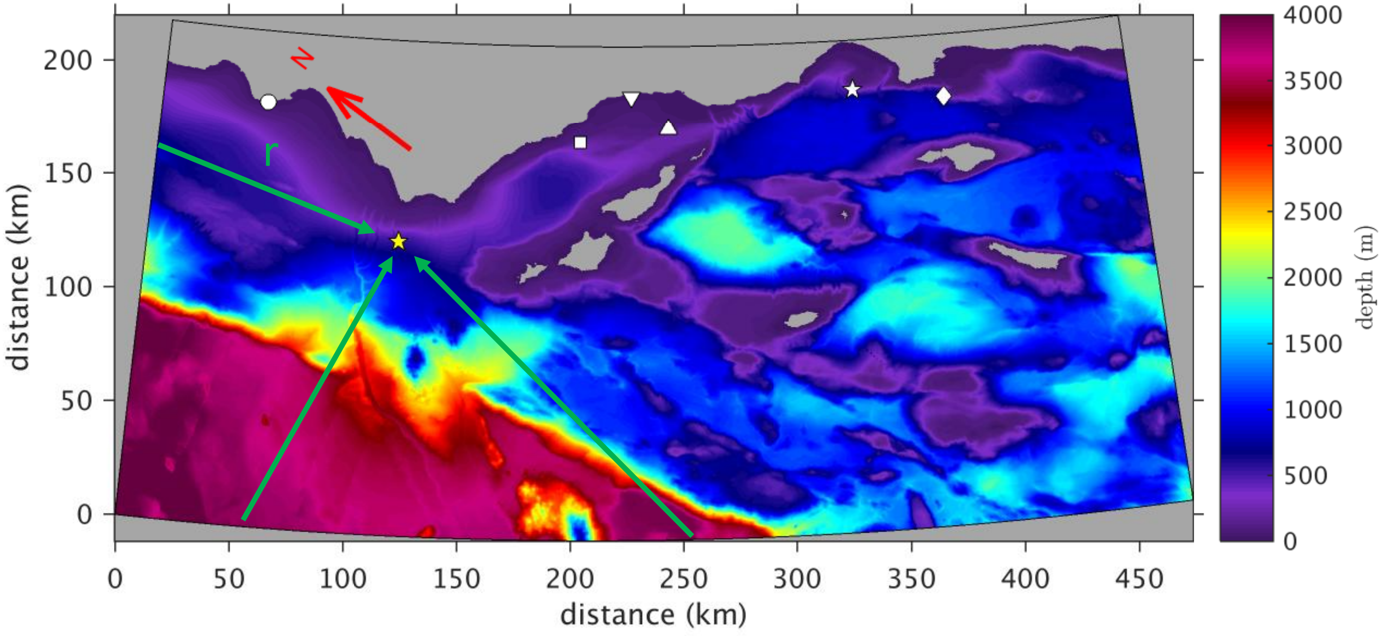

Time Series at Harvest Buoy (Dec. 2006)

Control Run:
- Wave propagation and depth-induced refraction without additional forcing

Significant Wave Height $(H_s = 4\langle\eta^2\rangle^{1/2})$

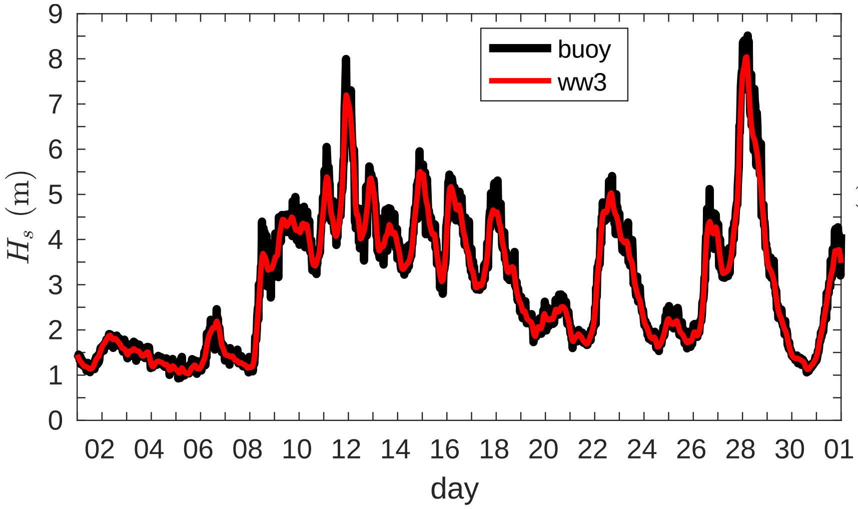

Peak Period

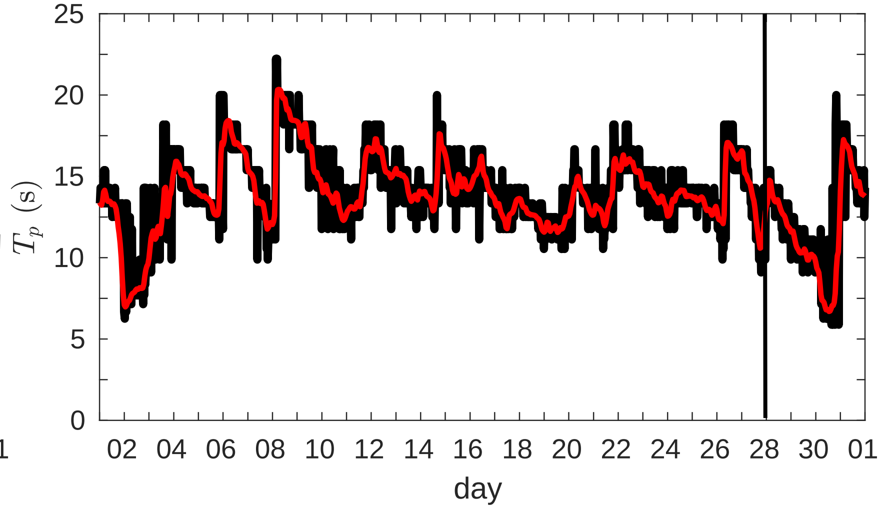

Directional frequency spectrum $F(f,\theta)$ at Harvest buoy on Dec 28 3:00, 2006.

T_p = 15 s towards the southeast

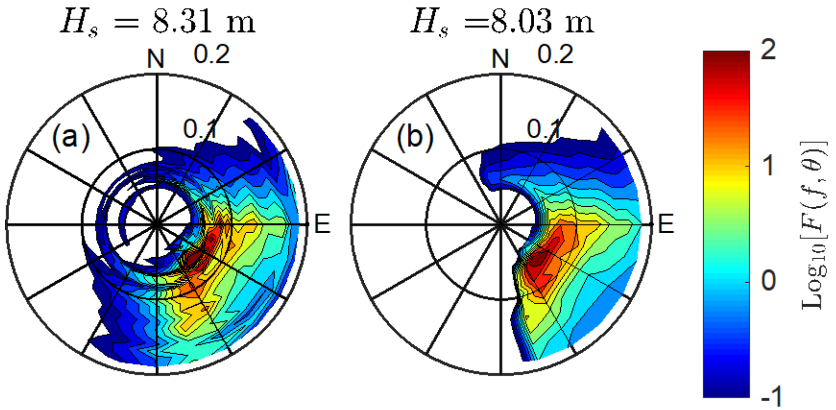

Buoy Obs.

Model (ww3)

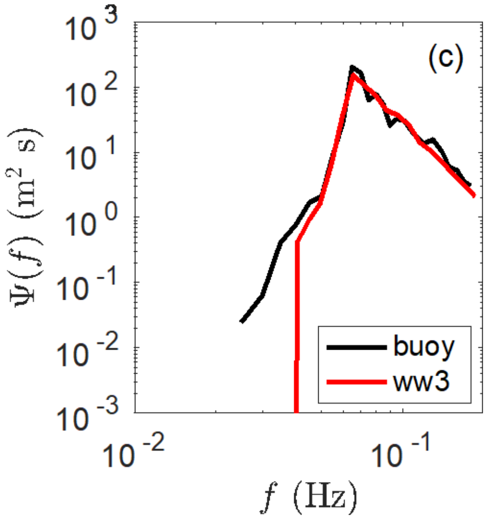

Snapshot of Significant Wave Height (∆x= 270 m)

Directional Spectrum at Harvest Buoy

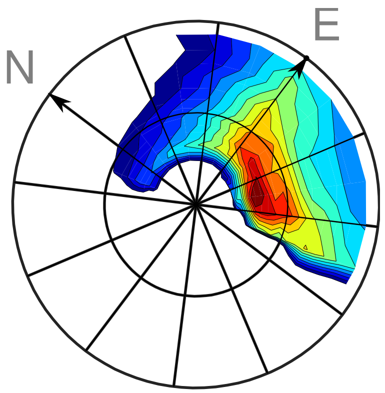

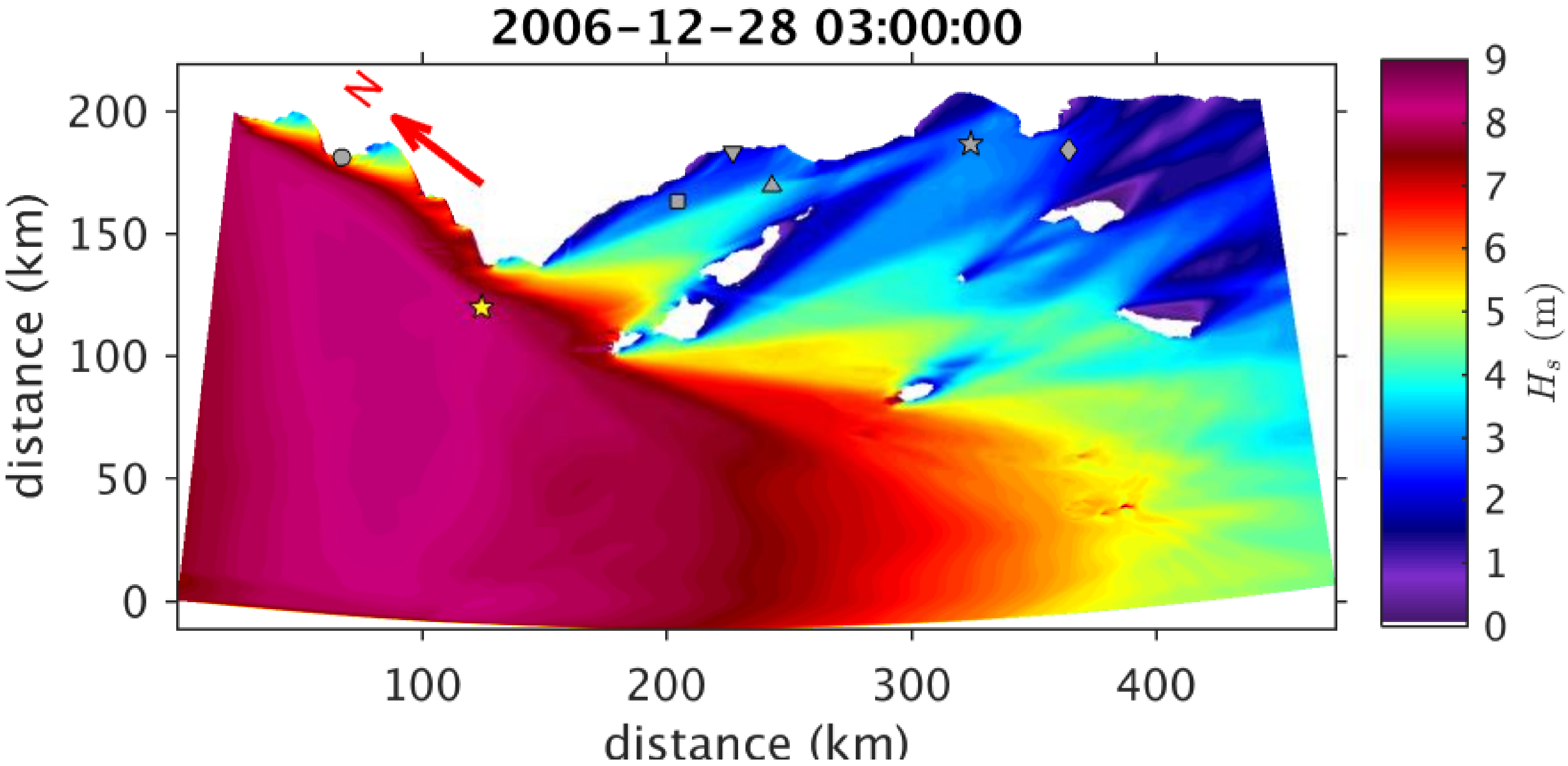

Control Run:

- Propagation and depth-induced refraction without additional forcing

Snapshot of Significant Wave Height (Δx= 100 m)

Directional Spectrum at Harvest Buoy

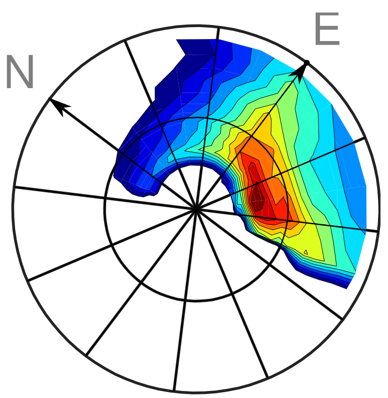

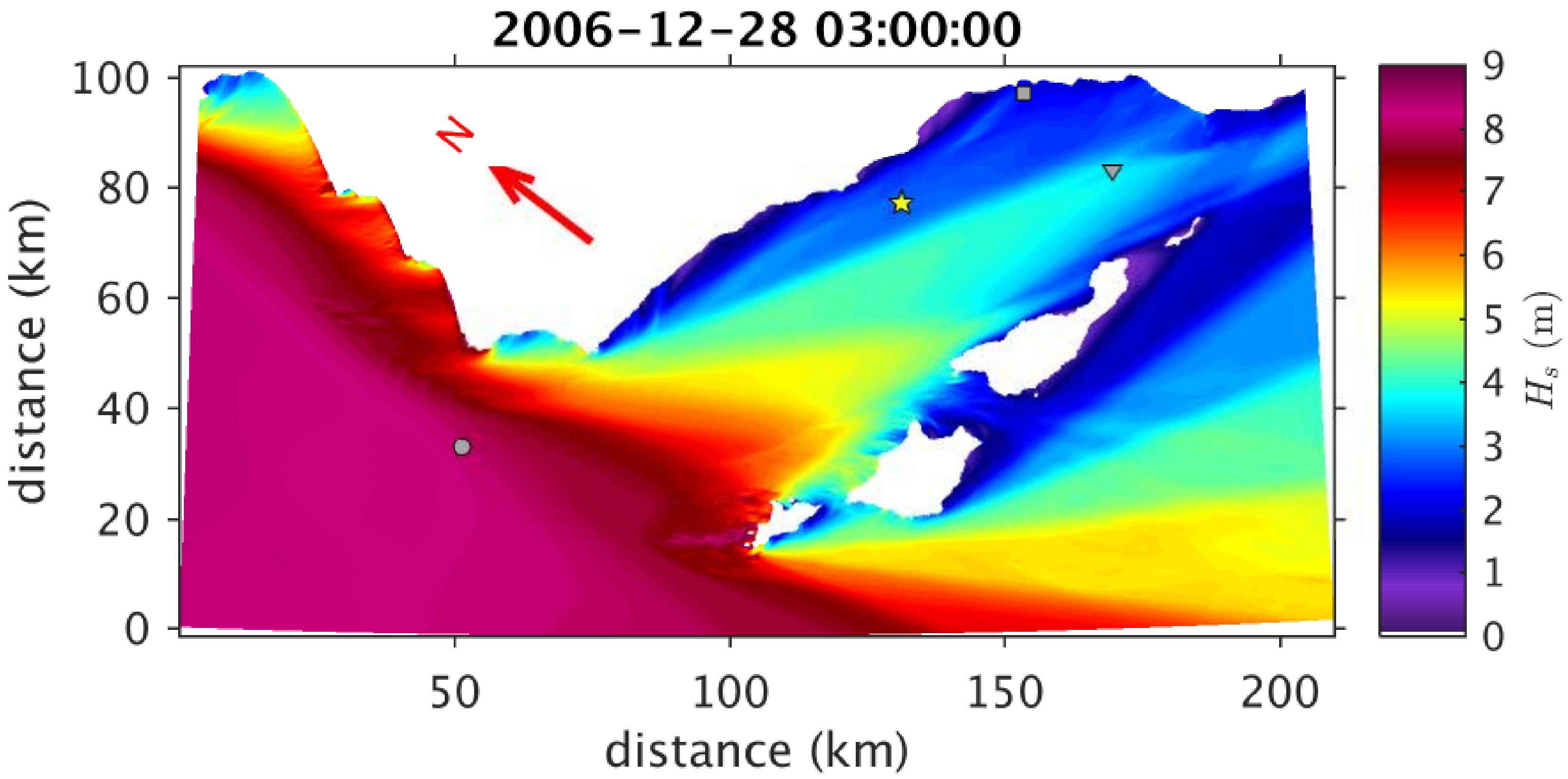

Model results at buoy locations give nearly identical solutions with two resolutions considered for water depths less than 10 m

This work focuses on the 270 m grid

Model Performance: Exposed vs. Sheltered Regions

Winter 2006

Significant Wave Height | Peak Period

Diablo Canyon (exposed)

San Pedro Basin (sheltered)

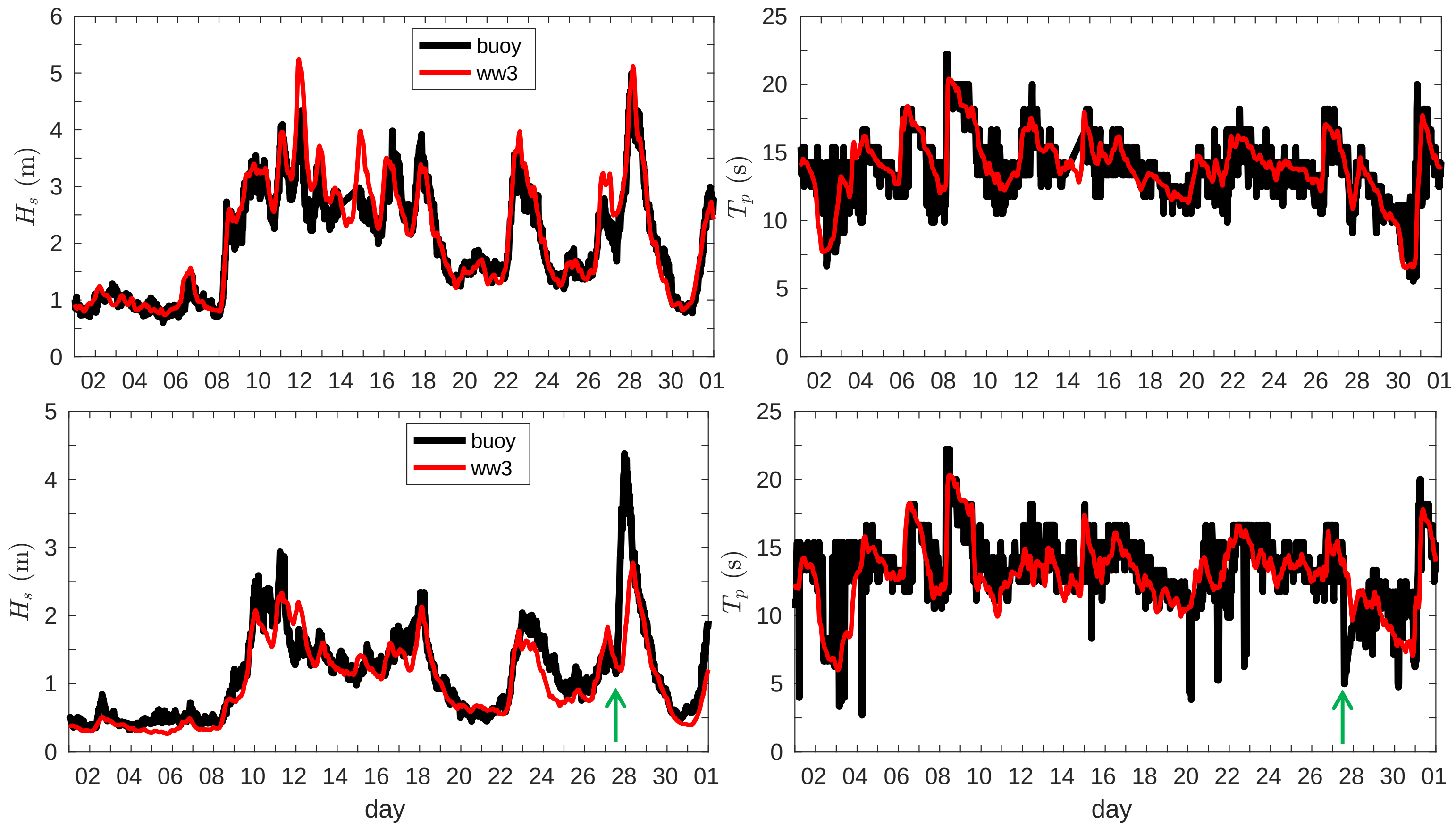

- Larger model errors at sheltered regions
- When H_s differences are large, T_p observed is low, indicative mixed wind-sea and swell

Model Performance: Exposed vs. Sheltered Regions

Spring 2007

Significant Wave Height | Peak Period

Diablo Canyon (exposed)

San Pedro Basin (sheltered)

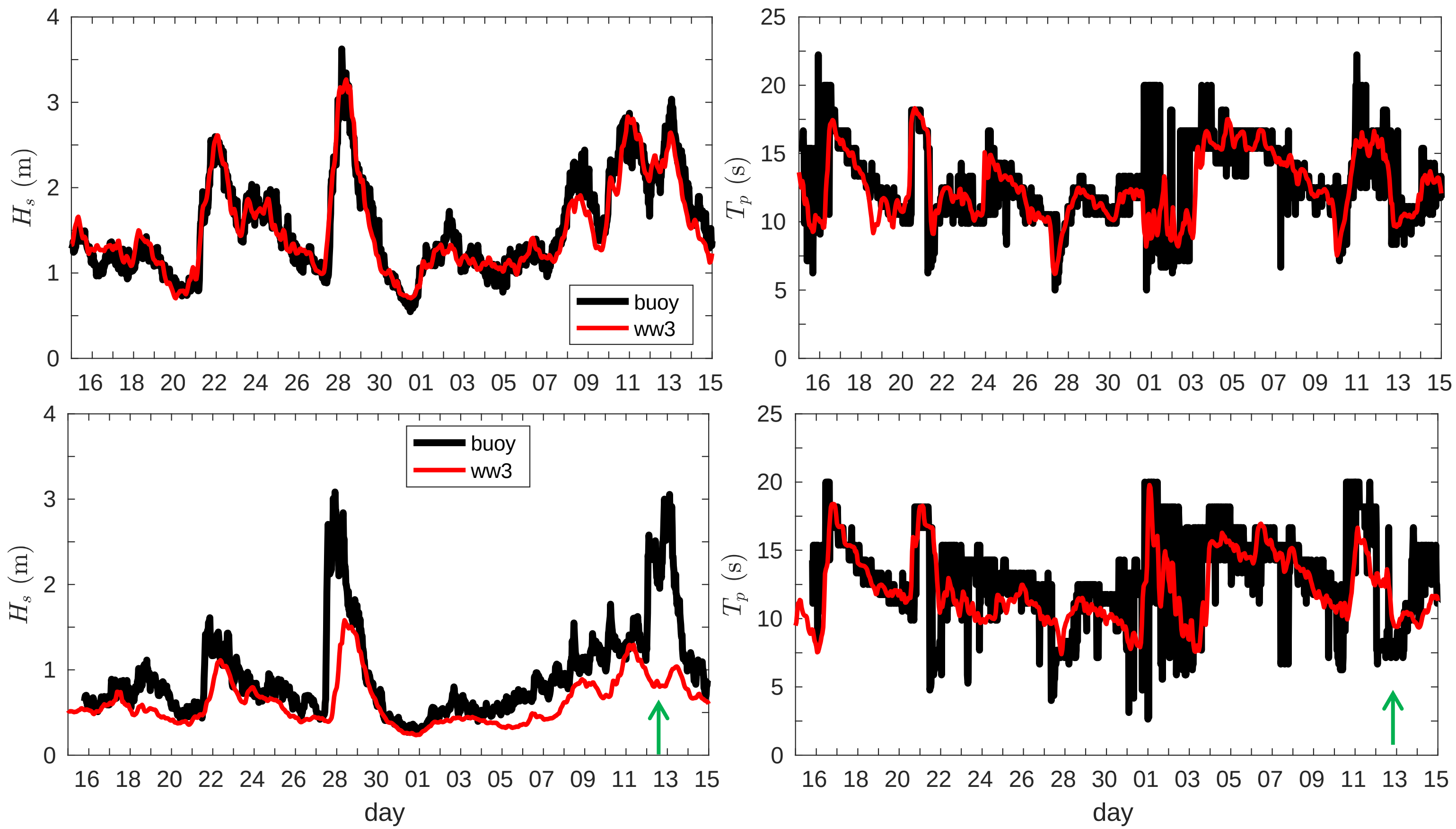

- Larger model errors at sheltered regions (5% vs 10% root-mean-square-errors and 0.96 vs 0.88 correlation)
- When H_s differences are large, T_p observed is low, indicative mixed wind-sea and swell

Wind Forcing

- Wind forcing can significantly improve model performance within sheltered areas during spring

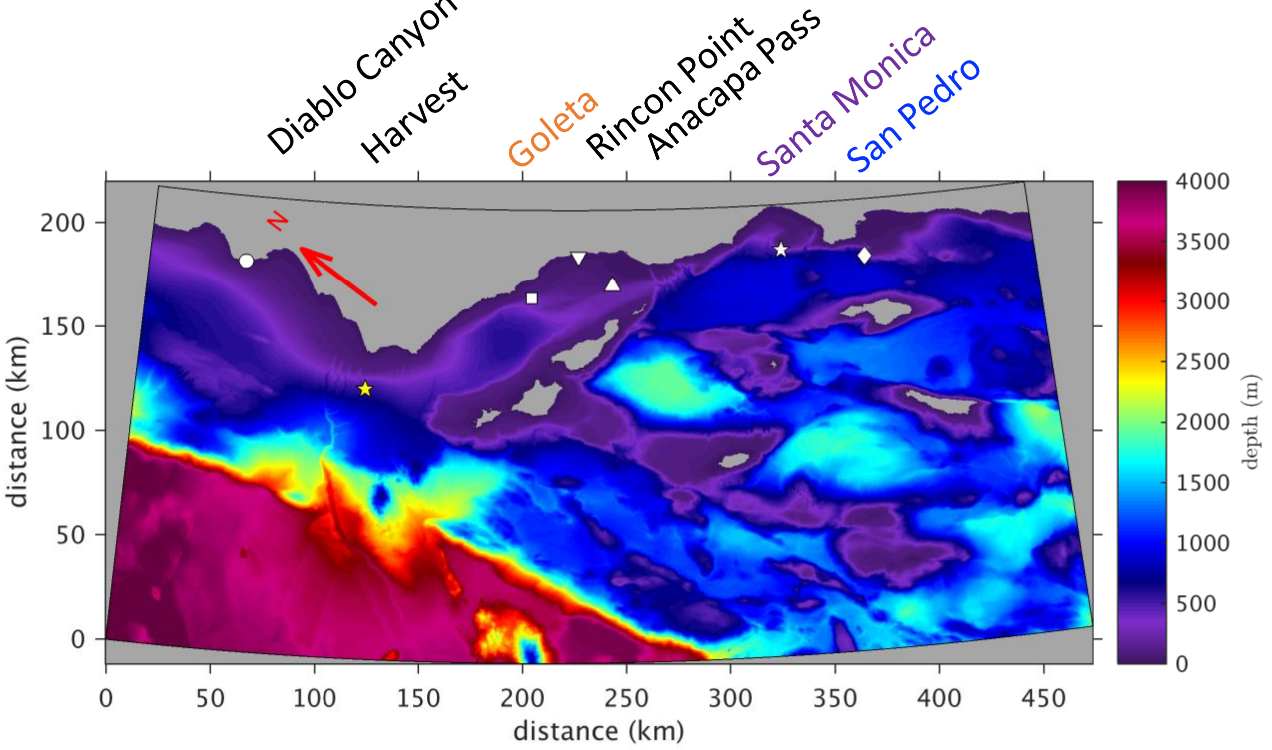

Spring 2007

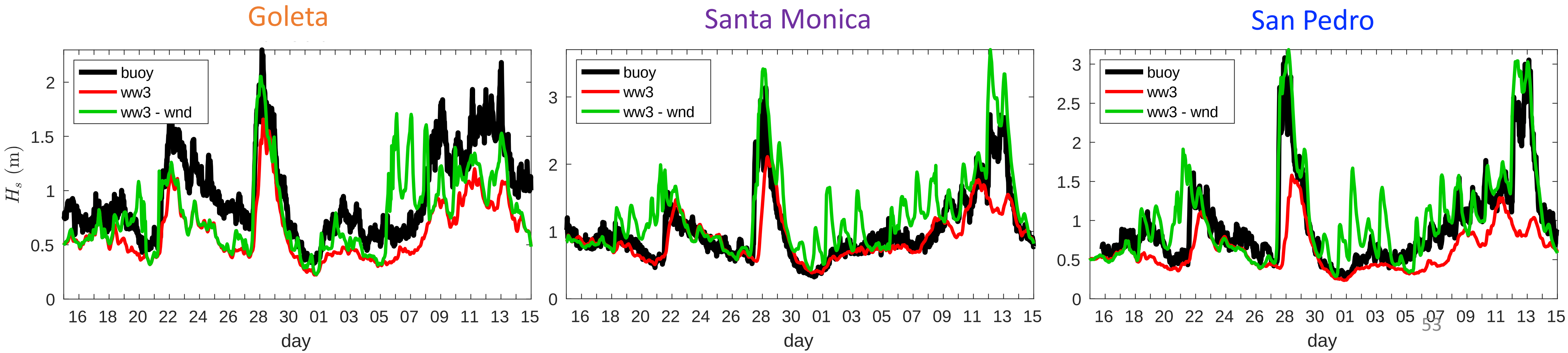

Wind Forcing

- Directional and One-Dimensional Frequency Spectra at San Pedro

March 28, 8:00 UTC, 2007

$H_s = 2.39$ m

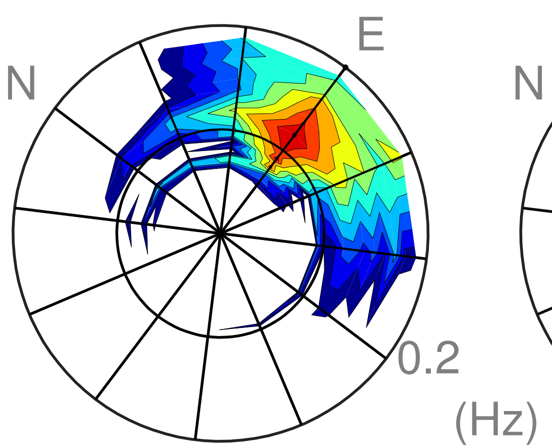

Observations

$H_s = 1.53$ m

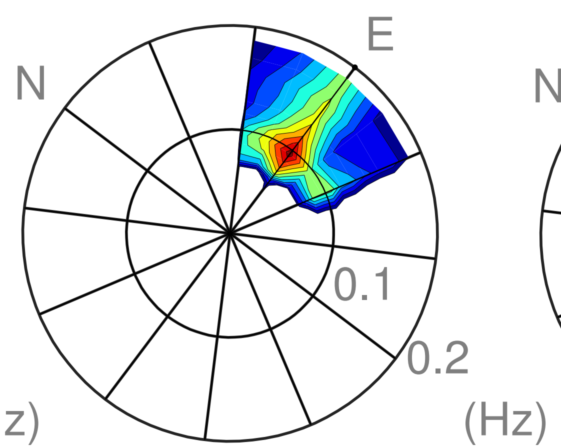

Control Run

$H_s = 2.79$ m

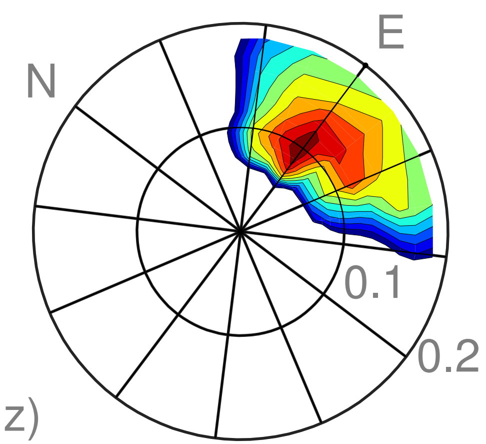

Wind Forced

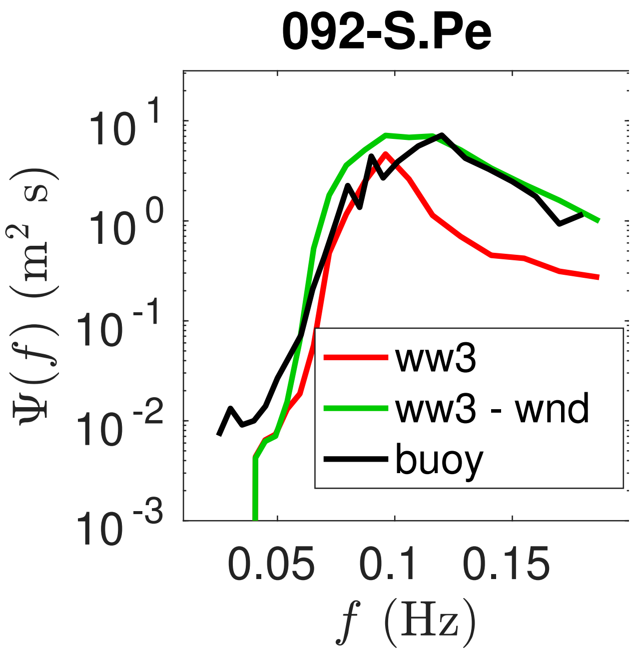

Spectrum forced by wind is in good agreement with observations

Current Effects on Waves (CEW)

- Significant wave height variability due CEW is around 20%, with larger values in the Santa Barbara Channel improving model performance during the 2006 winter

Winter 2006

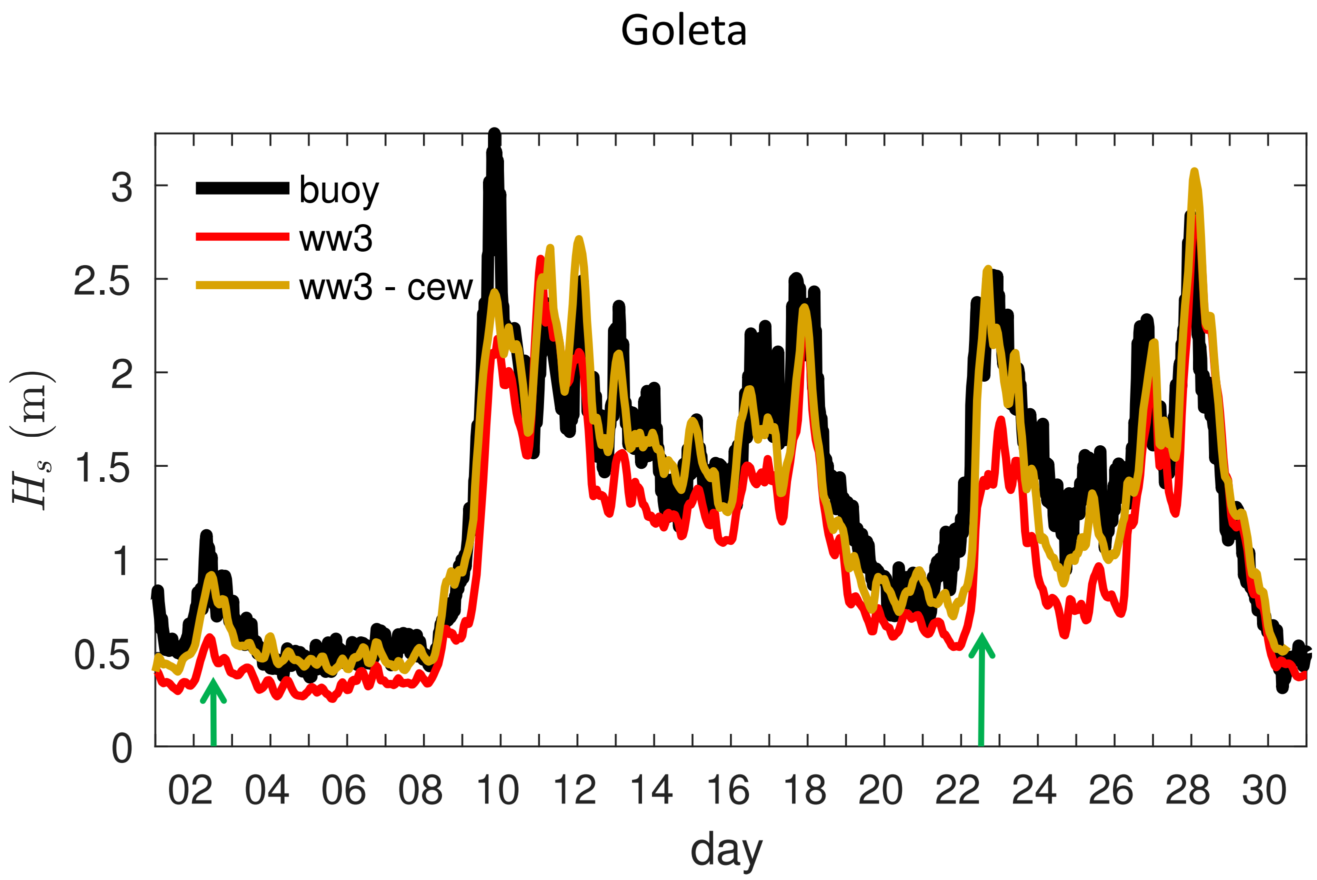

Current Effects on Waves (CEW)

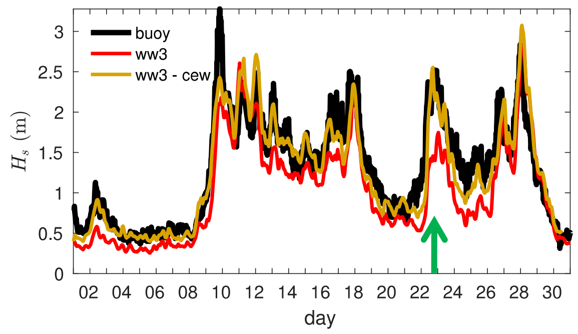

- Directional and 1-D Frequency Spectra at Goleta Point

Dec 22, 12:00 UTC, 2006

$H_s = 2.10$ m

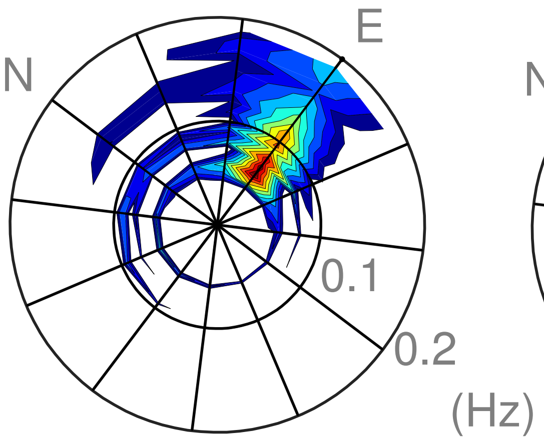

Observations

$H_s = 1.36$ m

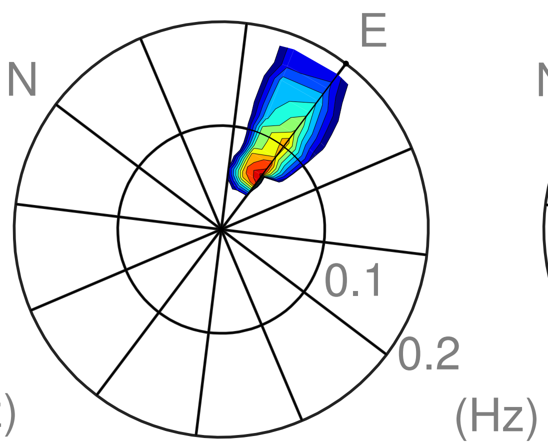

Control Run

$H_s = 2.09$ m

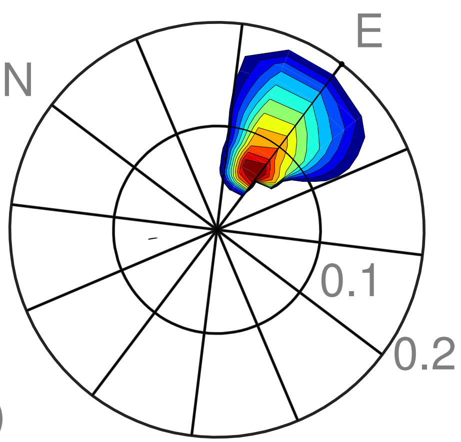

CEW

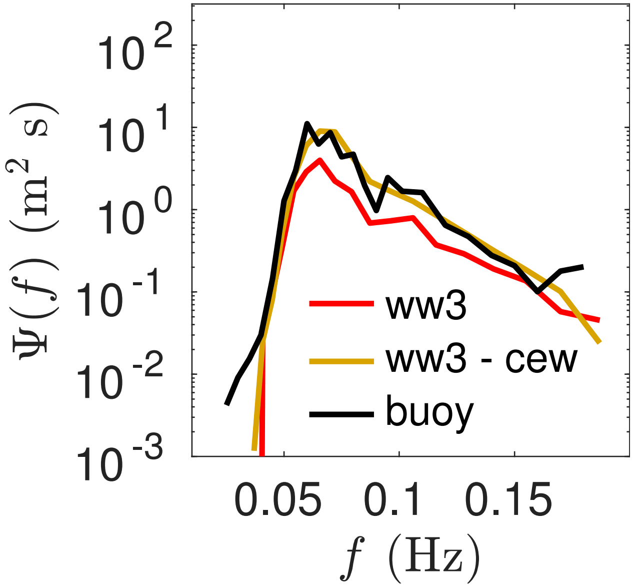

Spectrum forced by currents is wider and more energetic in better agreement with buoy data

ROMS Surface Currents and Vorticity Field

Dec 22, 12:00 UTC, 2006

Directional Spectrum at Harvest (☆)

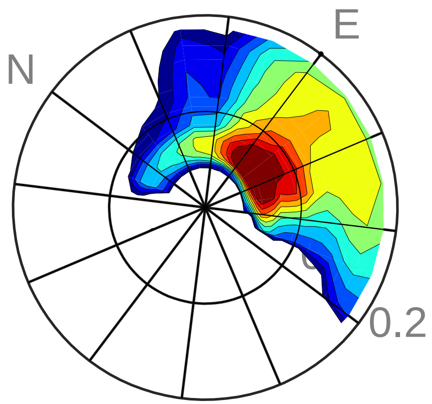

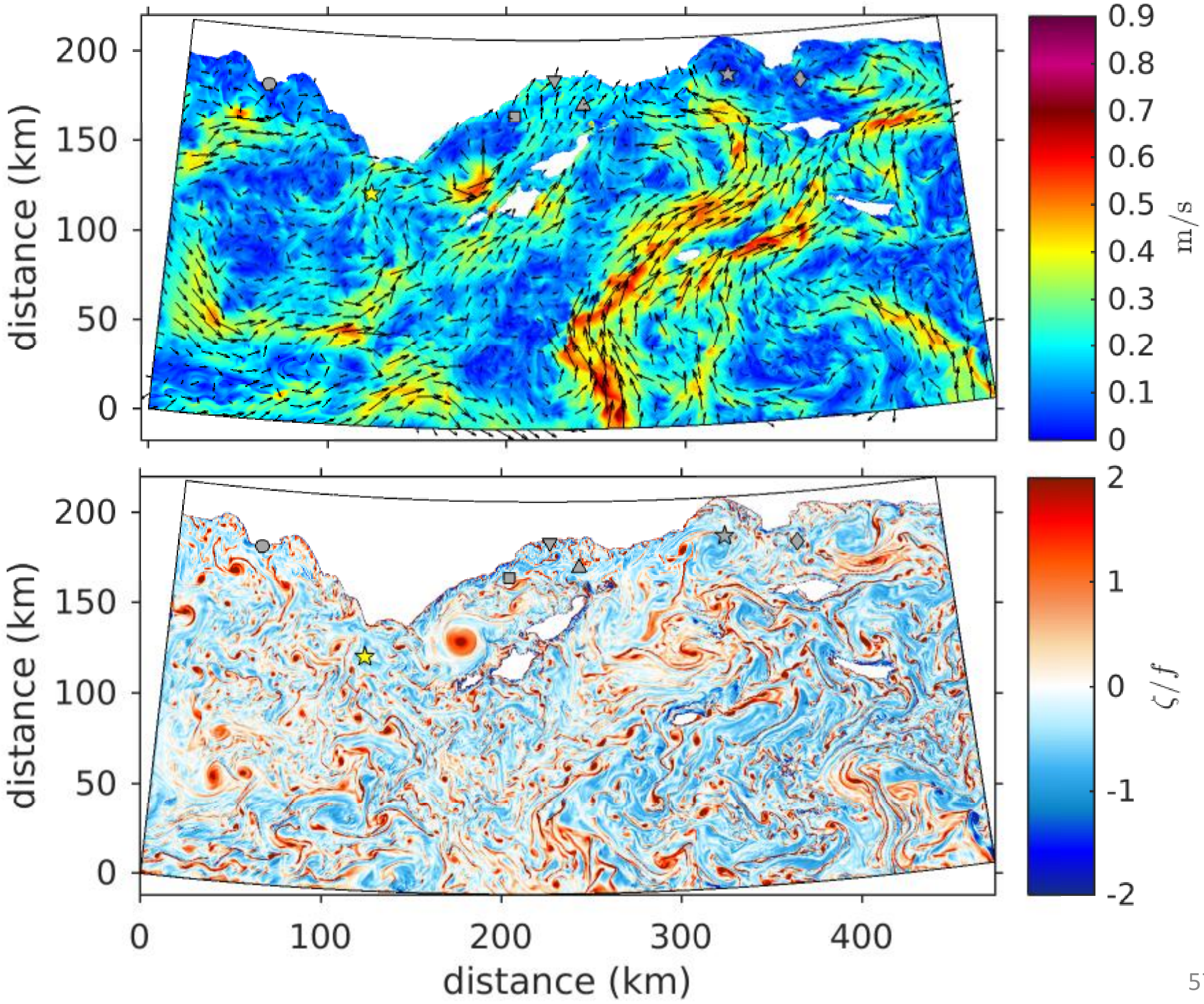

Significant Wave Height: Control Run vs WEC

Dec 22, 12:00 UTC, 2006

Directional Spectrum at Harvest (☆)

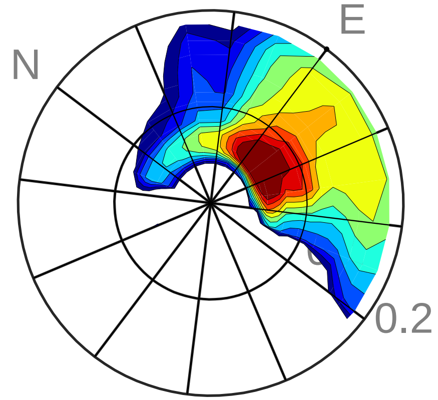

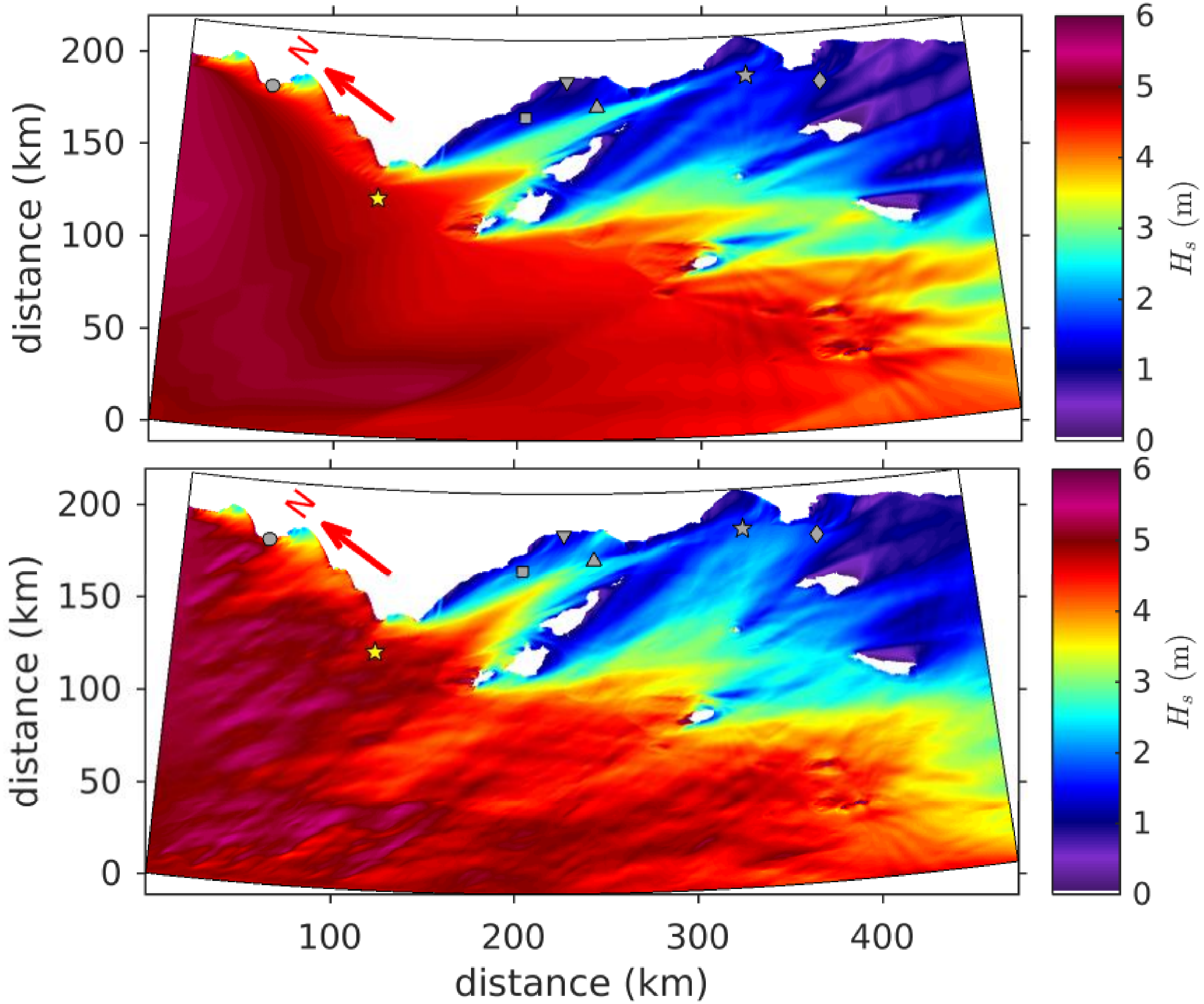

Significant Wave Height: Control Run vs WEC

Dec 22, 12:00 UTC, 2006

Directional Spectrum at Harvest (☆)

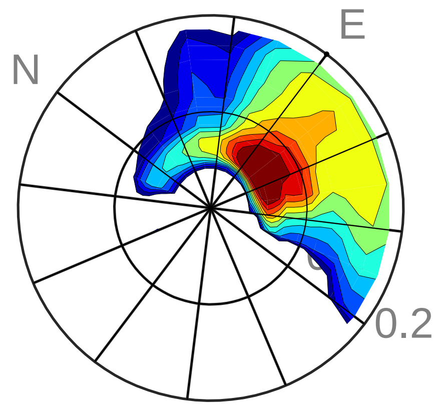

Percent Difference

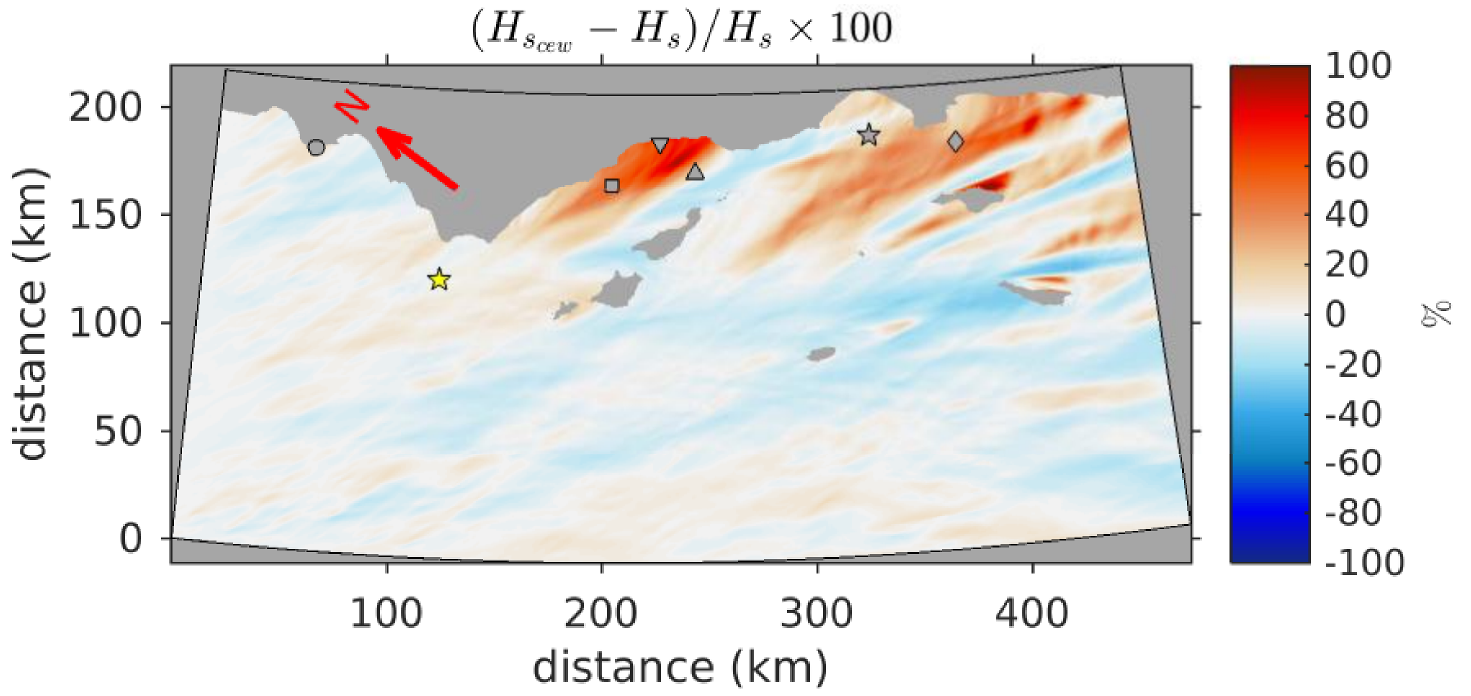

- Significant wave height variability due CEW is around 20%, with larger values in the sheltered areas

Surface Stokes Drift: Control Run vs WEC

Dec 22, 12:00 UTC, 2006

Directional Spectrum at Harvest (☆)

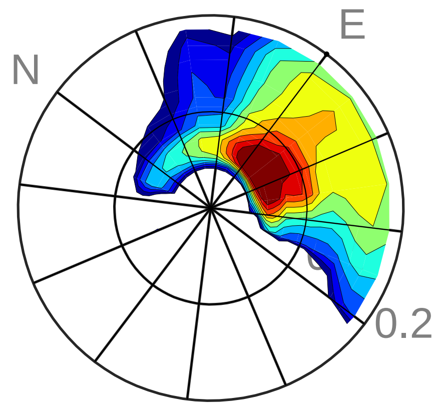

Percent Difference

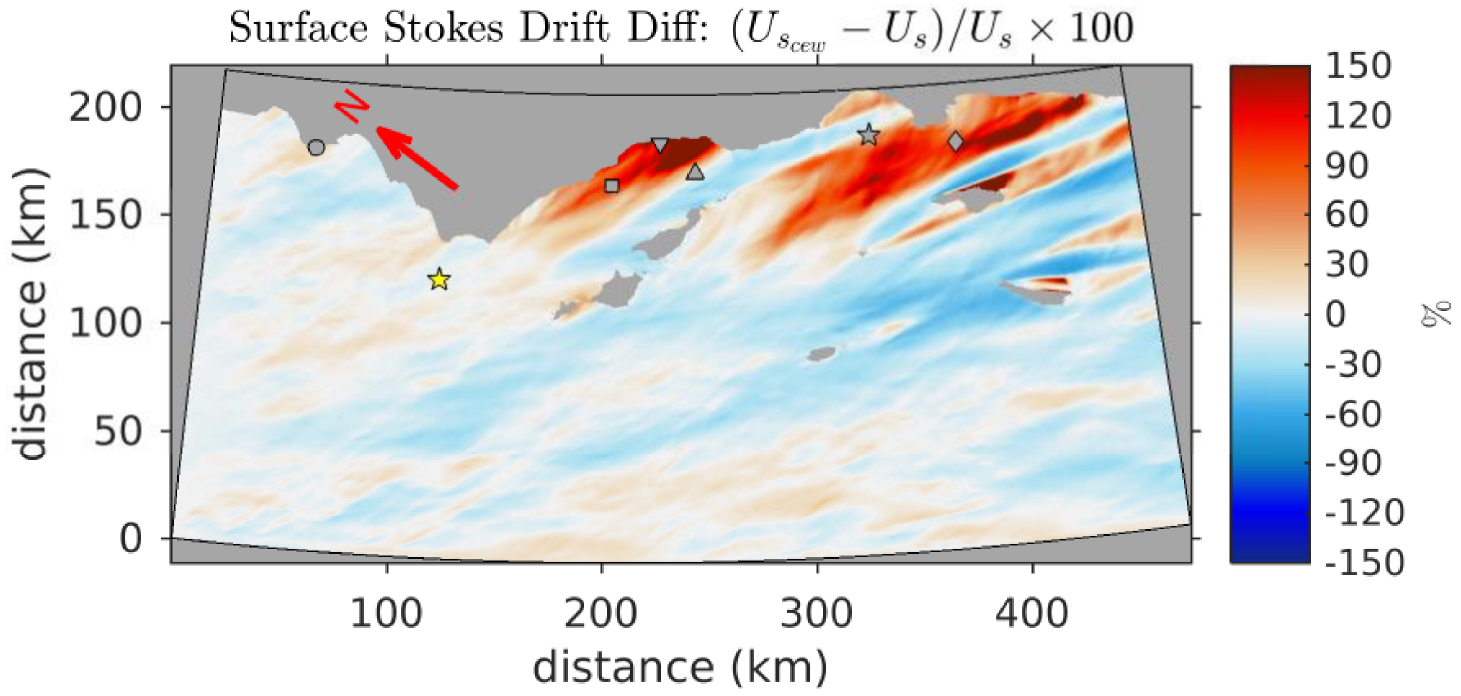

- Stokes drift spatial modulation is similar to that of Hs much with much larger percent changes with values around 30% over exposed areas and greater than 100% within the Bight
- Narrower spectrum over focal areas results in larger surface Stokes drift

Whitecap coverage modulated by submesoscale currents

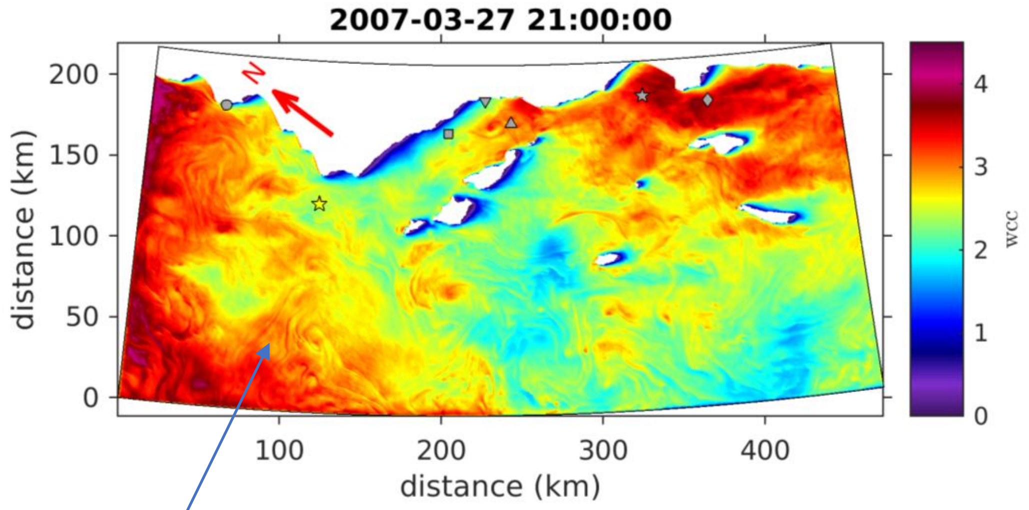

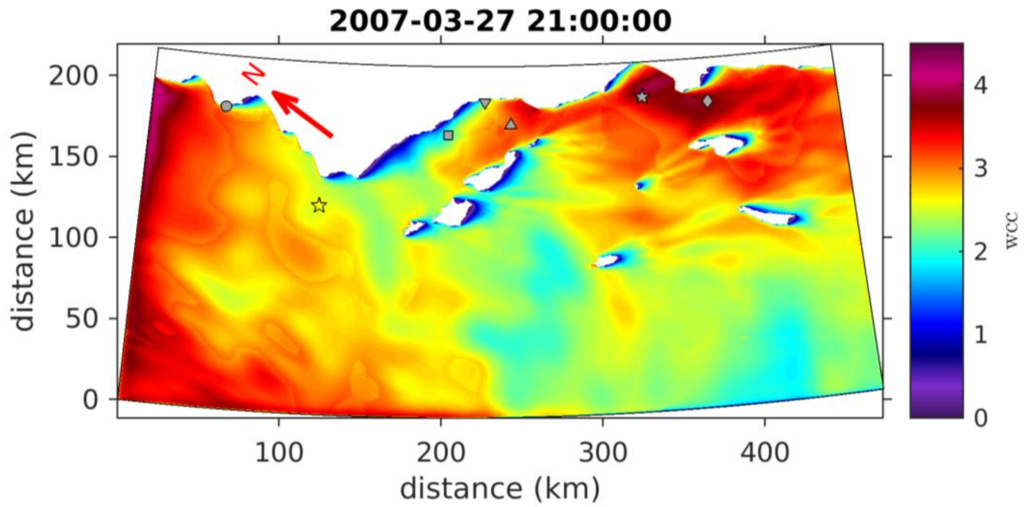

Forced by winds and currents

Wind only

Enhanced breaking at fronts and filaments (c.f. Romero et al 2017)

Whitecap coverage modulated by submesoscale currents

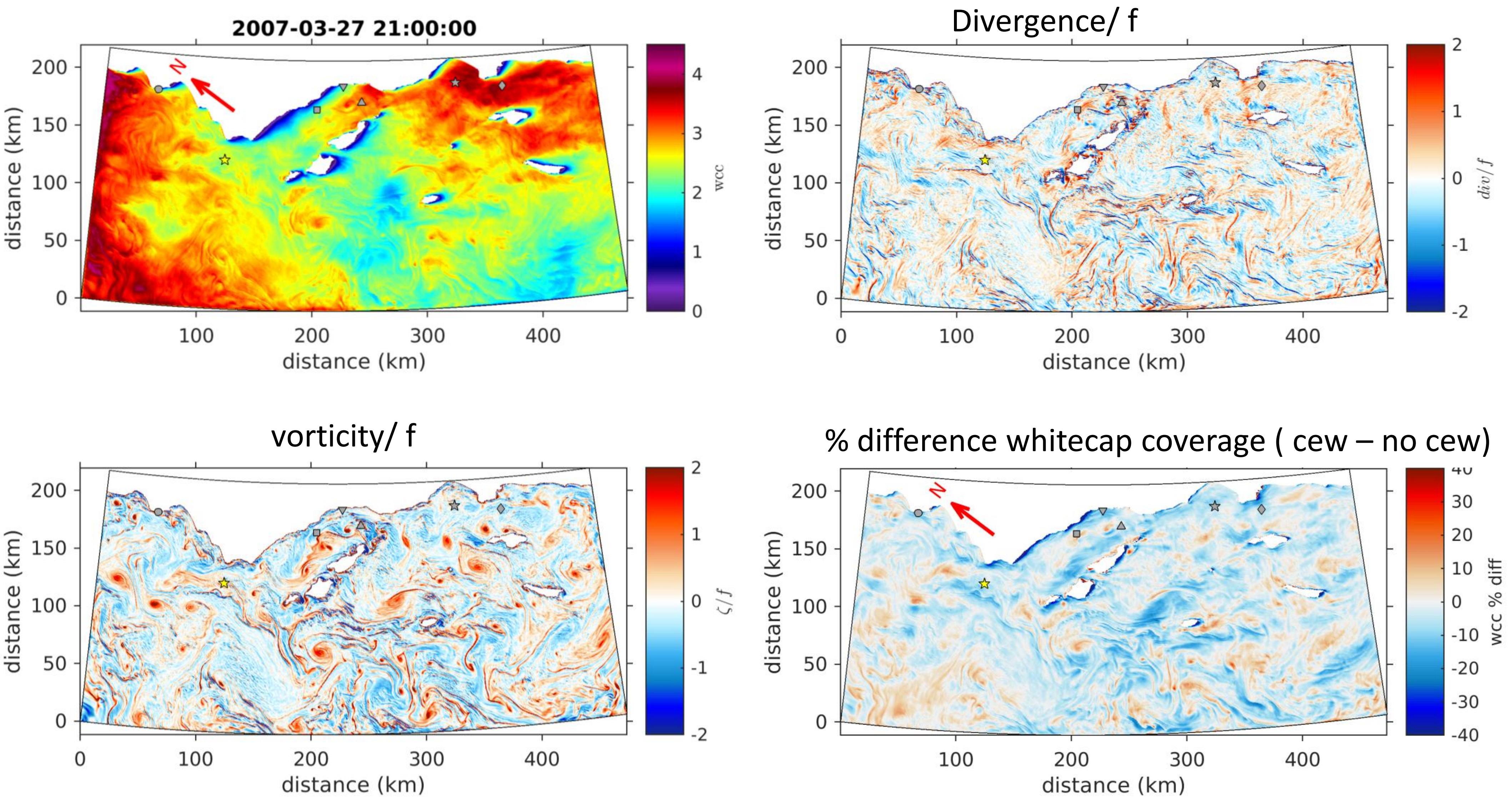

Whitecap coverage modulated by submesoscale currents

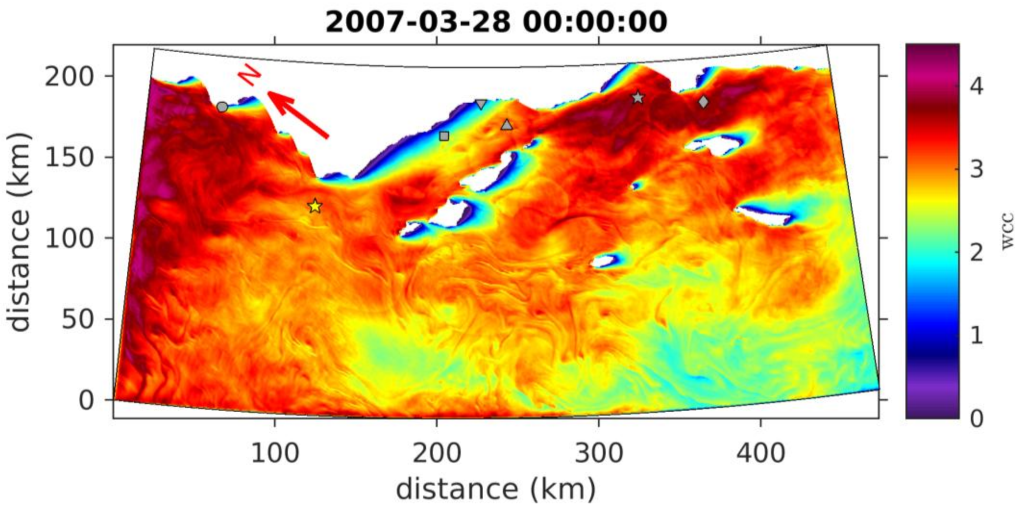

Divergence/ f

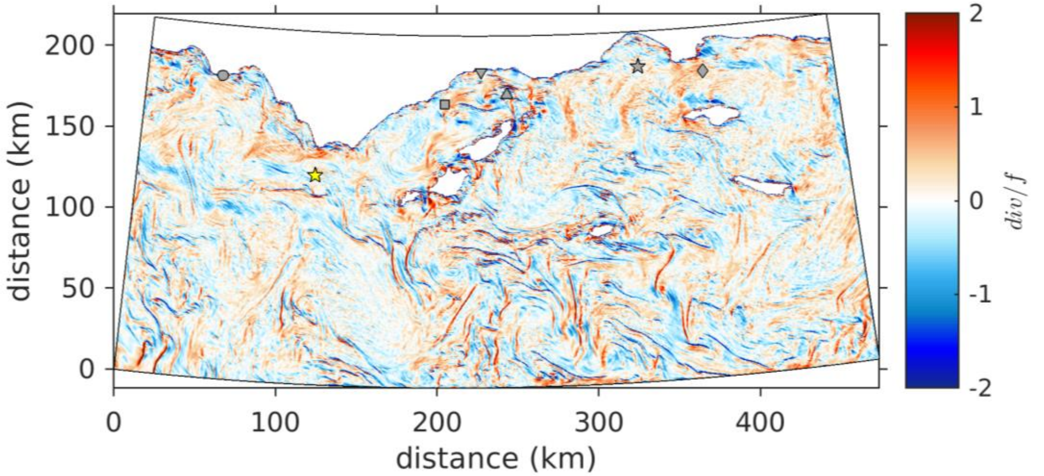

vorticity/ f

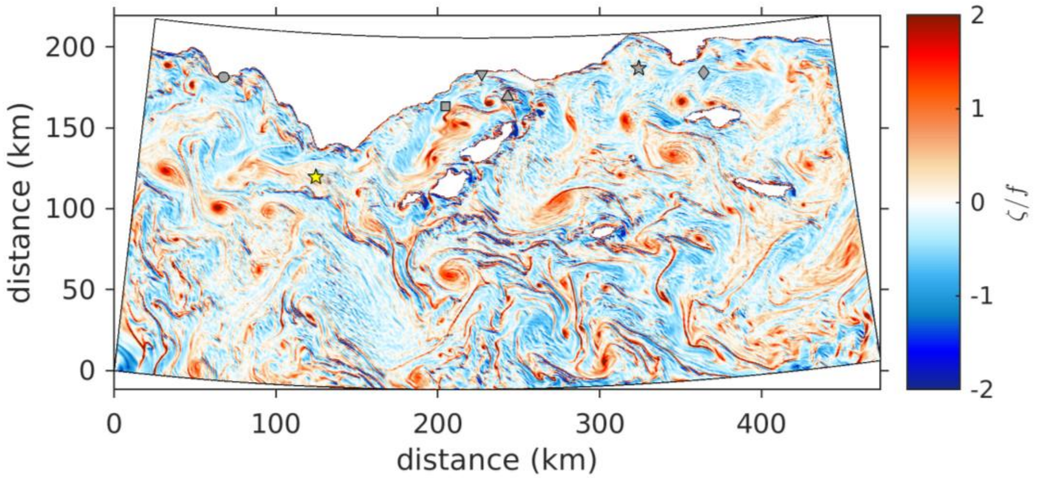

% difference whitecap coverage (cew – no cew)

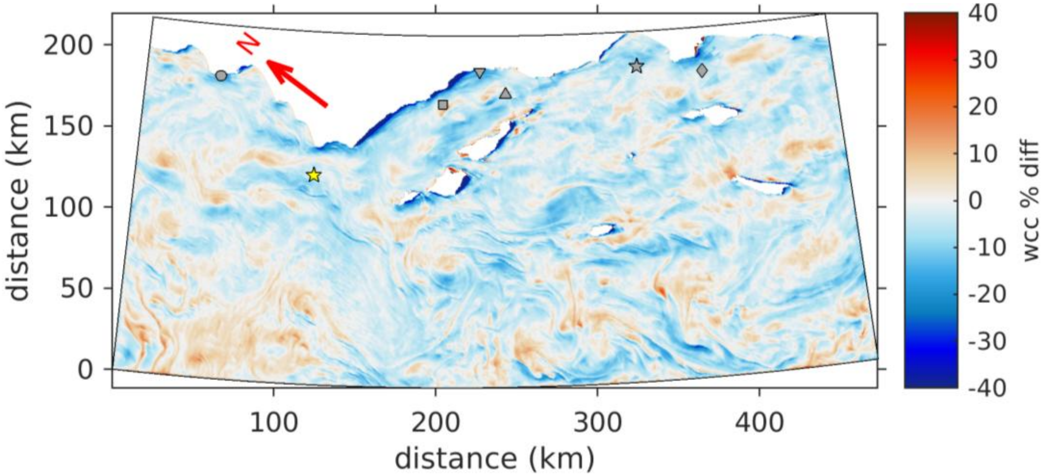

Whitecap coverage modulated by submesoscale currents

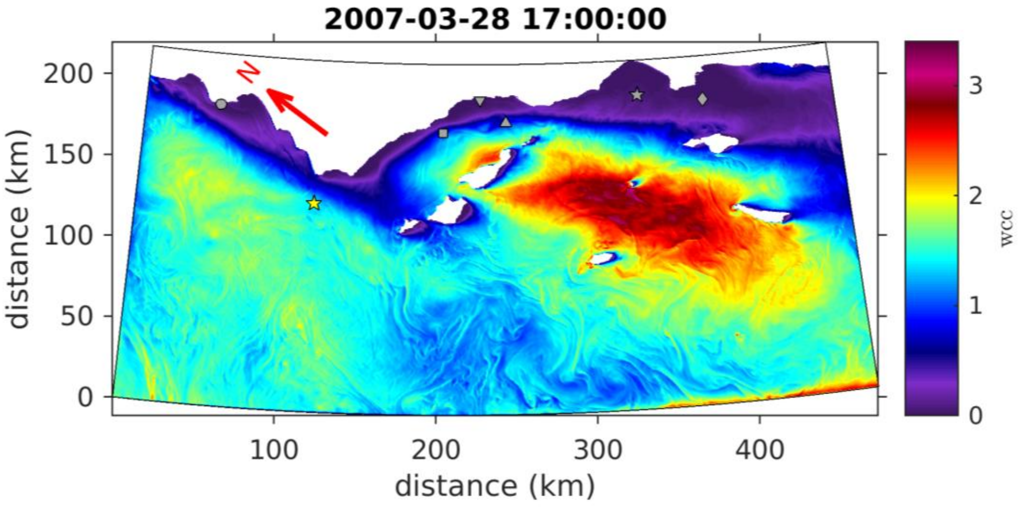

Divergence/ f

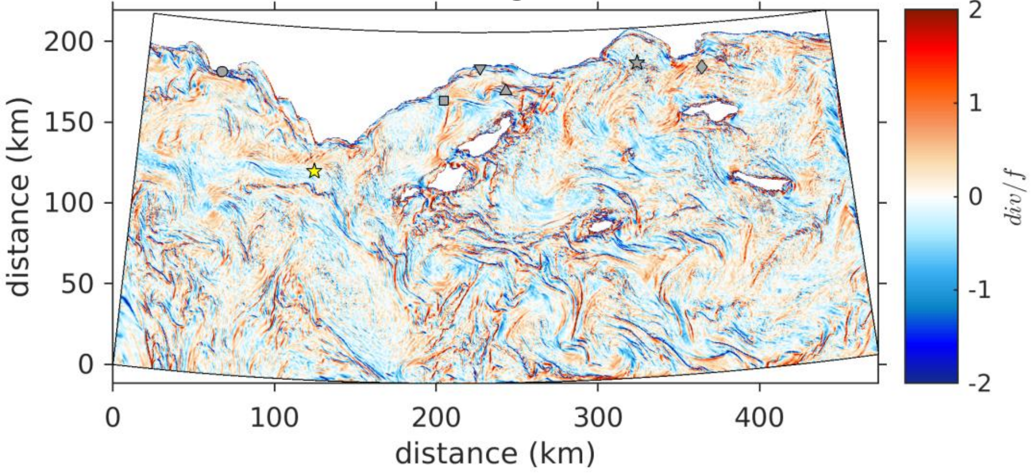

vorticity/ f

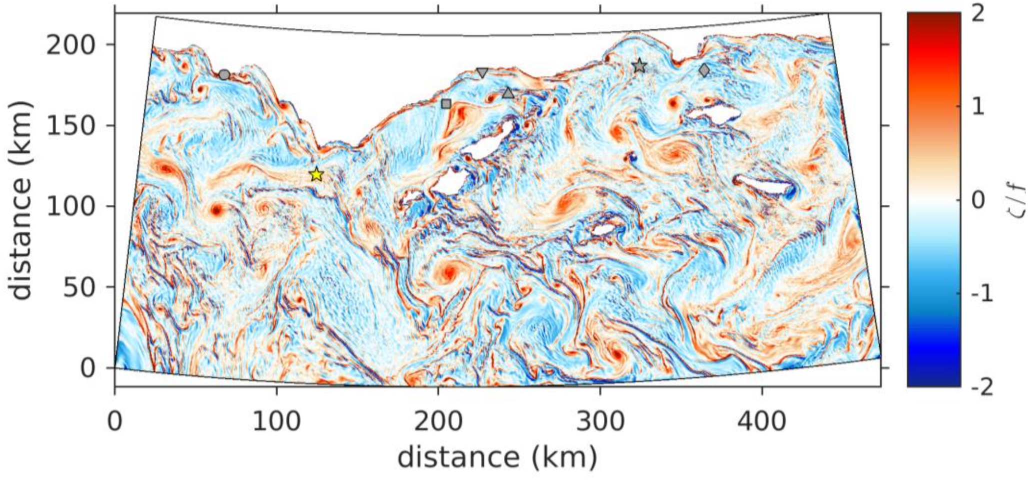

% difference whitecap coverage (cew – no cew)

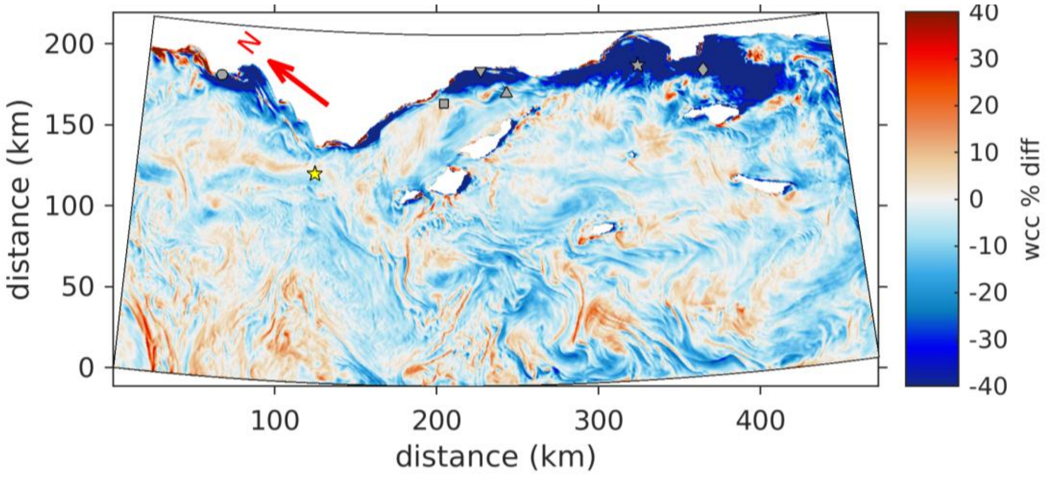

Summary and Conclusions

- New wave breaking parameterization implemented in WaveWatch III
- Model performance is very good reproducing observations, including high winds (< 40 m/s)
- Whitecap coverage at high winds saturates not exceed 10%
- Gas transfer velocities from DNS and CO2 from field observations are also well reproduced
- CEW results in modulation of H_s by 20% over wave exposed areas, with larger variability within the Bight (up 100%)
- CEW significantly modulate the Surface Stokes drift by 40% over exposed areas and by more than 100% within the Bight.
- CEW results in modulation of wcc by up to 40% over wave exposed areas, with larger variability within the Bight (up 100%)
- Large eddies (i.e. Santa Barbara eddy) can significantly increase the energy flux towards coast of Santa Barbara

ROMS surface vorticity: with and without wave effects on currents (WEC)

Forced by waves (vortex force)

Control

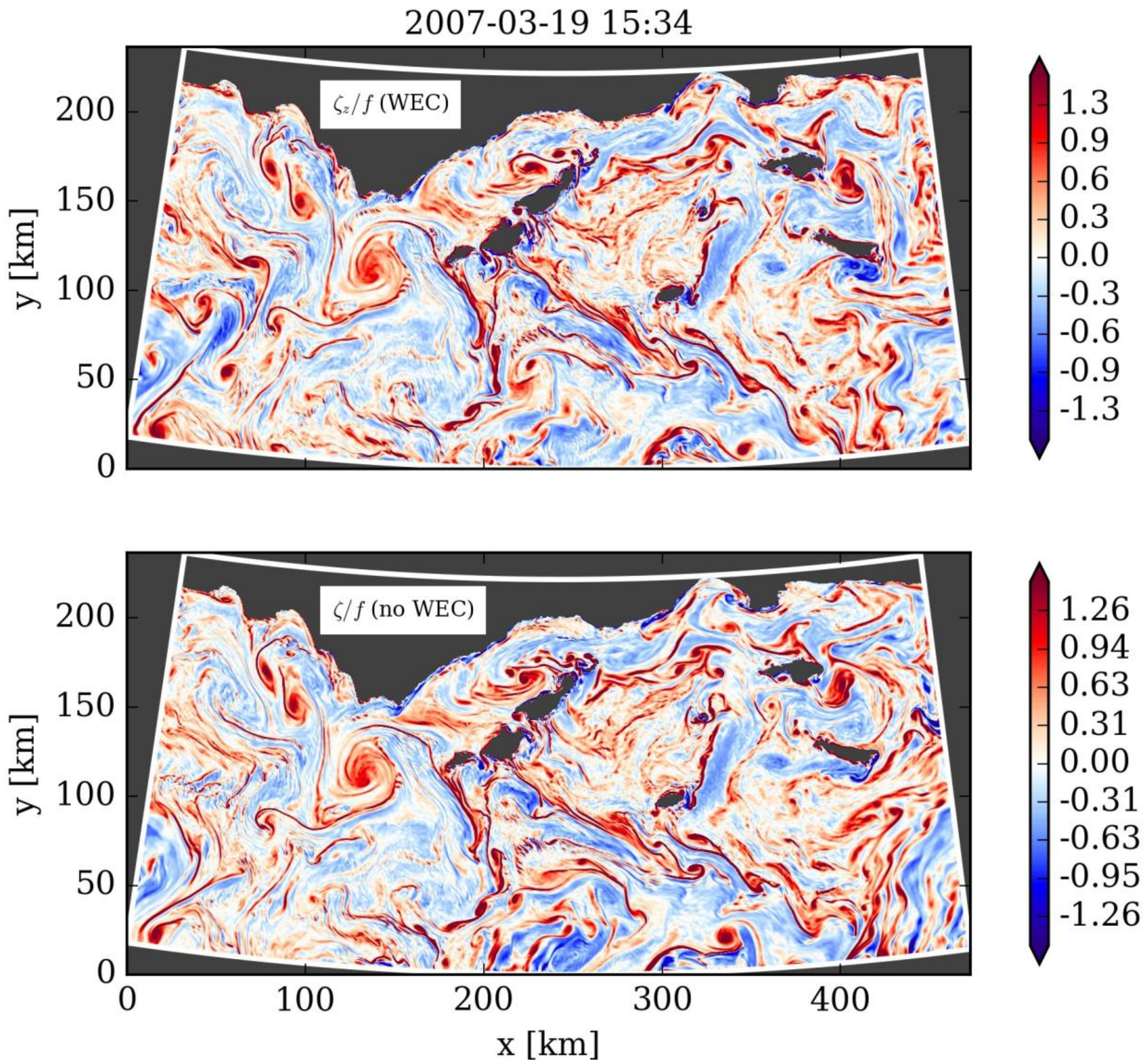

Ongoing and Future Work

- Wave model validation against Romero et al. 2017
- Two-way (online) coupling of ROMS and WW3 with OASIS3-MCT
  - Spectral peak coupling (i.e., H_s, T_p, and mean wave direction) following the framework by Uchiyama et al. 2010 (coupling of two-dimensional fields) – DONE
  - Fully coupled Stokes drift (required coupling of three-dimensional fields)
  - Coupling of non-conservative effects (wind stress from wave breaking)
- Two-way coupled ROMS-WW3 simulations in Southern California with validation against field observations (Langmuir DRI, Inner Shelf DRI)
  - Fully coupled vs spectral peak coupling (vortex forces)
  - Non-conservative effects (e.g., modification of the surface stress)
- Three-way coupled ROMS-WW3-WRF
  - coupled air-sea fluxes

Thank You

CIGoM
Consorcio de Investigación del Golfo de México

Office of Naval Research
ONR
Science & Technology